T.R.
Inonu University
Graduate School of Nature and Applied Sciences

EPILEPTIC SEIZURE DETECTION WITH POWER SPECTRAL DENSITY METHOD

Master of Thesis

Rabia TUTUK

Department of Biomedical Engineering

Thesis Supervisor: Assistant Prof. Dr. Reyhan ZENGİN

DECEMBER 2022

T.R.
Inonu University
Graduate School of Nature and Applied Sciences

EPILEPTIC SEIZURE DETECTION WITH POWER SPECTRAL DENSITY METHOD

Master of Thesis

Rabia TUTUK
(36203630007)

Department of Biomedical Engineering

Thesis Supervisor: Assistant Prof. Dr. Reyhan ZENGİN

DECEMBER 2022

ACKNOWLEDGMENTS AND PREFACE

I would like to thank my advisor Asst. Prof. Dr. Reyhan ZENGİN, guided me in every aspect of this thesis, without withholding her guidance, help, suggestions, criticism, knowledge, experience, and support at every stage of this thesis.

I would like to express my gratitude to my family for their trust, encouragement, kindness, and all kinds of support in my education.

I would also like to thank my friends who stood by me during this process, did not spare their moral support, listened to my problems patiently, and sought solutions.

WORD of HONOR

I proudly confirm that this work titled "Epileptic Seizure Detection with Power Spectral Density Method", which I submitted as a master's thesis, was written by me without resorting to any help that would be contrary to scientific morals and traditions, and that all the sources I have used are those shown in accordance with the method both in the text and in the bibliography.

Rabia TUTUK

CONTENTS

List of Tables

List of Figures

INDEX OF SYMBOLS AND ABBREVIATIONS

CNS	:	Central Nervous System,
EPSP	:	Excitatory Postsynaptic Potential,
IPSP	:	Inhibitory Postsynaptic Potential,
EEG	:	Electroencephalography
DC	:	Direct Current
AP	:	Action Potential
Hz	:	Hertz
BRE	:	Benign Rolandic Epilepsy
JAE	:	Juvenile Absence Epilepsy
JME	:	Juvenile Myoclonic Epilepsy
Fp	:	Pre-frontal
F	:	Frontal
T	:	Temporal
P	:	Parietal
O	:	Occipital
C	:	Central
Z	:	Zero
BC	:	Before Christ
DWT	:	Discrete Wavelet Transform
ANN	:	Artificial Neural Network
PSD	:	Power Spectral Density
HD	:	Hyperdimensional
LBP	:	Local Binary Pattern
AUC	:	Area Under Curve
HFO	:	High-Frequency Oscillations
FFT	:	Fast Fourier Transform
TIRDA	:	Temporal Intermittent Rhythmic Delta Activity

Master of Thesis

EPILEPTIC SEIZURE DETECTION WITH POWER SPECTRAL DENSITY METHOD

RABİA TUTUK

Inonu University
Graduate School of Nature and Applied Sciences
Department of Biomedical Engineering

81+xii page

2022

Supervisor: Assistant Prof. Dr. Reyhan ZENGİN.

Detection of pre-seizure signs in epileptic signals may help patients to survive the seizure with minimal damage. This thesis aims to detect the pre-seizure and the seizure patterns using different two databases. The first EEG dataset was provided by the Department of Epileptology, the University of Bonn, Germany (A, C, and E sets were used). The database collected at Boston Children's Hospital was used as the second data set. The power, frequency, and amplitude values of all EEG signals in this data set were examined and compared. The power spectral densities (PSD) of each signal were analyzed graphically. The maximum PSD of the signals and high-frequency oscillations (HFOs) in the signals are investigated. The frequency subbands of the maximum PSD are examined. It was determined that the maximum power at the time of seizure was in the delta and theta subbands (these subbands are pathologic). The maximum power of F4 and T3 channels for all patients included only delta and theta subbands and HFOs are detected in these channels. Furthermore, frequency increase rates of pre-ictal and ictal signals are investigated, and increasing PSDs of HFOs are then calculated. In addition, the frequency of signals is observed to be 80 Hz and above in the Fp2, C4, P4, O2, and Pz channels, which are common to all patients. Also, when the subbands with the maximum power before seizure were examined, it was determined that the T8-P8 and P7-T7 channels had alpha and beta subbands in most of the patients. Consequently, determined the differences between healthy, pre-seizure, and epileptic patterns.

Keywords: Epilepsy, Maximum power, Subband, Ripples.

Yüksek Lisans Tezi

GÜÇ SPEKTRAL YOĞUNLUĞU YÖNTEMİ ile EPİLEPTİK NÖBET TAHMİNİ

RABİA TUTUK

İnönü Üniversitesi
Fen Bilimleri Enstitüsü
Biyomedikal Mühendisliği Bölümü.

81+xii sayfa

2022

Danışman: Dr. Öğr. Üyesi Reyhan ZENGİN

Epileptik sinyallerde nöbet öncesi belirtilerin saptanması hastaların nöbeti en az hasarla atlatmasına yardımcı olabilir. Bu tez, farklı iki veri tabanını kullanarak nöbet öncesi ve nöbet paternleri tespit etmeyi amaçlamaktadır. İlk EEG veri seti, Almanya Bonn Üniversitesi Epileptoloji Bölümü tarafından sağlandı (A, C, E setleri kullanıldı). İkinci veri seti olarak Boston Çocuk Hastanesinde toplanan veri tabanı kullanıldı. Bu veri setlerindeki tüm EEG sinyallerinin güç, frekans ve genlik değerleri incelendi ve karşılaştırıldı. Her sinyalin güç spektral yoğunlukları (PSD) grafiksel olarak analiz edildi. Sinyallerin maksimum PSD'si ve sinyallerdeki yüksek frekanslı salınımlar (HFO'lar) araştırıldı. Maksimum PSD'nin frekans alt bantları incelendi. Nöbet anında maksimum gücün delta ve teta alt bantlarında olduğu belirlendi (bu alt bantlar patolojiktir). Tüm hastalar için F4 ve T3 kanallarının maksimum gücü sadece delta ve teta alt bantlarını içermekte ve bu kanallarda HFO'lar tespit edilmektedir. Ayrıca preiktal ve iktal sinyallerin frekans artış oranları incelenerek HFO'ların artan PSD'leri hesaplanmıştır. Tüm hastalarda ortak olan Fp2, C4, P4, O2 ve Pz kanallarında sinyallerin frekansı 80 Hz ve üzerinde olduğu gözlenmiştir. Ayrıca nöbet öncesi maksimum güce sahip alt bantlar incelendiğinde hastaların çoğunda T8-P8 ve P7-T7 kanallarında alfa ve beta alt bantlarının olduğu belirlendi. Sonuç olarak, sağlıklı, nöbet öncesi ve epileptik paternler arasındaki farklar belirlendi.

Anahtar Kelimeler: Epilepsi, Maksimum güç, Altbant, Dalgalanmalar.

1. INTRODUCTION

Epilepsy is a non-infectious chronic brain disease that influences nearly fifty million people of all ages globally. It consists of repetitive seizures which are a consequence of aberrant discharges of electrical in collective brain cells [1]. These can be caused by brain damage, head trauma, chromosomal and developmental disorders, hereditary diseases, and genetic reasons, or they can occur for unknown reasons [2]. Epilepsy is a curable disease, and despite all known treatments, seizures may not be controlled [3]. Due to these uncontrollable seizures, the quality of life of individuals suffering from epilepsy decreases. Since the time and place of seizures are not known, these people are in constant danger, so the early detection of seizures is really important manner [4]. Due to this manner, in this thesis study, the determination of the differences between healthy, pre-seizure, and epileptic seizure signals was investigated.

The brain consists of millions of interconnected neurons. The necessary information about the brain system is obtained from its signals and measurements. Measurements are made at larger scales with a large collection of neurons, but smaller scales are measured with a single nerve cell [4].

1.1 Neural Activities

A neuron is an electrically excitable cell that communicates with other cells by synapses. Each neuron consists of three parts; axon, dendrite and cell body. Each of these nerve cells responds to stimuli and transmits information over long distances. A neurocellular body consists of a single nucleus. It also contains most of the nerve cell metabolism, particularly involved in protein synthesis. Proteins formed in the cell body are transmitted to other parts of the nerve. The axon is a long cylinder that transmits an electrical impulse. Dendrites transmit signals to other nerves. Activities in the Central Nervous System (CNS) are related to synaptic currents transferred between cells' axon, dendrite, or dendrite connections. Under the membrane of the cell body, a varying negative polarity potential can be recorded with changes in synaptic activities of 60-70 mV. If an action potential moves along the fiber ending in an excitatory synapse, an excitatory postsynaptic potential (EPSP) occurs in

the neuron. If two action potentials move along the same fiber over the same short distance, there will be a sum of EPSPs producing an action potential on the post-synaptic neuron. If the fiber terminates at an inhibitory synapse, hyperpolarization occurs, which indicates the inhibitory postsynaptic potential (IPSP). After the formation of an IPSP, there is a flow of cations or anions in the nerve cell. This situation is in the form of cation overflow or anion entry into the nerve cell. This flow mobility eventually causes a change in potential. Primary transmembrane currents produce secondary ional currents across cell membranes in the intracellular and extracellular space. These currents (passing through the extracellular space) produce field potentials. These field potentials generally have a frequency of less than 100 Hz. Also, these field potentials are called EEGs when there is no change in the signal average. But if they have slow shifts that can mask the real EEG signals, they are called DCs. A combination of EEG and DC potentials is often observed for certain brain abnormalities (such as seizures, hypercapnia, and asphyxia) Action potentials in the excitatory and inhibitory presynaptic fibre respectively lead to EPSP and IPSP in the postsynaptic neuron (see Figure 1.1) [5].

1.2 Action Potentials

An action potential (AP) is defined as a transient change in membrane potential conducted along the axon and is also defined as the information produced by a nerve cell. APs are caused by an ion exchange across the neuron membrane. Generally, APs initiated in the cell body normally move in one direction. The membrane potential depolarizes and forms a spike. After the peak of the spike, the membrane repolarizes. The potential becomes more negative than the resting potential. Then the potential returns to normal. Action potentials last between 5-10 milliseconds in most nerves. Figure 1.2 shows an example AP [5].

1.3 The Brain and Epilepsy

The brain is a part of the central nervous system. Each part of the brain has its own task. The cerebral cortex is called a thin layer covering the entire surface of the brain and has different functional regions. These regions consist of the temporal, parietal, occipital, and frontal lobes. It is responsible for cognitive and memory func-

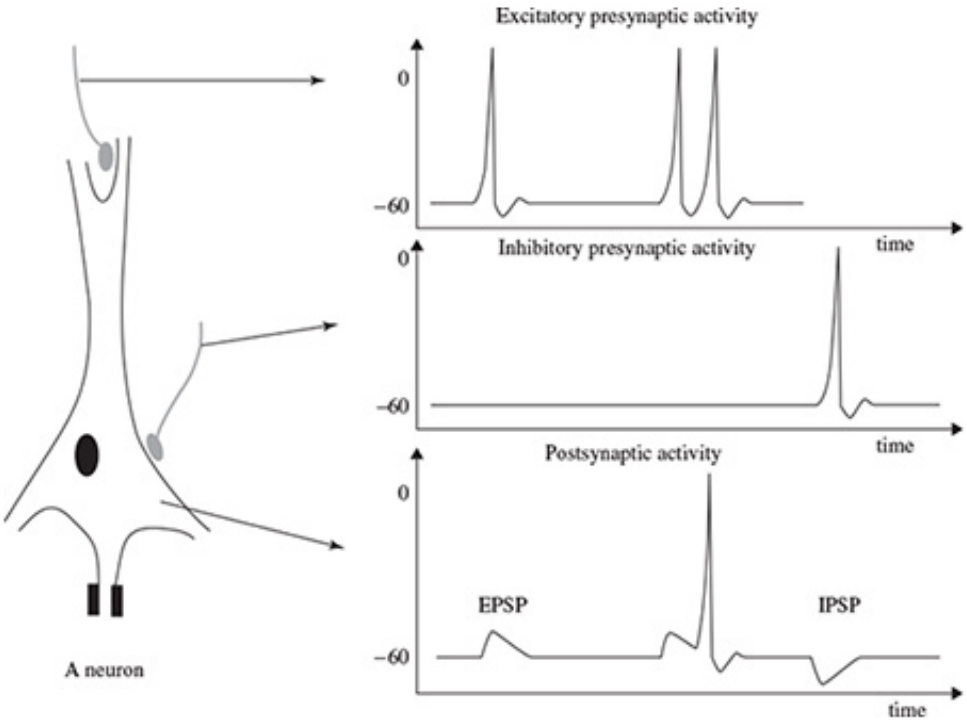

Figure 1.1 : The neuron membrane potential changes and current flow during synaptic activation recorded by means of intracellular microelectrodes [5].

tions as well as motor control. The cerebral cortex consists of 10-100 billion nerve cells or neurons. Densely interconnected neurons are difficult to understand. In particular, the interconnected neurons in the cerebral cortex of humans are denser than those of animals. This is due to the more complex abilities of humans. We can also describe the function of the brain in relation to different temporal and spatial scales. This is due to neural-generating conditions. We can list these scales as macroscopic, mesoscopic, and microscopic. Mesoscopic scales are associated with 10-1000 Hz activity. Because events faster than the behavior of aggregated neurons are neglected. Microscopic scales are generally associated with frequencies above 1000 Hz. The reason for this is that the mechanisms in single neurons are very fast. Macroscopic scales are associated with frequencies from 1 to 100 Hz, as the spatial average of a larger number of neurons is to filter out higher frequencies.

Epilepsy affects a large part of the brain, not whole the brain, so it is defined as a scale problem (macroscopic phenomenon). In order to understand the macroscopic events, it is sometimes necessary to understand the microscopic events [4].

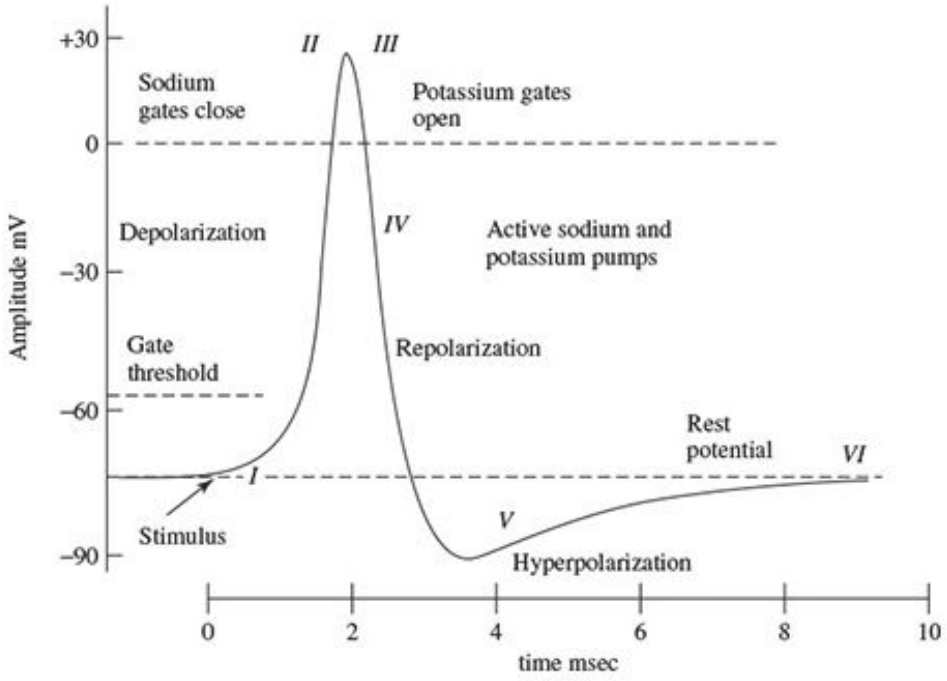

Figure 1.2 : Diagram showing the phases of an action potential [5].

An epileptic seizure is a neurological condition that occurs when the normal activity of the brain with disrupted as a result of abnormal discharge in nerve cells. The cause of this abnormal discharge may be various diseases. However, there are some cases where the cause cannot be determined and how the seizure occurs is not known. The causes of epileptic seizures can be listed as brain tumors, developmental disorders in brain tissue and brain vessels, hereditary diseases, and genetic causes. Epilepsy can occur at any age and at any time. Epilepsy is the most common neurological disease in children up to the age of 16 [6].

1.4 Types of Epileptic Seizures

Epilepsy is a status arising from basic physiological abnormalities in which seizures indicate an infrequent phenomenon of changing degrees [4].

We can classify epileptic seizures into two types. The first one consists of focal epileptic seizures, also called partial, and the second one consists of generalized epileptic seizures.

1.4.1 Focal (partial) seizures

Partial seizures begin in only one part of the brain and affect only this part. It is divided into simple and complex. In simple partial seizures, the patient is conscious. Abnormal twitching, drowsiness, sweating, nausea, disturbances of perception and memory, and a feeling of 'Deja Vu may occur. In complex partial seizures, the patient's consciousness changes, and loss of consciousness is observed. This causes mental confusion. The patient may think that she/he is dreaming. The patient may exhibit emotional outbursts or strange and repetitive behaviors such as winks and tics [7].

1.4.2 Generalized seizures

Generalized seizures occur as a result of abnormal activity in both halves of the brain at the same time. We can list these seizures as absence, myoclonic, tonic, clonic, atonic, and tonic-clonic seizures. An absence seizure is a type of seizure that can recur many times during the day, lasting 10-20 seconds, have a sudden onset and end, and complete loss of consciousness. In typical absence seizures, the EEG finding is in the form of bursts of symmetrical spike-wave complexes. A typical absence seizure has a more uncertain beginning and end, can last longer, and shows more pronounced changes in muscle tone. EEG shows normal background activity, asymmetric 2.0-2.5 Hz irregular spike waves, spike slow wave bursts, and paroxysmal fast activity. In a typical absence seizure, discharges on EEG tend to be slower and asymmetric. In the interictal period, a slowdown in ground activity may be observed. In absence seizure with the tonic component, activity is observed in symmetrical and asymmetrical flexor and extensor muscles. In absence seizures with atonic symptoms, a sudden decrease in tone is observed in the extremity and posture muscles. In absence seizures with a mild clonic component, there are beats ranging from subtle clonic twitches to marked tremors. In addition, clonic movements that are synchronized with spike-wave activity are seen in EEG recordings [8].

Myoclonic seizures, myoclonus, are involuntary sudden, rapid, and arrhythmic contractions of muscle groups. It can be generalized on the face, torso, especially the upper extremities, and/or generalized. It may occur as a single seizure or cluster.

EEG often shows multiple spike-wave discharges. Tonic seizures usually last less than a minute and are observed as a sudden increase in tone in the extensor muscle groups. EEG shows low-voltage fast activity or rhythmic activity with increasing amplitude as the frequency of 10 Hz decreases. Clonic seizures are characterized by recurrent and rhythmic clonic beats and are more common in infancy. The postictal duration of such seizures is short. In the EEG, this period occurs at rhythmic activity of 10 Hz or higher. Atonic seizures are characterized by a decrease in muscle tone, and sudden loss of tone is observed in falls. For this reason, injuries are seen as common. Seizures in the form of head falling forward are included in the scope of atonic seizures. EEG shows multiple spike-wave complexes or flattening. Tonic-clonic seizures are the most common and most severe seizure type and were formerly described as grand mal. It can be primary or it can develop as a result of the secondary spread of simple or complex partial seizures. Some patients experience a prodromal period. During this period, symptoms may begin hours or days before the seizure. When the seizure is over, the patient may fall asleep or be agitated. This state, called the postictal period, lasts for 5-20 minutes. It is observed less frequently in newborns and early infancy than in other seizure types. Because, during these periods, synaptic development, myelination, and interhemispheric connections are not completed [8].

1.5 Epileptic Seizure Types Syndromes

There are three seizure-type syndromes. The first type is called focal epilepsy seizures. These syndromes are divided into three among themselves. Benign rolandic epilepsy (BRE), one of the most common types of epilepsy, accounts for more than a third of all epilepsy cases. At 3-13 years of age, the onset of symptoms begins. At 7-8 years of age, the symptoms peak. Benign occipital epilepsy, an inherited type of epilepsy, accounts for about 3 percent of all childhood epilepsy cases. It is more common in girls than boys. The most common seizures of early childhood, febrile seizures affect 2 to 5 percent of all children. It occurs in children between the ages of 6 months and 5 years. However, the average age of onset is between 18 and 22 months. These seizures usually occur on the first day of a child's illness due to a high fever (>102℉) [9].

The second type of syndrome is called generalized seizures. This type of syndrome is divided into four among themselves. The first is childhood absence epilepsy, which is characterized by short-term changes in consciousness and gaze. The second is Juvenile absence epilepsy (JAE), a common type of epilepsy that begins between the ages of 10 and 17, typically at or after puberty. About one-third of patients with this type of epilepsy syndrome have a family history of seizures. Third, juvenile myoclonic epilepsy (JME) is an inherited form of epilepsy that begins during puberty. Febrile seizures that can occur in any child tend to be inherited and are also more common in boys than girls [9].

The last one is the mixed seizure type epilepsy syndromes. This type of syndrome is also divided into two. The first is Lennox-Gastaut syndrome, a severe form of epilepsy. In about one-third of children with this syndrome, the first symptom is a prolonged seizure. The child usually has more than one seizure during the day. This type of syndrome is called tonic seizures (muscle stiffness), which usually occurs during sleep. They usually last about 10 seconds or they can last up to a minute. The second one is West syndrome. This syndrome type is a rare type of epilepsy in children. It is also considered a serious brain disease [9].

1.6 How Is Epilepsy Diagnosed?

The information provided by the patient and their relatives is very important in the diagnosis of epilepsy. The diagnosis is made with this information received by the specialist neurologist about the seizure. Along with seizure histories, electroencephalography (EEG), sleep EEG, cranial images and blood tests are also necessary for differential diagnosis [10].

1.7 Electroencephalography (EEG) and Major EEG Findings

EEG is of great importance in the diagnosis of epilepsy and is also effective in the differentiation of specific epilepsy syndromes [24]. EEG lasts for about 30 minutes and is the process of transferring the signals received through the electrodes placed at certain specific points on the skull, to be strengthened and poured on a paper [11]. EEG waves show potentials at various frequencies and amplitudes. Figure 1.3

shows some EEG waves. An activity with a frequency of 8-13 Hz is observed in the

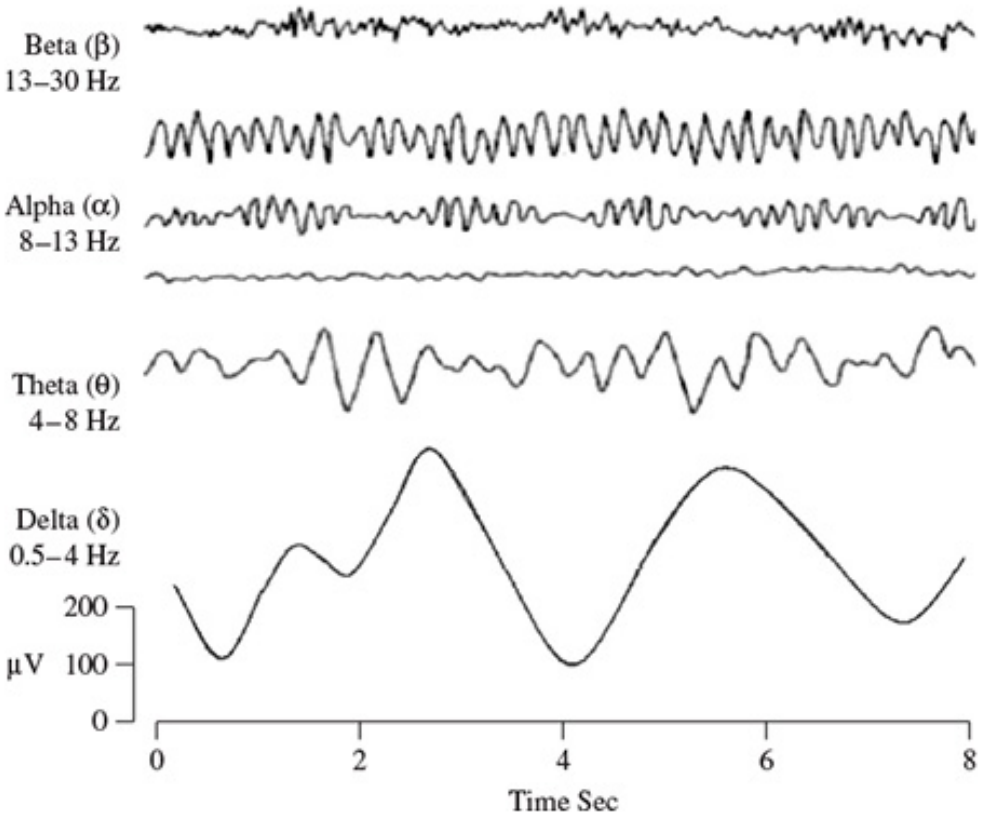

Figure 1.3 : Subbands of EEG [5].

parieto-occipital regions. This activity is called alpha activity and occurs in a normal adult when awake and with eyes closed, together with the basic activity varying according to age. This activity is lost or suppressed when the eyes are opened. Beta activity is a rhythm with a frequency of 13-30 Hz, which is evident in the frontal and central regions. For this activity (with high amplitude) usually one suggests the use of a sedative-hypnotic drug. Pathological findings in EEG are divided into two main groups. These are nonspecific slow waves and epileptiform activity. Slow wave activity is grouped as theta (4-8Hz) and delta (1-4Hz). It is important to know where the slow wave occurs. Its frequency, amplitude, and other relevant factors are all recorded. Focal slow wave finding suggests the presence of a structural brain lesion in the region where it is recorded with a probability of 70%. However, this finding can sometimes be seen in focal epilepsy without lesions [12].

1.7.1 EEG generation

The EEG signal is defined as a measurement of the currents flowing during synaptic excitation of the dendrites of many pyramidal neurons in the cerebral cortex. Synaptic currents in dendrites are produced when neurons are activated. This current produces a secondary electric field on the scalp that can be measured by EEG systems. Figure 1.4 shows the structure of a neuron, and Figure 1.5 shows a schematic representation of the main parts of the brain [5].

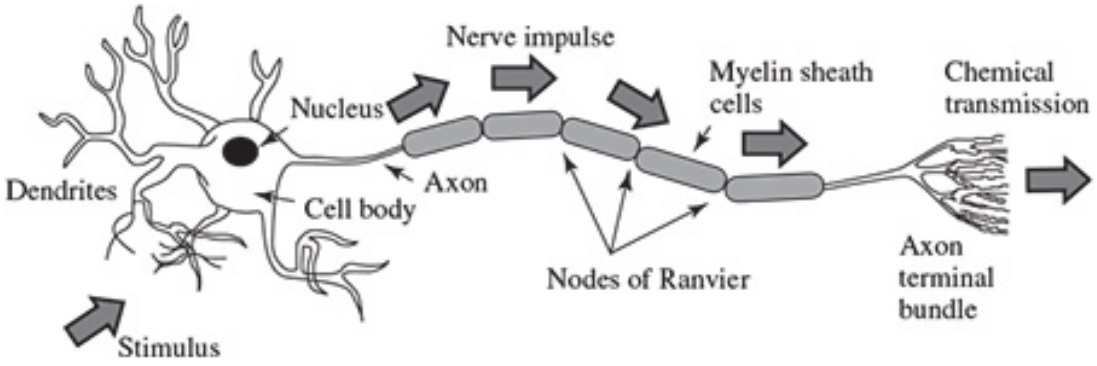

Figure 1.4 : Structure of a neuron [5].

1.7.2 Investigation of EEG signals in clinical problems

It is common for the examination of EEGs to be used in the diagnosis of many neurological disorders and abnormalities in the human body. EEG signals from humans and animals can be used to investigate the following clinical problems [5]:

- monitoring states of wakefulness, coma, and brain death;
- detecting all areas of damage, together with the presence of head trauma, paralysis, and whether there is a tumor;
- finding afferent pathways with evoked potentials;
- monitoring the alpha rhythm;
- generating biological feedback situations;

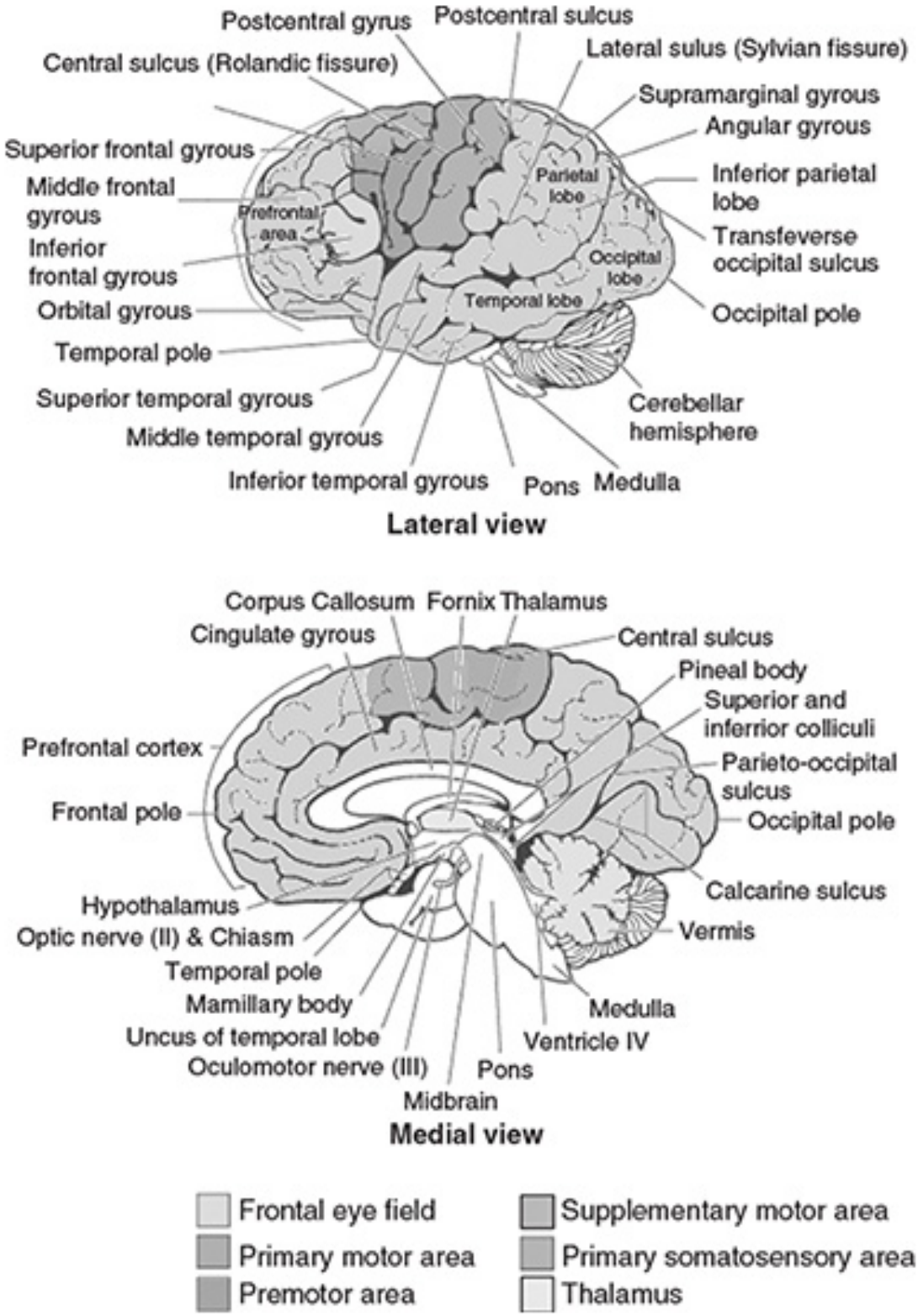

Figure 1.5 : Diagrammatic representation of the major parts of the brain [5].

- controlling the depth of anesthesia;
- examining epilepsy and finding the source of the seizure;
- testing the effects of drugs used for epilepsy;
- assisting in the removal of tissue in which the epileptic focus is located;
- monitoring of all brain-related development;
- controlling the drugs for shocking effects;
- examining of sleep physiology and disorders
- examining mental disorders;
- providing a hybrid data logging system with other imaging modalities [5].

1.8 Fundamentals of Electrophysiology

An EEG is a voltage-time graph where the vertical axis (y) represents the voltage and the horizontal (x) axis represents the frequency. The voltage is obtained from the difference in the voltages between two electrodes (at least one of which is on the scalp) placed at a given moment. The cellular activity produces the EEG, and it is basically cortical postsynaptic potential changes that change the electrical charge across the pyramidal cell membrane. The temporal and spatial summation of the electrical currents originating from postsynaptic potentials is accepted as the source of different EEG waves. During the EEG recording, the electrical changes collected in the electrodes on the scalp and the underlying cortex are recorded. Meanwhile, far-field potentials and extra-brain potentials can be recorded. Factors affecting the amplitude of recorded potentials are the density of the electrical source, the distance of the recording electrodes, and the electrical resistance and capacitance of the structures between the source and the recording electrodes. EEG electrodes are placed on the scalp with the international 10-20 system [13].

1.9 10-20 Electrode System

The 10-20 electrode system is an internationally accepted method that standardizes the EEG electrode placement. It ensures that the distance between the electrodes is

equal [14]. "10" and "20" refer to the fact that the actual distances between adjacent electrodes are 10% or 20% of the total anterior-posterior or right-left distance of the skull [15]. Figure 1.6 shows the placement of the electrodes on the skull according to the 10-20 electrode system.

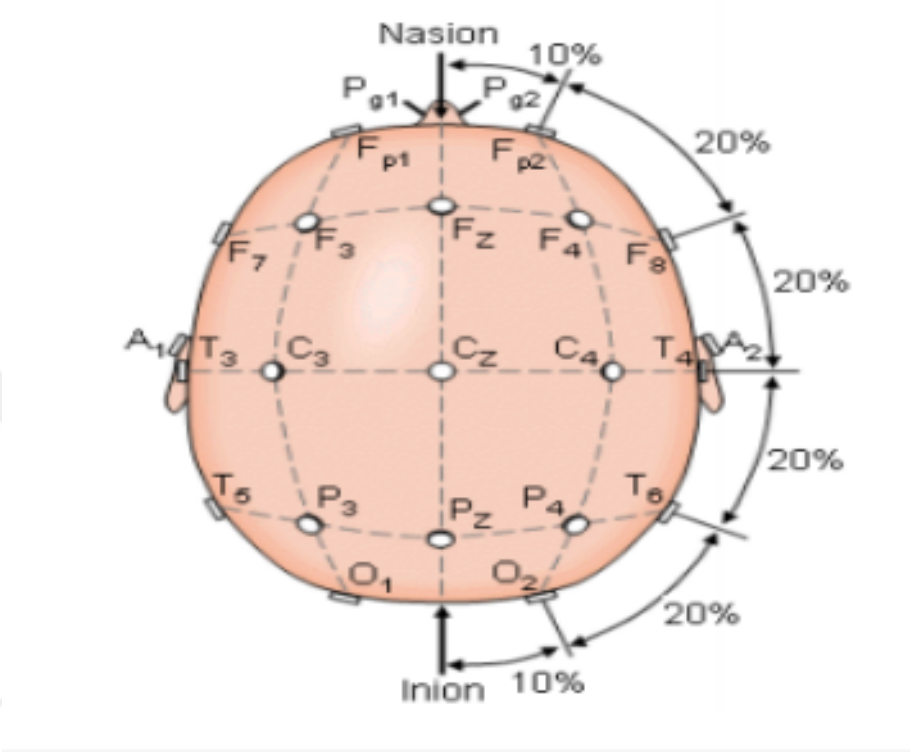

Figure 1.6 : Skull representation of the 10-20 electrode system [16].

1.9.1 Electrode placement

The letters **Fp, F, T, P, O,** and **C** are used for all electrode insertion points to indicate the areas of the brain. These letters represent the prefrontal, frontal, temporal, parietal, occipital, and central regions, respectively. The **"C"** electrodes represent the EEG activity more typical for anterior, temporal, some parietal, and occipital activities. **"Z"** electrodes are used in polysomnography sleep studies. It is also often used as a "reference" to diagnose possible clinical brain death or epileptiform seizure activity on clinical EEG montages. **(Z)** electrodes used mostly for reference/measurement points. The **"Z"** (zero) refers to an electrode placed in the midline sagittal plane of the skull **(FpZ, Fz, Cz, Oz)**. The even-numbered electrodes

(2,4,6,8) are used to represent the electrode placement on the right side of the brain. The odd-numbered electrodes **(1,3,5,7)** are used to represent the electrodes on the left side of the brain. The prominent bony part behind the outer ear usually represents **"A"**. For all electrodes, **Cz** and **Fz** represent "ground" or "common" reference points. **A1** and **A2** electrodes are used for the contralateral reference of all EEG electrodes [15].

1.9.2 Measurement of EEG

For Z electrodes, marks are made between these points along the midline at the intervals of 10%, 20%, 20%, 20%, 20%, and 10%. The point in front of each ear is called a preauricular point. This point can be found more easily with light taps. Furthermore, if it is necessary, the patient may be asked to open his mouth slightly. T3, C3, Cz, C4, and T4 electrodes are placed on the marks measured from the top of the head at 10%, 20%, 20%, 20%, 20 and 10% intervals, respectively. Skull circumference is measured just above the ears where the T3 and T4 electrodes are located, just above the bridge of the nose where the Fpz electrode is placed, and just above the occipital point in Oz. When measured from the front, that is, over the Fpz electrode, the Fp2, F8, T4, T6, and O2 electrodes are placed at 5%, 10%, 10%, 10%, 10%, and 5% intervals, respectively. The same procedure is done for the odd-numbered electrodes on the left side to complete the entire circumference. The measurement methods for the placement of the F3, F4, P3, and P4 electrodes are different. If the measurement is made from front to back (Fp1-F3-C3-P3-O1 and Fp2-F4-C4-P4-O2), they can be 25% "up" from the front and rear points (Fp1, Fp2, O1, and O2). If the measurement is made side by side (F7-F3-Fz-F4-F8 and T5-P3-Pz-P4-T6), they can be 25% "up"from the side points (F7, F8, T5, and F7, F8, T5, and T6). When the measurement is made diagonally from Nasion to Inion, it will be 20% in front of and behind points C3 and C4. Each of these measurement methods gives different results for each nominal electrode placement [15].

1.10 Recording the EEG

The components of EEG recording are given as following:1) **Electrodes:** Attached to an individual's scalp. 2) **Amplifiers:** The amplitude of the input signals from the

electrodes is in the order of microvolts. Therefore, differential amplifiers are used to amplify this level. These amplifiers must have high input impedance. 3) **Filters:** Before recording EEG signals, it is necessary to filter them to eliminate interference. For this purpose, high-pass, low-pass, and notch filters are used. 4) **Recording unit:** It is used for permanent EEG signal recording [44].

1.10.1 EEG activity scopes

The electrical potential change between two electrodes, regardless of the waveform, is called a wave. These waveforms can be regular or irregular. They are classified as monophasic, biphasic, triphasic, and polyphasic. There are rhythmic and arrhythmic wave repetitions. In rhythmic repetitive waves, there are similar intervals between waves. They are usually in the form of regular and sinusoidal waves. In arrhythmic repetitive waves, there are variable and irregular intervals between the waves. The frequency of a wave is calculated by measuring the duration and wavelength of a single wave. EEG waves are divided into five subbands: theta, beta, alpha, delta, and gamma. The amplitude of EEG waves is measured at the level of microvolts. EEG distribution can be in large areas on both sides of the head, it can be found in a single hemisphere or it can be limited to a small area. Phase expresses the timing and polarity of the wave components in one or more channels. Waves with different frequencies may appear in different channels. Phase encounter is the biggest indicator of the source of EEG potentials in bipolar recordings. Phase shows the time relationship between different components of a rhythm in a single channel. The timing of the waves in different areas of the head may be the same or different. While the term synchronous is used for the exact simultaneous occurrence, persistence describes how often a wave occurs during a recording. Reactivity is a concept used to describe the changes that may occur in some normal and abnormal waves with various maneuvers (frequent breathing, eye blinking, or light reaction) [24].

1.11 EEG Indications about Epilepsy

We can list the epilepsy-related indications as 1) Clinical epilepsy or suspected seizure, 2) Classification of a patient diagnosed with epilepsy, 3) Changes in seizure pattern,4) Suspicion of nonconvulsive status epilepticus, 5) Monitoring of status

epilepticus, 5) Antiepileptic treatment interruption plan, and 6) Surgical evaluation [17]. EEG is effective in the differentiation of specific epilepsy syndromes. EEG always remains normal in 10% to 40% of epileptic cases. Sleep, sleep deprivation, photic stimulation, and hyperventilation facilitate the emergence of discharges in epileptic patients. West Syndrome, Lennox-Gastaut Syndrome, Childhood Absence Epilepsy, Benign Rolandic Epilepsy, Juvenile Myoclonic Epilepsy, and Temporal lobe seizures can be easily recognized by special EEG findings [24].

1.11.1 EEG in epilepsy diagnosis

EEG recording analysis is the primary method in the diagnosis of epilepsy. Interictal indications of epilepsy can be identified from a short period of EEG recordings. However, the rarity of seizures requires long EEG recordings. Before the advent of portable recorders, EEG recordings were made in private hospitals with trained personnel. Usually, seizures were detected either when the patient stated or when the patient was observed. However, with the use of portable EEG systems, the patient is recorded in her/his own environment before the seizures end in one session [44]. The EEG recording should be reviewed by a trained technician, because it is not clear when the seizures will occur, and often nocturnal seizures cannot be marked [44].

1.11.2 Anatomical distribution of abnormal waves in EEG

Knowing the anatomical distribution of abnormal waves in EEG will provide a faster and more accurate evaluation of it. When the distribution of epileptic waves according to the anatomical parts of the brain was evaluated, no statistically significant difference was observed between the parts (p=0,557, p=0,999). However, frontal and temporal regions were seen to be more prominent in terms of producing epileptic activity. Figure 1.7 shows the cerebral distribution of epileptogenic waves [18].

In a study, When epilepsy is evaluated according to age groups, it was observed that these epileptic activities were significantly more common in the right frontal region in the 21-40 age group, and in the bilateral frontotemporal regions in the 8-20 and 41-60 age groups compared to other regions (p=0.01, p=0.001). Figure 1.8 shows the cerebral distribution of epileptogenic waves by age [18].

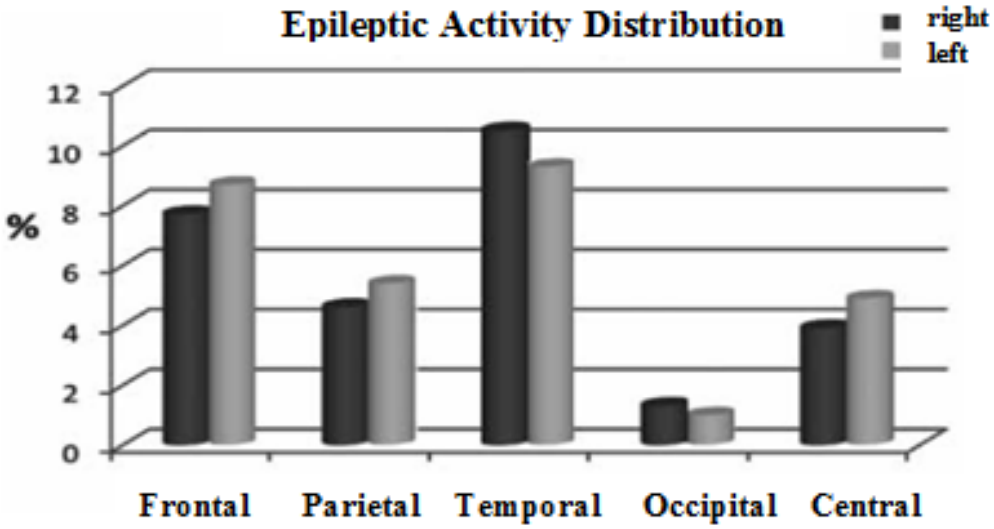

Figure 1.7 : Cerebral distribution of epileptogenic waves [18].

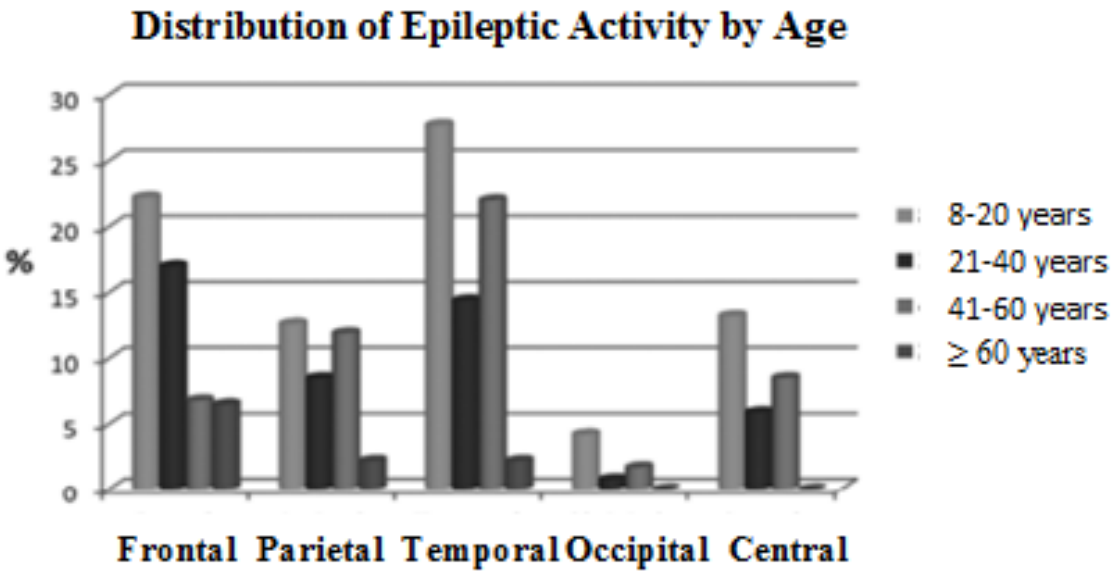

Figure 1.8 : Cerebral distribution of epileptogenic waves by age [18].

Epileptiform anomalies are spike (with bases of less than 70 ms) and sharp (with bases of 70 to 200 ms) waves, and the underlying physiological event of these waveforms is paroxysmal (comes in sudden transient crises) depolarization shift.

Localized epileptiform activities, usually are located in the temporal or frontotemporal areas. The frontal lobe is the most common region of epileptic activity after the temporal lobe. According to data from the epilepsy surgery series, 20-30% of treatment-resistant focal epilepsies originate in this region. Epileptic activities originating from the parietal lobe are rare. The occipital lobe accounts for 8% of all cases [18].

1.12 Can Epilepsy Be Treated?

Since epilepsy has no specific cause, the response time and level of the patient's response to treatment varies from person to person. In the treatment of epilepsy, which starts with drug therapy, drugs have the effect of suppressing the disease rather than curing it [3]. Correct drug selection and dose adjustment are effective to stop seizures. However, in some patients, the use of medication may not be effective to stop seizures. In this case, as a second treatment method, surgical treatment is applied. In order to apply surgical treatment, the patient must be resistant to drugs. There are two types of surgical treatment methods. The first and preferred one is to eliminate the seizure focus, and the second is to reduce the spread and frequency of seizures [19]. However, if the patient is not suitable for surgical treatment, there is no treatment to stop or control the seizures [3].

1.13 History of Epilepsy

Epilepsy is one of the oldest known illnesses, with written records dating back to 4000 BC [1]. Figure 1.9 shows an ancient tablet describing epilepsy symptoms and different types of epileptic presentation. In these records, a person with epilepsy was described as "with his neck turned to the left, his hands and feet tense, his eyes wide open, foams coming out of his mouth unconsciously" (Figure 1.10) [20].

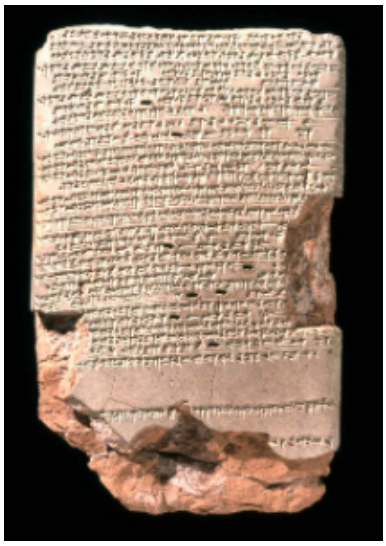

Figure 1.9 : Tablet 26 of a series of 40 which compose the ancient Babylonian diagnostic manual entitled Sakikku [20].

Figure 1.10 : Saint Severin image showing him healing a woman from a 'falling sickness demon' [20].

Nearly a millennium later, it was defined as a mental illness by Babylonian doctors and it was suggested that it could be treated on only a spiritual level [21]. Evidence of epilepsy was found around 1700 BC. The Egyptians created a case report of the brain's direct stimulation by physiological feedback. They proved that seizures could result from cortical deterioration. Egyptians' documents about epilepsy were also found in Chinese texts dating back to 770-221 BC [20]. In the 5th century BC, Hippocrates decided that epilepsy was a brain disease and wrote a book called

"The Sacred Disease" [21]. In this book, Hippocrates opposed the divine origin of epilepsy. He recognized that epilepsy was not compared to other diseases more sacred, but had the same nature and caused the rise of individual diseases. He combined the etiology of epilepsy and brain dysfunction and suggested that heredity plays a role in the disease [22]. In the 4th century BC, Aristotle suggested epileptic seizures and sleep arose from akin mechanisms. His ideas have influenced the scientific community for centuries. From the 17th century, Hippocrates' epilepsy idea began to spread in Europe. A Scottish physician, William Cullen, proposed that seizures can appear without causing loss of consciousness. A French doctor agreed that individuals suffering from epilepsy should be treated in a hospital. In 1849, it is hypothesized that "electrical discharges" in the brain may be the cause of seizures. John Hughlings Jackson established the scientific base of epileptology and examined the location of abnormal tissues that could cause seizures [20].

1.14 Review of the Literature on Epilepsy

Researchers have been studying the detection of epilepsy with EEG signals nearly for a century. In a study in 1934, it was stated that there was evidence that the pH value increases with the body temperature of individuals with epilepsy, especially before seizures, and stated that the increased pH value is usually accompanied by the retention of water [23]. In 1991, it is shown in Spehlmann's EEG Primary book that EEG has great importance in the diagnosis of epilepsy, and is effective in the differentiation of specific syndromes. It is claimed that the EEG always remains normal in 10% to 40% of epileptic cases, and explained that sleep, sleep deprivation, and hyperventilation (excessive breathing) facilitate the emergence of discharges in epileptic patients [24]. Meldrum and Chapman examined the synaptic release of amino acid neurotransmitters by in vivo microdialysis in 1999. They reported that extracellular hippocampal concentrations of glutamate and aspartate were increased before seizure onset in patients with epileptic foci in the temporal lobe. [25]. Andrzejak et al. stated that there was a consistent decline in the strength of the delta subband in the pre-ictal term by comparison to the inter-ictal period [26].

Zhao et al. obtained a decrease in hemoglobin oxygenation 20 seconds before the onset of seizure [27]. It is also proposed that the ephemeral focal tissue oxygen defi-

ciency and insufficient blood supply to the extremities are good signs for the epileptic centers and may occur prior to the outset of the ictal case [28]. Varvsky et al. stated that for the sake of fully agreeing with the epileptic brain, the term after the seizure is as well as crucial in terms of how the brain affects the seizure. They also defined structures like alterations in chemical (adenosine) or rebalancing of the chemical inequality accountable for onsetting the seizure [4]. As a result of a study conducted in 2012, individuals suffering from epilepsy were not nominees for surgical operation with vagal nerve stimulation, for some patients, it was possible to reduce or stop the seizures [29]. In 2014, the prediction of epileptic seizures was performed prospectively [30]. In the same year, Moghim and Corne noted that before the onset of seizures, an increase in the availability of oxygen, amount of oxygen in the blood, cerebral blood outflow, and any changes in heartbeat rate are involved [31]. Performing analysis of venous blood gas based on pH, bicarbonate, base surplus and lactate just one hour after the recent epileptic seizure attack could be used to predict the seizures [32]. In 2016, Teixeira et al. showed that before the onset of the seizure, a decrease in band power of the EEG because of lower frequencies leads to a decrease in the correlation process [33]. In addition, a method of predicting an epileptic seizure by combining a method of detecting changes in heart rate and identifying an abnormal condition was proposed [34]. In another study, it was shown that impending seizures in multi-channel EEG data can be predicted with mean phase coherence, a measure of phase synchrony [35].

Lai and Chiang explained that automatic detection of epileptic seizures in EEG could be performed with machine learning methods using the dataset consisting of five different patient categories [36]. MJN Neuroserve has developed a device that predicts epileptic seizures based on real-time monitoring of stress and heart rate in 2018 [37]. After one year, Wang and colleagues automatically identified epileptic cases using a compound of Gradient Boosting Machine and system [38]. In another study, researchers developed an auto-detection method that effectively filters noise and takes into account variability in EEG signals, potentially making it suitable for clinical diagnosis of epileptic seizures [39]. Furthermore, an epileptic seizure detection based on signal processing in the time-frequency domain with multilevel Discrete Wavelet Transform (DWT) and nonlinear Artificial Neural Network (ANN)

model was presented [40]. In 2020, Slimen et al. estimated based on EEG sudden detection that spikes in the ictal (during seizure) period increased by comparison to other periods and that spikes increased suddenly in the pre-ictal period compared to the inter-ictal period [41]. In a recent study, it was stated that continuous EEG monitoring is a standard approach for epilepsy detection to distinguish between epileptic seizures and non-epileptic seizures [42].

Power spectral density (PSD) is the most widely used feature for epileptic seizure detection. Spectral power properties such as absolute band powers in specific bands, relative band powers, or spectral power ratios between these are known to be good properties for seizure detection or prediction. [43] . Automatic analysis of the human EEG began in the early 1970s for helping in the diagnosis of epilepsy. Total signal strength can be a useful measure of discrimination of the variation between ictal and non-ictal EEG. In addition to variations in the aggregate signal power, it is feasible that the power in specific frequency bands will expose differences between epileptic and non-epileptic signals. The epileptic EEG generally includes spike and wave ingredients of frequencies up to approximately 20 Hz. It would be acceptable to await that the power of this frequency band, for a certain subject and recording, would be higher for epileptic EEG than non-epileptic. A consistently higher mean power was demonstrated in the ictal EEG compared to the non-ictal period [44]. PSD has been used in many epileptic seizure classification studies to detect seizures in EEG segments. In similar studies, in addition to different feature extraction, the PSD of each EEG data is calculated with different spectral analysis methods, and these features are taken as input to classifiers, deep learning methods, or different machine learning methods. These methods have been used to optimize feature subsets such as PSD and to train the models [**?**]. In a study, spectral power was calculated in nine bands and this was used as a feature set for seizure prediction [54]. Another study in 2019 showed that the spectral power ratio in two distinct bands, rather than its characteristics in a particular band, can obtain importantly better performance for seizure prediction [55]. Moreover, the spectral energy of the frequency subbands carrying the maximum information in the EEG signal was determined and various subband combinations were obtained [56]. In a recent study, the feasibility of binary Hyperdimensional (HD) computation for de-

tecting seizures from EEG data using both local binary pattern (LBP) coding and PSD features was presented. As a result of that study, it was seen that the PSD method outperformed the LBP method in test sensitivity, specificity, accuracy, and AUC (Area Under Curve) [57].

High-frequency oscillations (HFOs) are assigned as an effective factor in determining seizure activity. HFOs are promising biomarkers for epileptogenic tissue. HFOs are divided into ripples (R; 80–250 Hz) and fast ripples (FRs; 250–500 Hz). Most studies have reported higher HFO rates in epileptogenic tissue than in non-epileptogenic tissue [58]. In recent years, many studies have been done on the automatic detection of HFOs [**?**]. In 2021, Schoenberger et al. showed in an electrical stimulation study that 'pure' ripples, as opposed to epileptic surges, are essentially physiological [62].

In this thesis, we used two EEG datasets, one is from the Department of Epileptology, University of Bonn, Germany, and the other one is from Boston Children's Hospital. First, these datasets were preprocessed. The power, frequency, and amplitude values of all EEG signals in this data set were examined and compared. Then, the EEG signals were divided into subbands, and the subbands with the maximum power spectral density were determined. These procedures were applied to healthy, pre-ictal, and ictal datasets. In addition, the HFOs in the EEG signals, and the maximum amplitude ratios of the pre-ictal and ictal EEG signals in the frequency subbands were calculated. The frequency values of the pre-ictal and ictal EEG signals between the reference electrode (Fz) and the remaining channels were examined. Consequently, in this study, we determined the differences between healthy and epileptic seizure signals.

1.15 Objectives of the Thesis

Epileptic seizures and pre-seizure differences should be determined by examining feature extraction, spectral analysis methods, and signal processing methods. These methods are necessary for the detection of pathological findings. The goals set are as follows:

- Conversion of time-domain EEG signals to the frequency domain, because it is difficult to understand in the time domain.

- To decompose these signals into frequency subbands with DWT to make the signals clearer.
- Investigation and comparison of amplitude and frequency values of healthy, pre-seizure, and seizure signals.
- Graphical examination of PSDs of healthy, pre-seizure, and seizure signals.
- Detection of frequency subbands with maximum PSDs of signals. Investigation of frequency subbands with maximum PSDs of epileptic signals.
- Detection of HFOs in signals. Calculation of the increasing power of ripples and fast ripples.
- Detection of epileptic seizure patterns by using the obtained maximum PSD values and HFOs together.
- Minimizing the number of channels.

1.16 Thesis Outline

In Chapter 2, the EEG datasets, preprocessing step, feature extraction, and frequency domain analysis used to detect pre-seizure and seizure patterns are described.

In Chapter 3, the results obtained from the methods applied to both data sets used are included. Comparison of PSD plots, frequency, amplitude values, and HFOs of healthy, pre-seizure, and seizure signals are shown. In addition, the maximum power values of epileptic signals and their frequency subbands are shown. Each result is interpreted and how epileptic patterns are detected is explained. The conclusion is given in Chapter 4.

2. MATERIALS AND METHODS

The epileptic pattern detection consists of pre-processing, feature extraction, and post-processing parts.

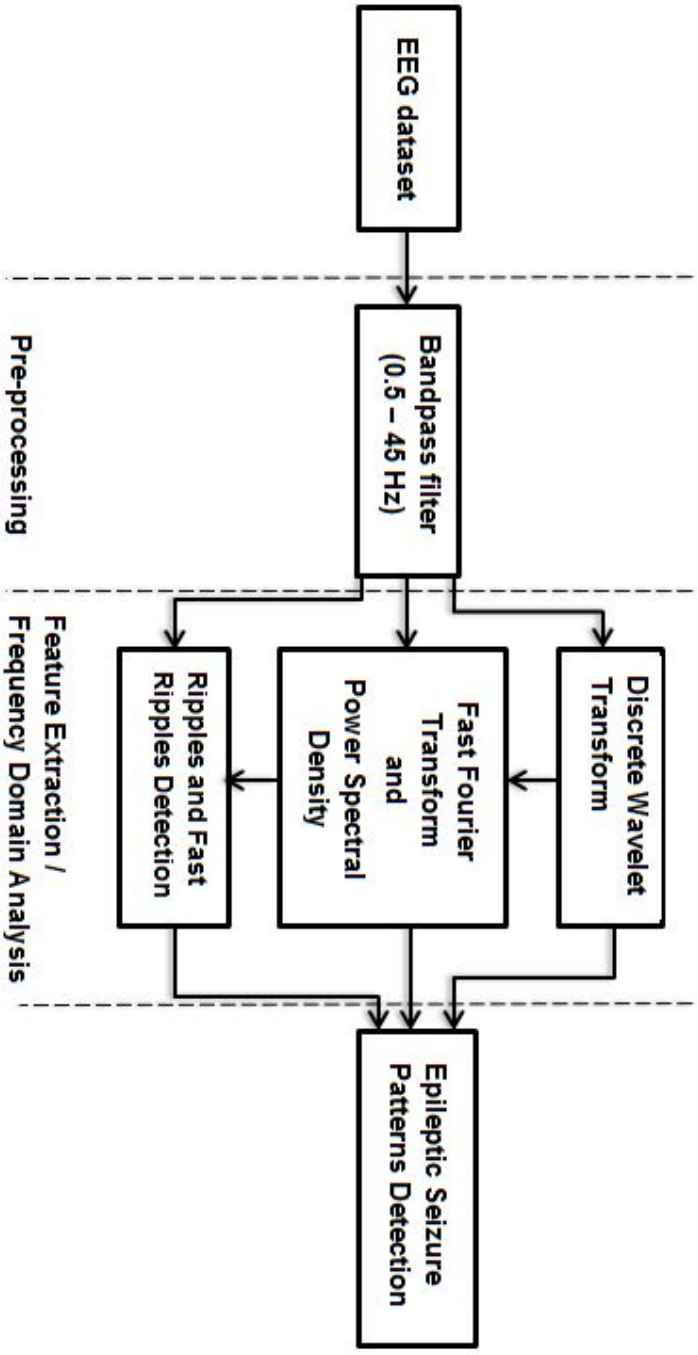

Figure 2.1 : Steps of the epileptic pattern detection system.

The flow diagram of the epileptic pattern detection system used in this study is given in Figure 2.1. EEG data is first filtered with a band-pass filter as a preprocessing step. Secondly, due to the difficulty of understanding the EEG signals in the time domain, the signals are transformed into the frequency domain. Thirdly, the EEG signals are separated into subbands with the discrete wavelet transform method to make the signals clearer. Then, the frequency subbands with the maximum PSDs of the signals are examined. Afterward, the HFOs in the signals are detected and increasing the power of spectral density of ripples and fast ripples are calculated. Finally, as post-processing, with the resultant maximum PSD values and HFOs, epileptic seizure patterns can be detected.

2.1 Explanation of EEG Data

In this study, we used two different EEG datasets. The first one is provided by the Department of Epileptology, University of Bonn, Germany [63]. A standard 10-20 electrode system was used to record this dataset (see Figure 2.2). The second one is provided by Boston Children's Hospital.

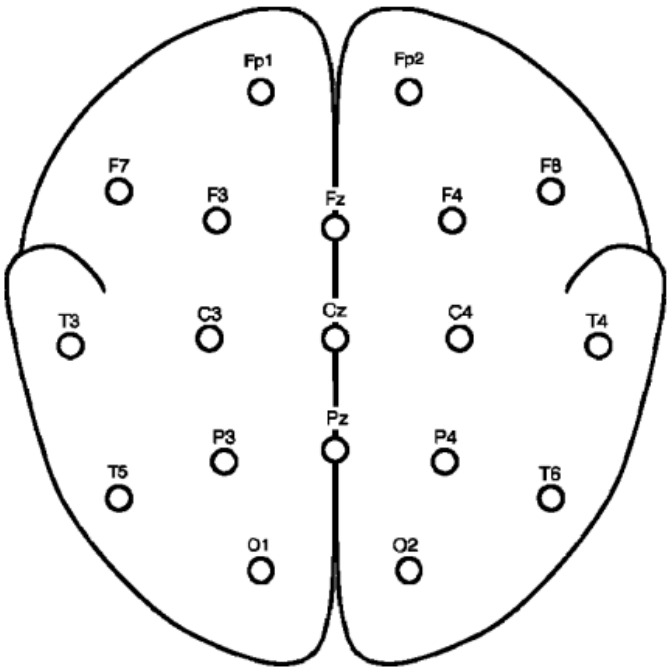

Figure 2.2 : Positions of the surface electrodes correspondingly the international 10-20 electrode system [63].

The first EEG dataset consists of 5 sets named A, B, C, D, and E. Each set contains 100 channels. A and B sets consist of EEG recordings from five healthy individuals. Set A consists of recordings taken with eyes open and set B with eyes closed. Other sets are taken from the EEG archive and belong to the pre-operative period. The records in set D were recorded from the region that caused epilepsy. Set C was recorded from the opposite hippocampal part of the brain. C and D sets were included only in activity measured at non-seizure intermissions. Set E includes only seizure activities. The sampling frequency of the data is 173.61 Hz. All .txt files include 4096 samples [63]. EEG data of these five datasets were drawn with the MATLAB program (Figure 2.3). In this study, we decide to compare healthy (set A), pre-ictal (set C), and epileptic (set E) signals, so we used only A, C, and E datasets. In addition, as a second EEG dataset, the database collected at Boston

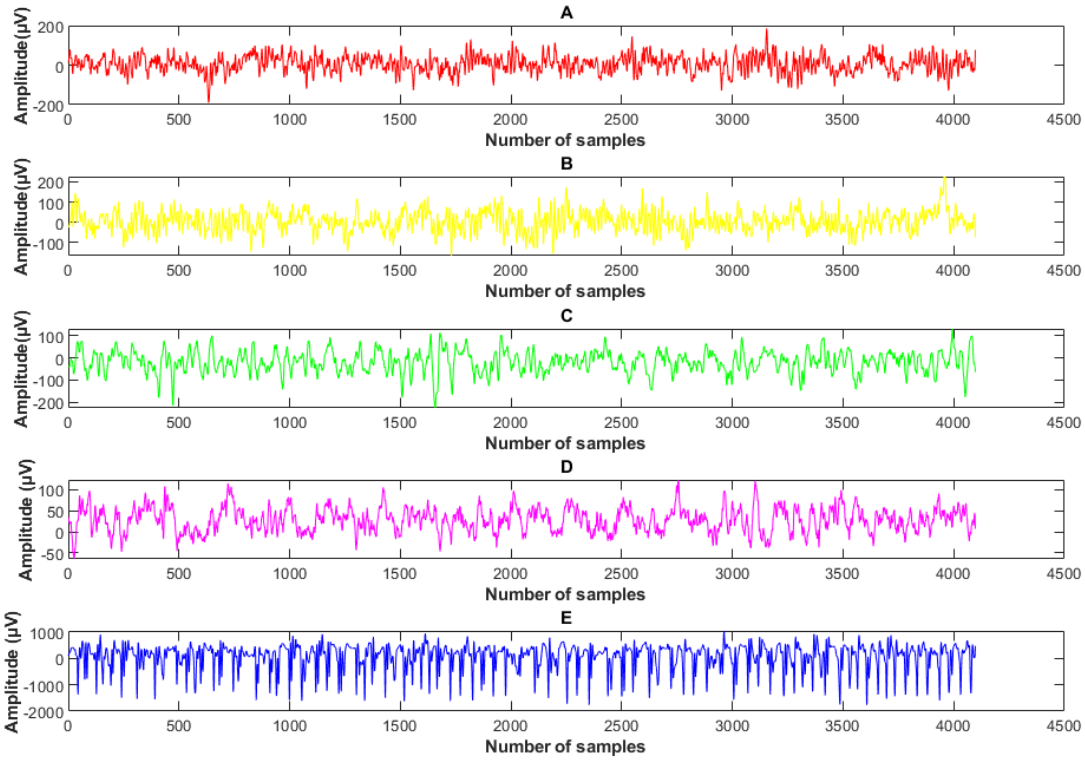

Figure 2.3 : Graphical representation of EEG signals from first channel.

Children's Hospital was used in this study. This database includes EEG recordings from pediatric subjects with persistent seizures. Records were obtained from 22

subjects, 5 males (3-22 years old) and 17 females (1.5-19 years old). However, the Chb21 (patient 21) case was grouped as 23 cases, as it was taken from the same female subject 1.5 years after the chb01 (patient 1) case. All signals are sampled at 256 samples per second. An International 10-20 EEG electrode system was used for these recordings. The records consist of 198 seizures in total [72]. Figure 2.4 shows MIT datasets drawn with the MATLAB program. The level of these signals is microvolts.

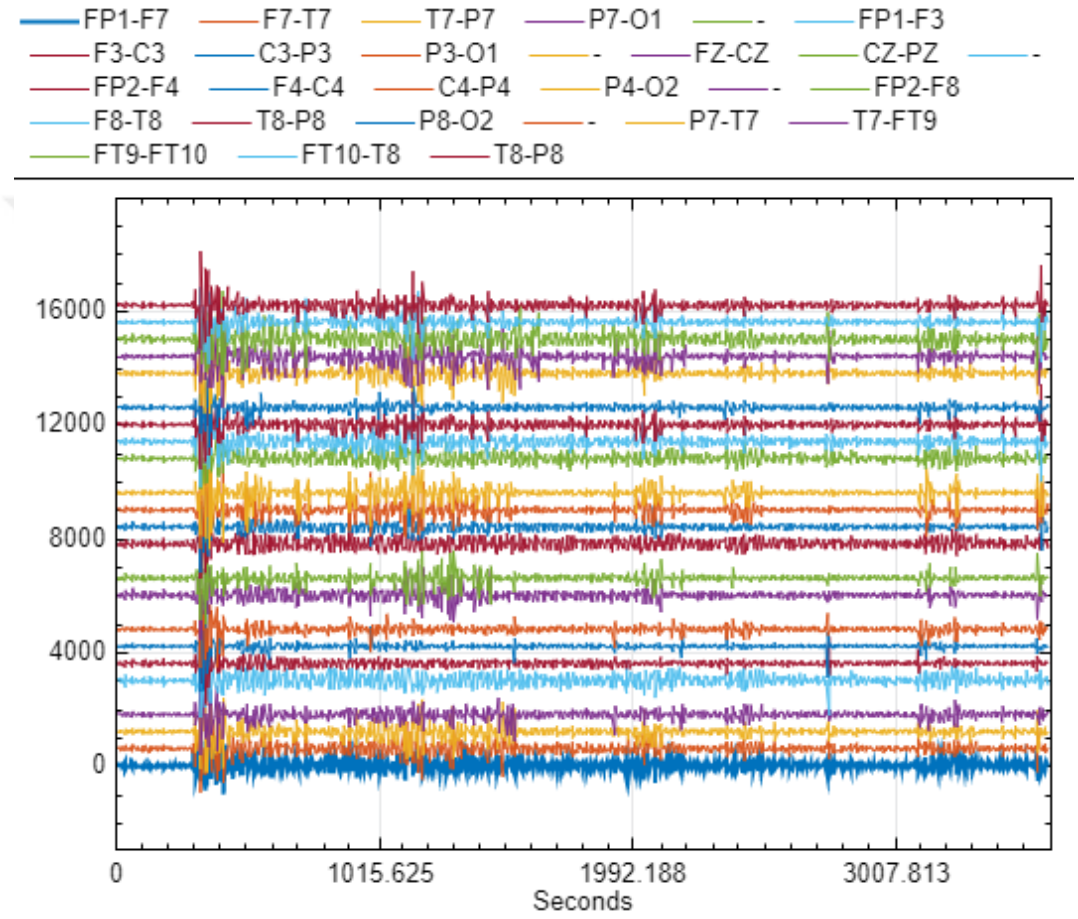

Figure 2.4 : Graphical representation of EEG signals from all channels (second dataset, MIT database).

2.2 Preprocessing of EEG Signals

To eliminate the noise in EEG signals, preprocessing should be done. Many artifacts such as eye-muscle movements or power line interference may occur during the recording of EEG signals [64]. The frequency interval of EEG artifacts does not

usually exceed 50 Hz, device artifacts rarely exceed 30 to 40 Hz [65], and power line interference remains at 50 or 60 Hz [66]. Therefore, a band-pass filter is applied to limit the frequency of the signals between 0.5-45 Hz, taking into account the EEG frequency bands.

2.3 Discrete Wavelet Transform (DWT)

Discrete Wavelet Transform (DWT) is a method for decomposing non-stationary signals into different frequency subbands. However, it does not contain any physical comments about the components [67]. This method splits signals into wavelet coefficients. It ensures exact time and frequency knowledge at both low and high frequencies, due to its conformity with the use of variant-size windows. It enables the signal to be decomposed into coarse approximation and detailed knowledge with consecutive low and high pass filters. If the filter produces the coarse approximation and detail coefficients, it is called a low-pass and a high-pass filter, respectively. The sizes of coarse coefficients decrease by a factor of two in the subsequent dissociation. At each step of decomposition, the time resolution is halved, while the frequency resolution is doubled (Figure 2.5) [64]. It is very important to choose the most suitable separation level in order to perform the DWT process correctly. We can directly determine the number of decomposition levels according to the dominant frequency ingredients [64].

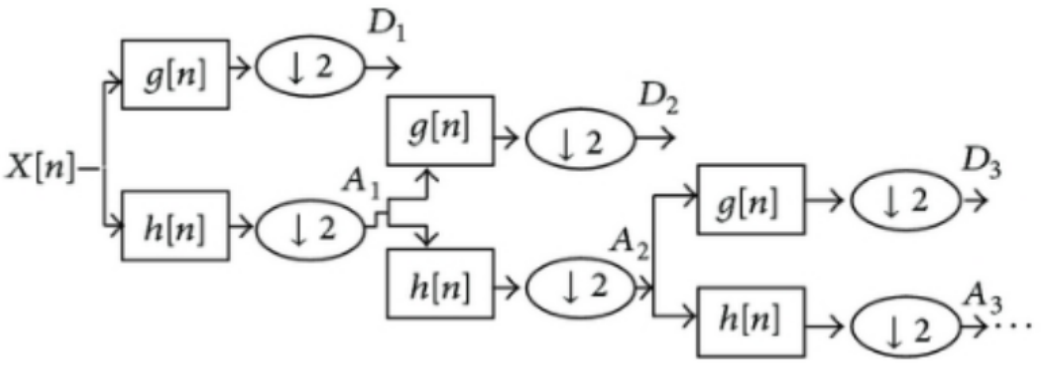

Figure 2.5 : Application of discrete wavelet transform [64].

2.4 Frequency Domain Analysis

In this study, we performed the frequency analysis of EEG signals. It is preferred due to its proven capability to distinguish between epileptic and non-epileptic EEG. Non-overlapping windows of EEG data with two seconds from a single channel are filtered in frequency bands to be suitable with dual style distributions in DWT analysis. These frequency bands are 2-4 Hz (delta), 4-8 Hz (theta), 8-12 Hz (alpha), and 13-30 Hz (beta), which contain all frequencies of epileptic seizures and generally do not contain higher frequencies of artifacts. After the filtering process, the mean signal strength is computed for each resultant frequency band [4].

2.4.1 Fast Fourier Transform (FFT) and power spectral density (PSD)

EEG signals contain events with different frequencies. Most of the events are not always clear in the time domain when cases at different frequencies interact with each other [4].

PSD is a significant analysis method to figure out both the static and dynamic properties of EEG. Dynamic features are reviewed to capture the time-varying nature of EEG. A locally stable behavior is referred to as static property. The most common method used to detect epileptic seizures is PSD. The features of the EEG signals with PSD estimation are computed to symbolize these signals selectively. The PSD is computed with the Fourier transform of the autocorrelation sequence found by non-parametric methods [67].

In order to make our signal more understandable, frequency transform is applied to the $y[n]$ signal. With this transformation n [4] is defined as ω. Frequency transform can be used for any signal consisting of a linear combination of fundamental (basic) functions ($b_n[k]$, at time k). These functions act as an implicit identity in the time domain and isolate the elements in time [4]:

$$b_n[k] = \begin{cases} 1 & \text{if k=n} \\ 0 & \text{otherwise} \end{cases} \tag{1}$$

The original signal ($y[n]$) in the time domain can be rewritten as follows:

$$y[n] = \sum_{k=-\infty}^{\infty} y[k]b_n[k], \quad n = 1, 2, 3... \tag{2}$$

Fundamental functions in the frequency domain isolate the different frequency components of the $y[n]$ signal by projecting them into sinusoidal fundamental functions. These basic functions were chosen due to their good performance in isolating items with different frequencies. In the next step, the signal is defined in the frequency domain in the point of frequency components. Frequency domain analysis is known as a method for estimating frequency-related features. For finite time domain signals with discrete time, the FFT of a random windowed signal $y[n]$ for $n = k + 1, k + 2 \ldots, k + N$ is given by [4]:

$$FFT[w, k] = \sum_{n=1}^{N} y[n + k]e^{-iwn}, \quad w = \frac{2\pi m}{N} \tag{3}$$

The sinusoidal fundamental functions $e-^{i\omega n} = cos(\omega n)$ - $isin(\omega n)$ are able to isolate action at different frequencies ω, measured in terms of radians.

The FFT is defined for $0 \leq \omega = \frac{2\pi m}{N} < 2\pi$ with $m = 0, 1..N - 1$. The range 0 to 2π is separated into equal divisions limiting the number of samples in the windowed $y[n]$. To properly scale the frequency array in Hz, the transform $\omega = 2\pi f/F_s$ is required, where F_s is the sampling rate of the data and f is the frequency in Hz among zero and F_s. [4].

PSD is defined as a function of ω. It also contributes each frequency item to the strength of the resultant signal $y[n]$:

$$PSD[w, k] = \left|FFT[w, k]\right|^2 \tag{4}$$

where $\left|\cdot\right|$ specifies the absolute value. The concept of power is kept among time and frequency domain [4].

2.4.2 Ripples and fast ripples in the EEG signal

We aforementioned that oscillations in EEG signals are good biomarkers for seizure detection. They produce EEG brain activities in the 80-500 Hz range, which are divided into high-frequency oscillations (HFOs) as ripples (80–250 Hz) and fast ripples (FRs; 250–500 Hz) [69]. HFOs are associated with seizures if there are HFOs in the transition from the pre-ictal to the ictal region. In addition, HFOs are increased from the inter-ictal (in the seizure-free period) to the pre-ictal periods and are spatially kept. Ictal oscillations are mostly related to the seizure onset site. Just before the seizure, inhibitory and spike activities decrease. Then the epileptogenic activity of the tissue increases and there is an increase also in HFOs. Therefore, in this study, a band-pass filter was first applied to the EEG signals using a sampling rate of 2 kHz to detect these ripples. As a result, signals with low-frequency components were eliminated, and just signals with high-frequency (80-500 Hz) components are used [69]. The increasing PSD's of ripples and fast ripples were then calculated. Finally, the labeling process was carried out by normalization.

3. RESULTS

In this study, we focused on detecting differences between healthy and epileptic seizure patterns using two different EEG datasets. The first one is obtained from Bonn university, the other one is from Boston University. The power, frequency, and amplitude of all EEG signals were reviewed, and the maximum PSD of the signals and HFOs in these signals are investigated. These methods were applied to all healthy and epileptic individuals including the A, C, and E sets of the first EEG dataset. All calculations and signal processing steps in this study were done online using Matlab (2021) [71]. First, the raw EEG signals were passed through a band-pass filter. By using the DWT method, the signals were decomposed into subbands and the complexity of the signals was reduced. Figure 3.1, 3.2, and 3.3 show the subband plots of sets A, C, and E with DWT applied, respectively.

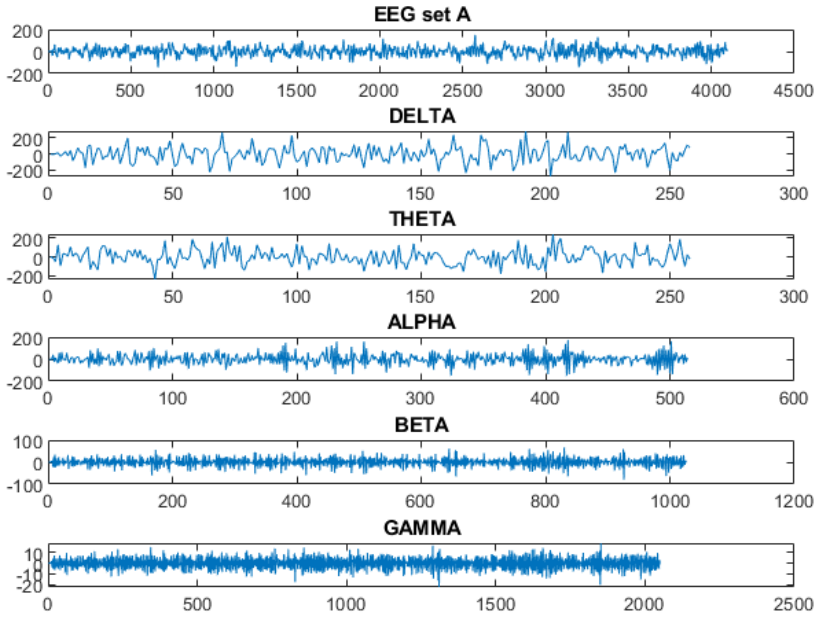

Figure 3.1 : Discrete wavelet transform of EEG set A.

Since EEG signals are not clear and comprehensible in the time domain, we applied Fast Fourier Transform (FFT). After taking FFT, we calculated the PSD of each signal and determined the frequency subbands with the maximum power. We compared

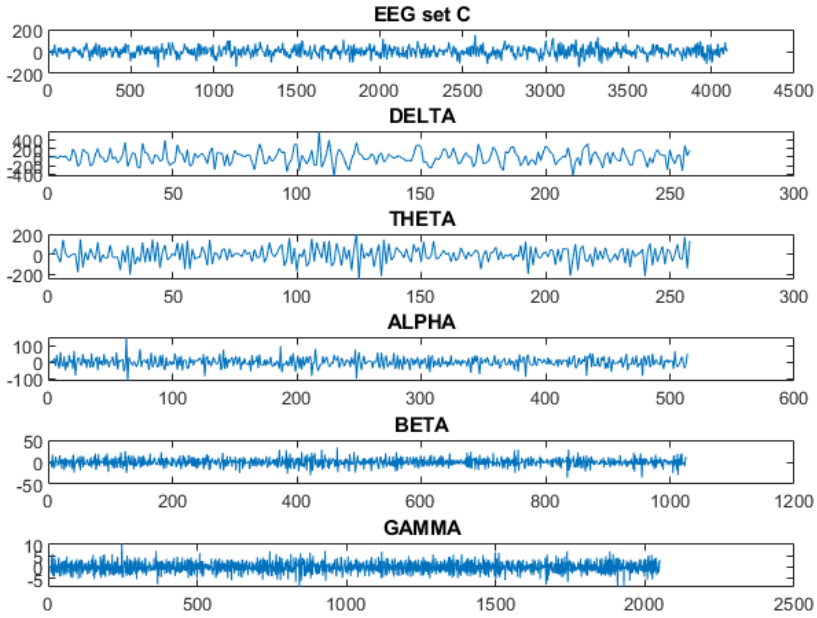

Figure 3.2 : Discrete wavelet transform of EEG set C.

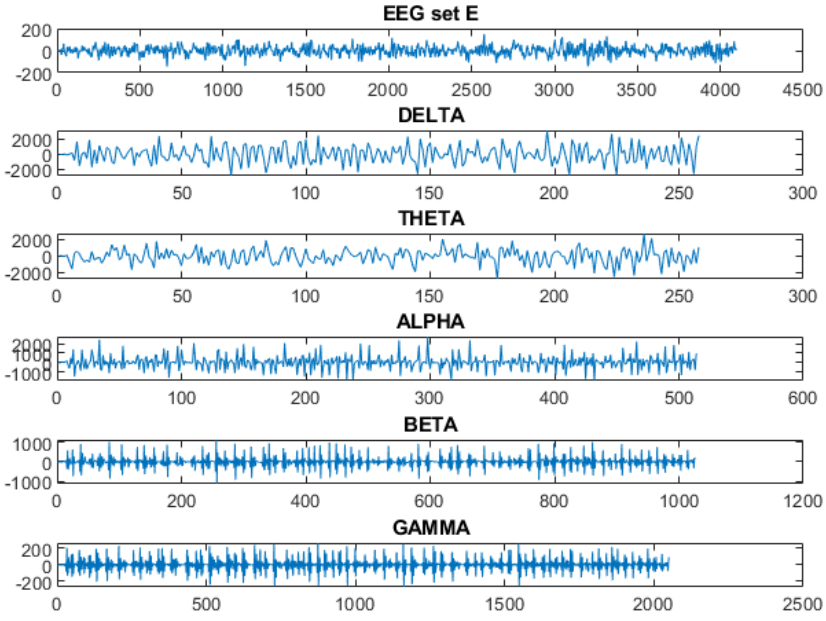

Figure 3.3 : Discrete wavelet transform of EEG set E.

each set with the PSD at each frequency subband. With this comparison, we determined the differences between healthy, pre-seizure, and epileptic EEG patterns.

In the frontocentral head regions, physiologically, the rhythm seen in deep sleep is the delta rhythm. In the case of generalized encephalopathy and focal cerebral dysfunction, the pathological delta rhythm occurs in awake states. People with temporal lobe epilepsy have temporal intermittent rhythmic delta activity (TIRDA). In the awake state focal theta activity, is an expression of focal cerebral dysfunction. In normal awake EEG recordings, there is a characteristic posterior dominant alpha rhythm in the occipital head region. This rhythm is a feature of the normal background rhythm of adult EEG recording. It is known that in normal adults and children, the beta rhythm is the most common rhythm [70].

Table 3.1 Frequency values and maximum PSD of each channel of five patients in set E (• delta • theta • alpha • beta • max(PSD)).

			Patient-1	Patient-2	Patient-3	Patient-4	Patient-5
Channels	Fp1	Frequency value in maximum power (Hz)/ Maximum PSD $(V^2/Hz)(\times 10^4)$	3.6/11.2	2.62/1.0	1.99/18.5	13.3/9.3	2.75/29.1
	Fp2		4.53/11.0	4.23/1.6	6.65/15.4	5.5/6.2	5.5/18.3
	F3		3.6/5.9	2.58/3.5	4.78/2.6	6.1/2.4	6.61/0.7
	F4		6.65/3.8	4.7/3.7	4.49/29.1	6.05/0.7	1.56/2.1
	C3		5.16/11.5	2.58/15.1	1.56/5.0	3.47/18.0	14.95/7.8
	C4		6.10/4.3	6.35/2.1	4.49/11.1	5.12/6.3	8.17/1.4
	P3		0.76/4.3	14.19/14.6	16.27/15.4	5.0/37.6	5.16/17.2
	P4		6.65/51.2	4.49/38.6	4.49/12.4	9.83/13.4	6.1/6.5
	O1		5.5/12.3	1.69/3.3	12.28/10.3	1.39/5.9	1.69/4.2
	O2		16.27/17.3	12.28/9.4	6.48/8.5	6.35/10.0	14.11/2.3
	F7		5.72/4.9	6.65/9.5	2.45/0.7	1.56/2.3	5.25/16.1
	F8		4.78/51.5	2.2/0.8	4.25/2.8	6.65/13.8	3.43/5.0
	T3		5.93/20.9	5.16/16.3	1.99/4.5	3.6/8.2	2.03/38.1
	T4		2.45/0.9	5.16/7.0	13.34/5.4	1.01/1.3	6.65/12.2
	T5		1.01/5.9	14.19/17.7	4.78/4.1	6.1/8.8	6.65/5.7
	T6		1.31/1.3	6.1/7.9	2.2/1.3	14.36/10.9	6.1/1.5
	Fz		4.53/23.3	1.94/15.6	6.65/10.4	11.77/0.6	6.65/48.0
	Cz		1.77/2.4	1.69/1.6	3.43/10.25	10.08/0.8	6.65/12.4
	Pz		3.6/18.3	5.65/1.9	4.49/51.7	5.29/25.8	9.57/9.8
	FCz		6.65/6.8	1.69/5.5	2.03/37.3	6.65/55.1	5.8/4.5

This information forms the basis of our study. When the frequency subbands with maximum power are examined, it has been determined that the majority of the channels that make up the signals in the E set are in the delta and theta subbands.

Also, a small part of the maximum power is in the alpha and beta subbands.

As given in Section 2.1, set E included only seizure activity. Therefore, since the E set includes delta and theta rhythms, our results are supported by this information. Table 3.1 contains the maximum power calculated from the EEG signals of all channels of the five patients in the E set and the frequency values with the maximum power.

Table 3.2 : The percentage ratio of the number of frequencies in each subband of the set E to all frequencies in the total subband at maximum PSD.

		Alpha (%)	Beta (%)	Delta (%)	Theta (%)	Total (%) (Alpha-Beta)	Total (%) (Delta-Theta)
Patients	Patient-1	0.0	5.0	40.0	55.0	5.0	95.0
	Patient-2	5.0	10.0	40.0	45.0	15.0	85.0
	Patient-3	10.0	5.0	35.0	50.0	15.0	85.0
	Patient-4	20.0	5.0	25.0	50.0	25.0	75.0
	Patinet-5	10.0	10.0	25.0	55.0	20.0	80.0

In Table 3.2, the percentages of the number of subbands of these frequencies in each channel according to the total channels are given. For example, one examines Patient 1 it can be seen that 5% of the channels contain alpha and beta subbands, while 95% contain delta and theta subbands. In Table 3.2, it is observed that these signals were epileptic signals for all patients in the E set. Apart from that, when the increase in PSDs of the A, C, and E sets was checked (not given in Table form), healthy, pre-seizure, and seizure signals were distinguished from each other. We choose channels F4 and T3 due to the frequency subbands with maximum power including only the delta and theta subbands for all patients. Furthermore, when the increases in PSDs of the A, C, and E sets were examined, it is seen that healthy, pre-seizure, and seizure signals were distinguished from each other. The PSDs of the F4, T3, and P3 channels of the first and second individuals at these sets used in Figure 3.4, Figure 3.5, and Figure 3.6 are plotted. As can be seen from these figures; the PSD of the epileptic signal is higher than the PSD of the pre-seizure signal, and the PSD of the pre-seizure signal is higher than the PSD of the healthy signal. In particular, the PSD of the epileptic signal is considerably higher than the

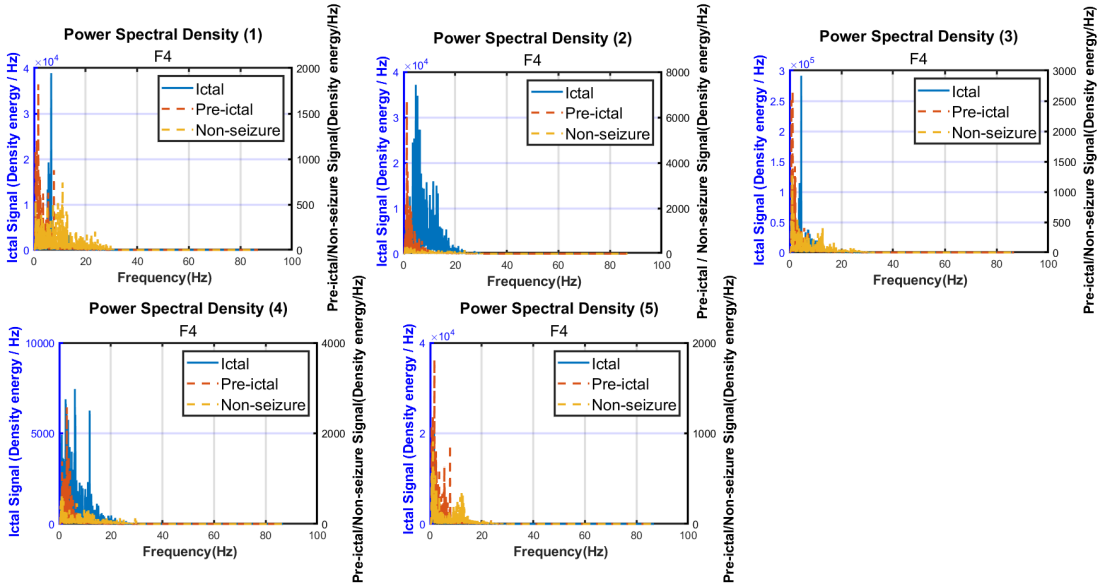

Figure 3.4 : PSDs of the signals of the F4 channel of all individuals (healthy and patient) of the sets A, C, E.

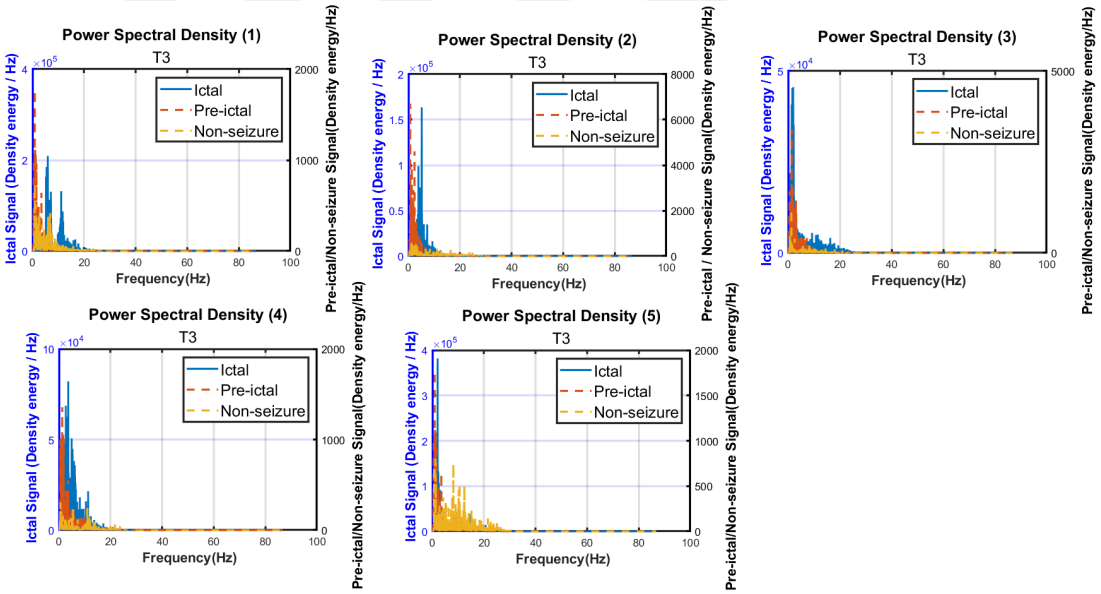

Figure 3.5 : PSDs of the signals of the T3 channel of all individuals (healthy and patient) of the sets A, C, E.

PSD of the healthy signal, which allows the two signals to be distinguished from each other. Furthermore, the frequency of the healthy EEG signal is spread over a wider band than the pre-seizure and epileptic EEG signals.

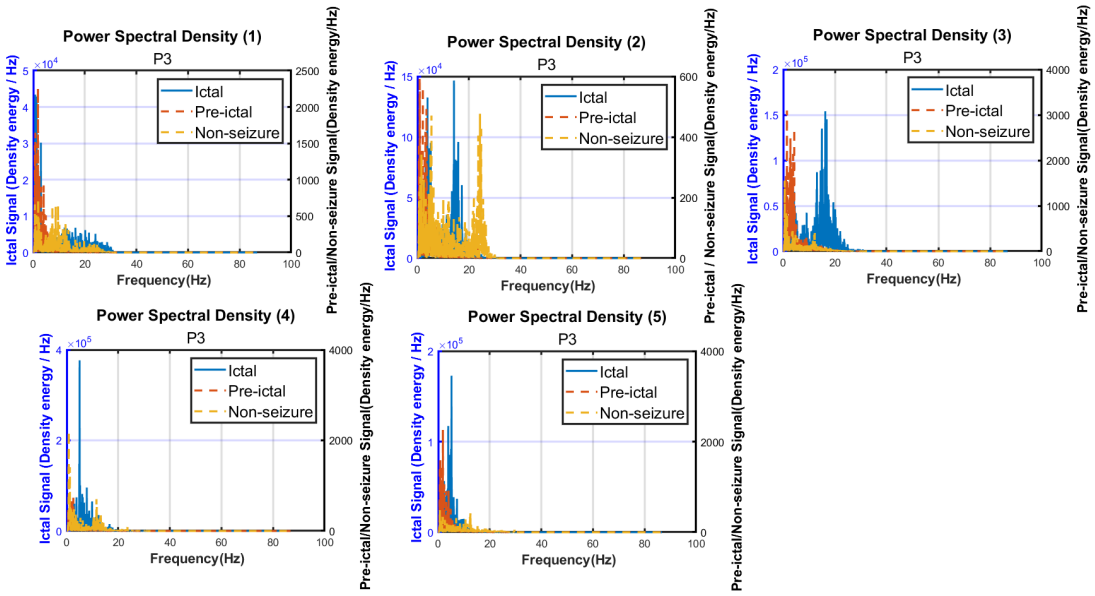

Figure 3.6 : PSDs of the signals of the P3 channel of all individuals (healthy and patient) of the sets A, C, E.

Moreover, to distinguish the ictal and pre-ictal signals from each other, we used another method as HFOs in the EEG signals. When the EEG signals of each channel of each patient in the E dataset were examined, ripples and fast ripples were detected. A band-pass filter was first applied to the EEG signals using a sampling rate of 2 kHz to detect these ripples.

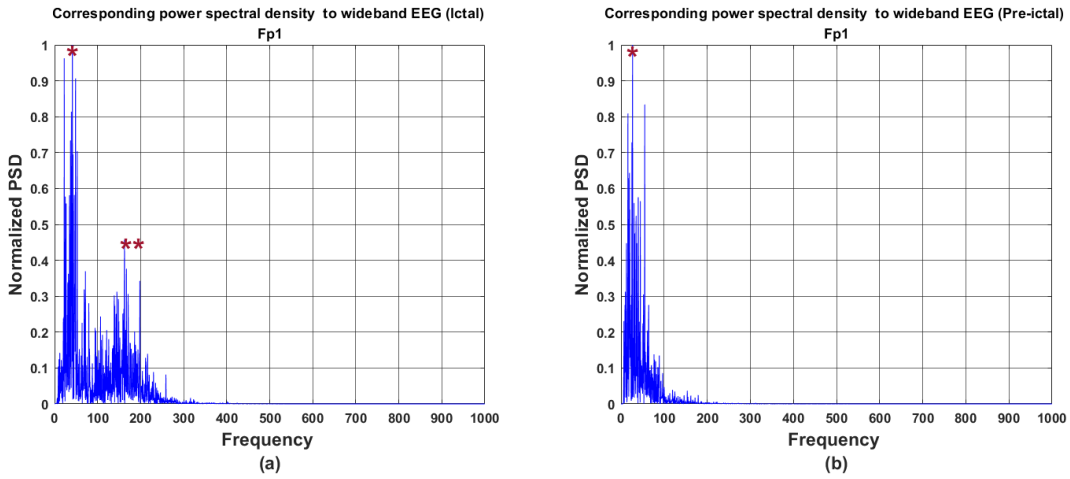

Figure 3.7 : Corresponding power spectral density to wideband ictal and pre-ictal EEG signal (Fp1 channel-Patient/1).

As a result, signals with low-frequency components were eliminated and only signals with high-frequency (80-500 Hz) components remained. The increasing

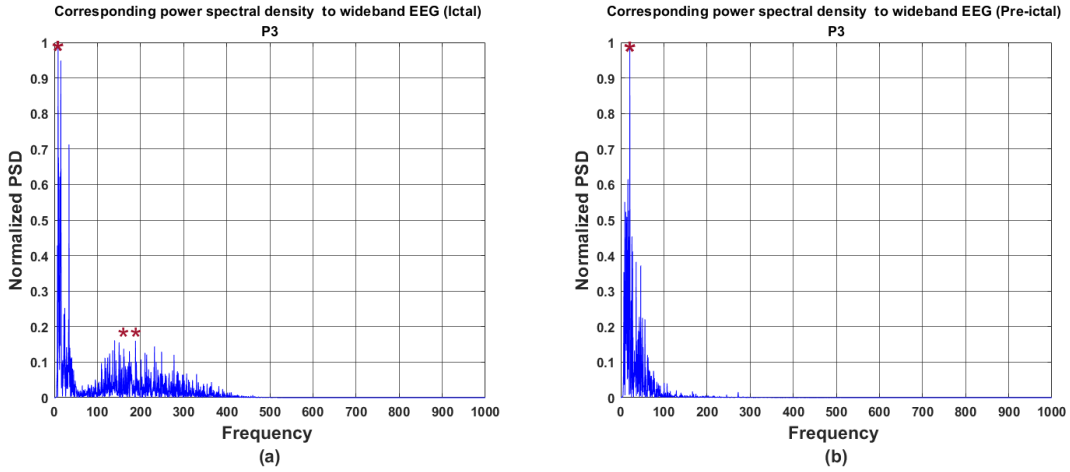

Figure 3.8 : Corresponding power spectral density to wideband ictal and pre-ictal EEG signal (P3 channel-Patient/1).

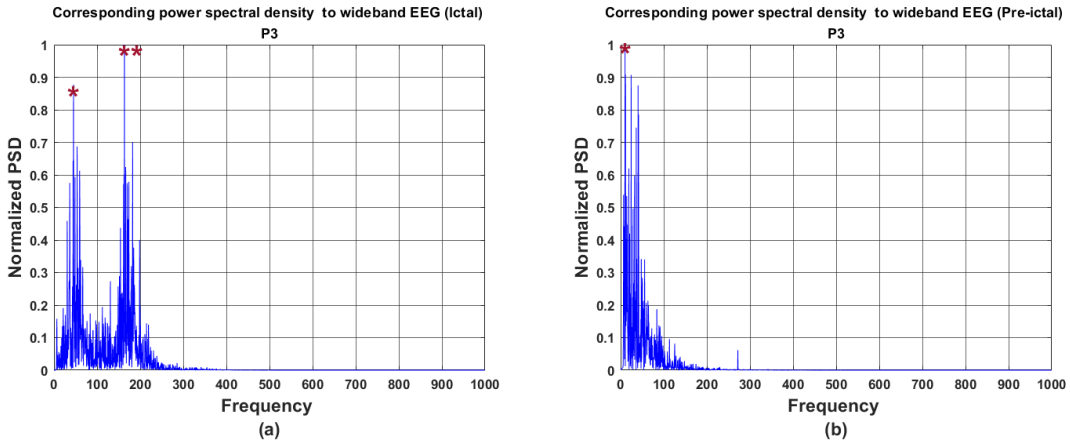

Figure 3.9 : Corresponding power spectral density to wideband ictal and pre-ictal EEG signal (P3 channel-Patient/2).

PSD of ripples and fast ripples was then calculated. Finally, the labeling process was carried out by the normalization process.

We detected low-frequency ripples followed by much higher-frequency ripples in 75%, 75%, 65%, 85%, and 75% of the channels of the five patients, respectively. Figures 3.7a, 3.7b, 3.8a and 3.8b show the graphs obtained by using broadband EEG segments representing HFOs in power spectral analysis using the criteria described in the methods (see Section 2.4.2). Figure 3.7a and 3.8a show how the HFO starts out as a low-frequency swing (indicated as *) that turns into a much higher-frequency swing (indicated as **). In Figure 3.7b and 3.8b, however, a much higher frequency ripple is not seen following the low-frequency ripple. This fact proves to us

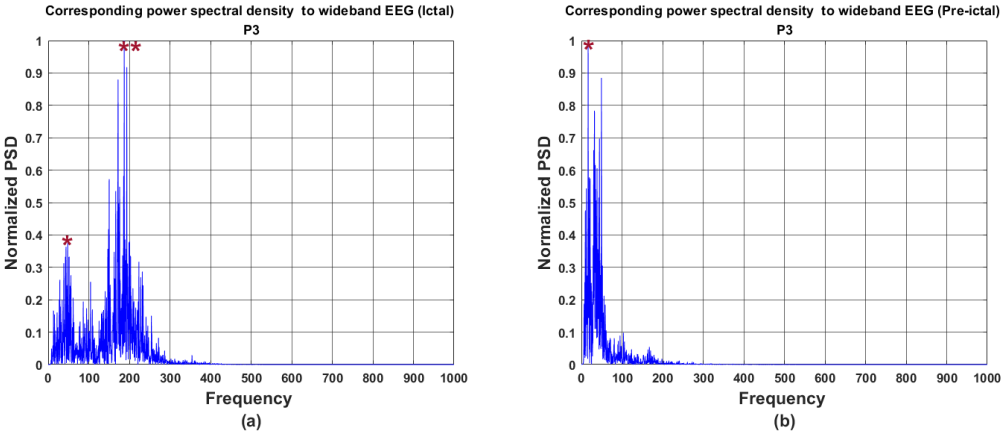

Figure 3.10 : Corresponding power spectral density to wideband ictal and pre-ictal EEG signal (P3 channel-Patient/3).

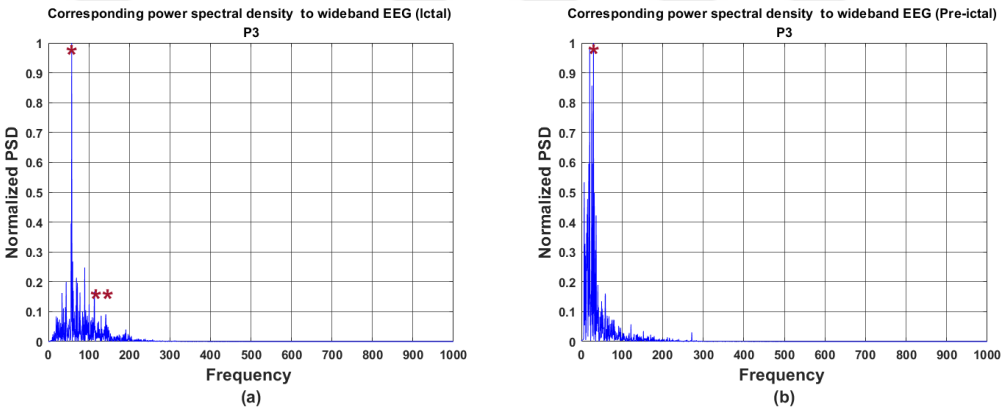

Figure 3.11 : Corresponding power spectral density to wideband ictal and pre-ictal EEG signal (P3 channel-Patient/4).

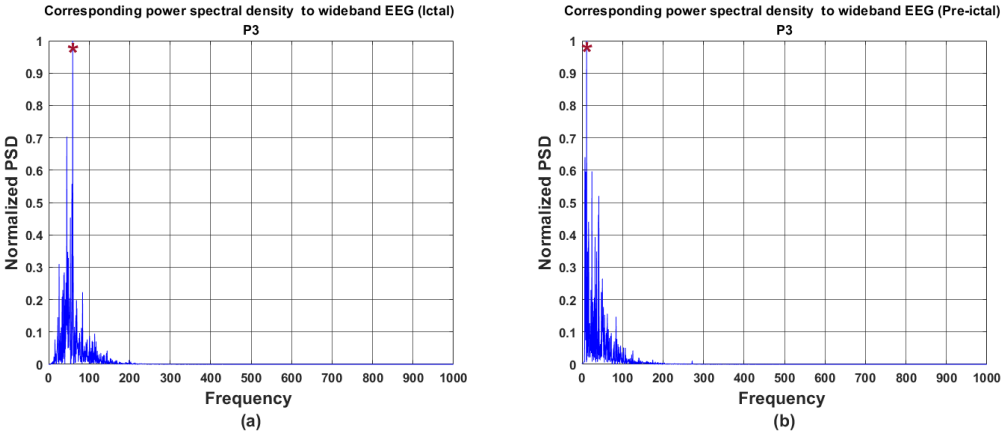

Figure 3.12 : Corresponding power spectral density to wideband ictal and pre-ictal EEG signal (P3 channel-Patient/5).

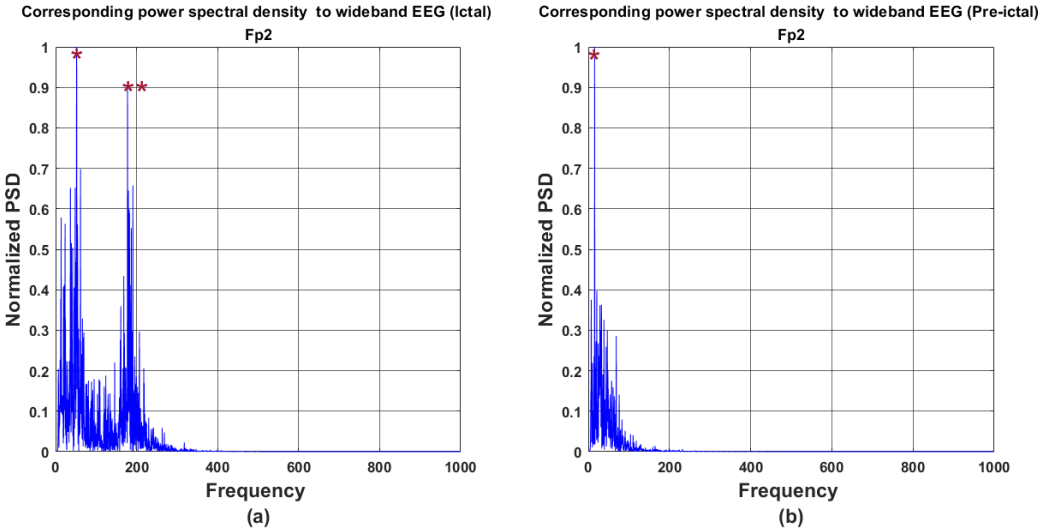

Figure 3.13 : Corresponding power spectral density to wideband ictal and pre-ictal EEG signal (Fp2 channel-Patient/1).

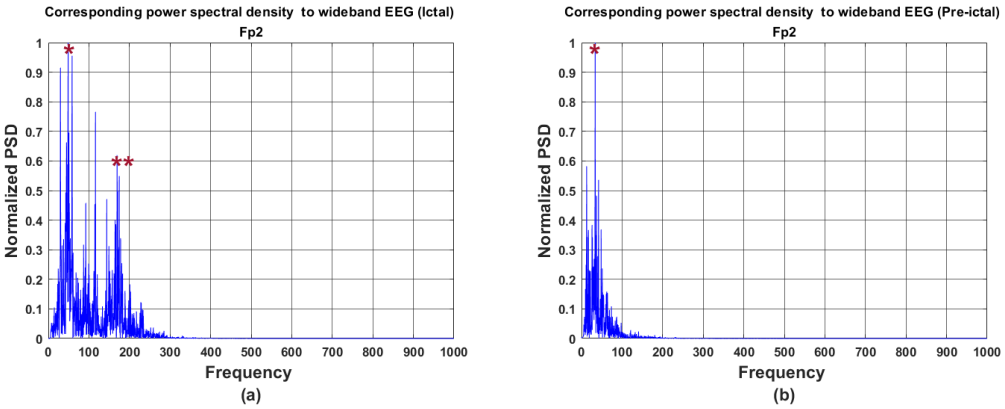

Figure 3.14 : Corresponding power spectral density to wideband ictal and pre-ictal EEG signal (Fp2 channel-Patient/2).

that Figure 3.7a and 3.8a contain the epileptic patterns. When the amplitude ratios between the pre-ictal and ictal signals are examined, the P3 channel was added because it is the common channel with an 80% amplitude increase. We also choose the Fp1 channel randomly. Figures 3.9, 3.10, 3.11 and 3.12 show corresponding power spectral density to wideband ictal and pre-ictal EEG signals in other patients' P3 channels. In Figures 3.12 much higher frequency ripple is not seen following the low-frequency ripple for the ictal data. Figures 3.13, 3.14, 3.15, 3.16 and 3.17 show corresponding power spectral density to wideband ictal and pre-ictal EEG signals in other patients' Fp2 channels. As seen in all these figures, HFO starts out

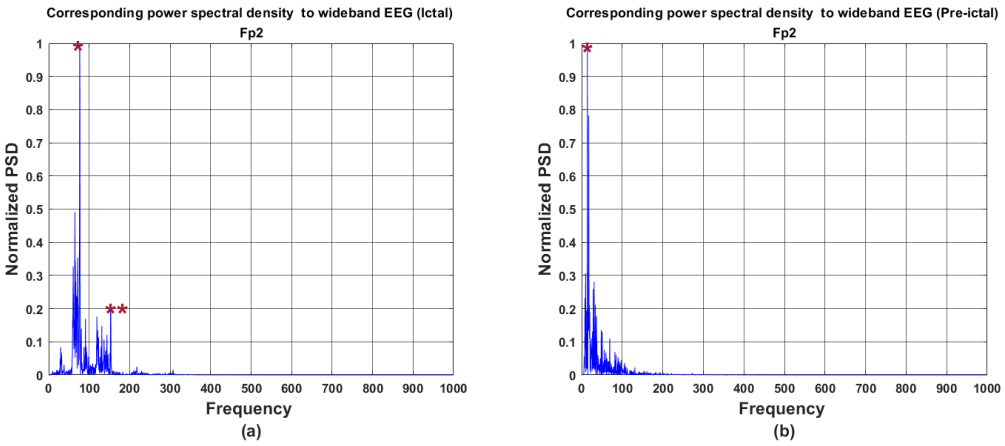

Figure 3.15 : Corresponding power spectral density to wideband ictal and pre-ictal EEG signal (Fp2 channel-Patient/3).

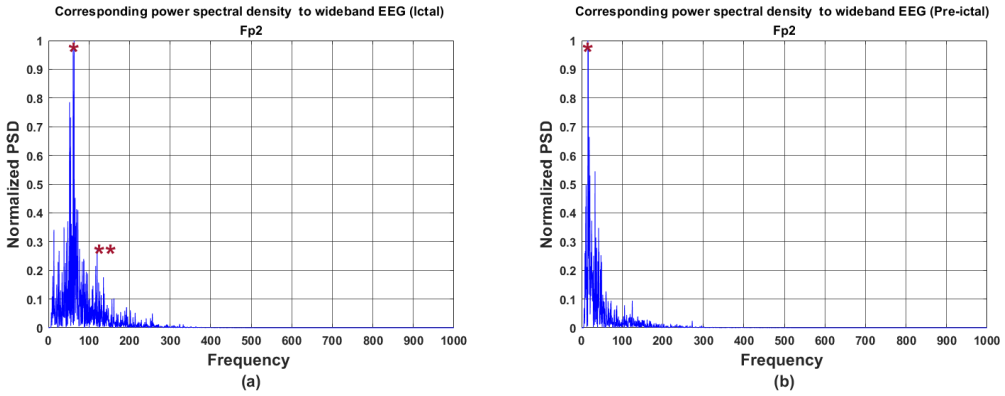

Figure 3.16 : Corresponding power spectral density to wideband ictal and pre-ictal EEG signal (Fp2 channel-Patient/4).

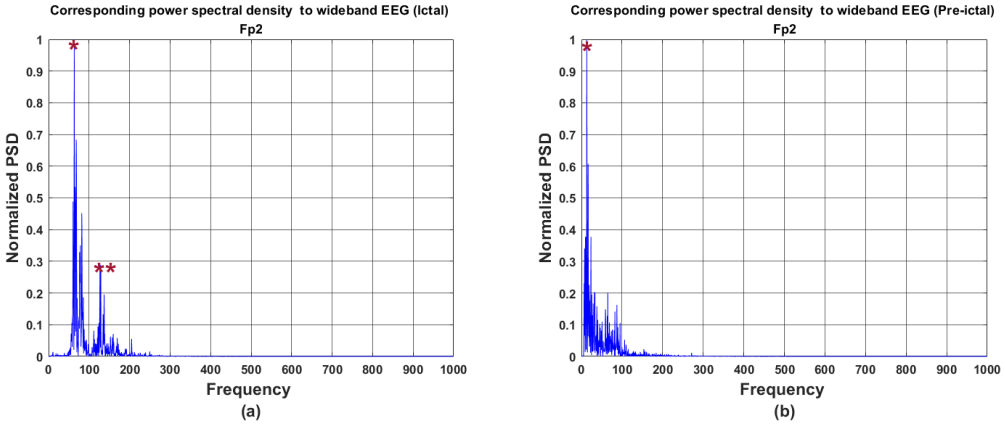

Figure 3.17 : Corresponding power spectral density to wideband ictal and pre-ictal EEG signal (Fp2 channel-Patient/5).

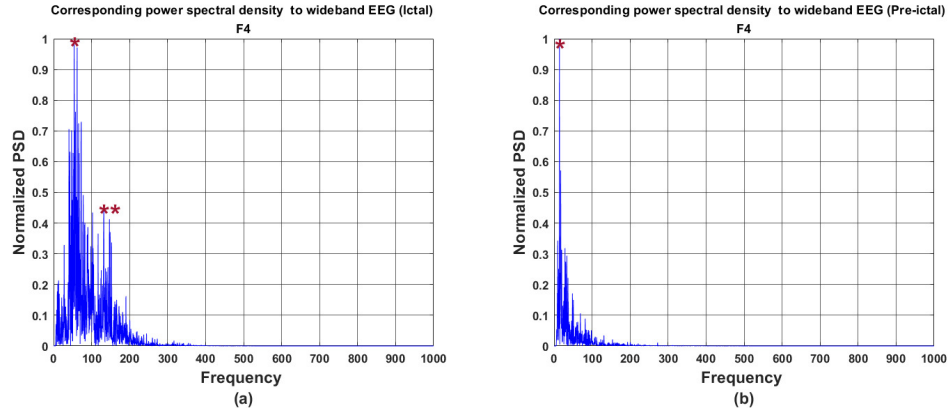

Figure 3.18 : Corresponding power spectral density to wideband ictal and pre-ictal EEG signal (F4 channel)

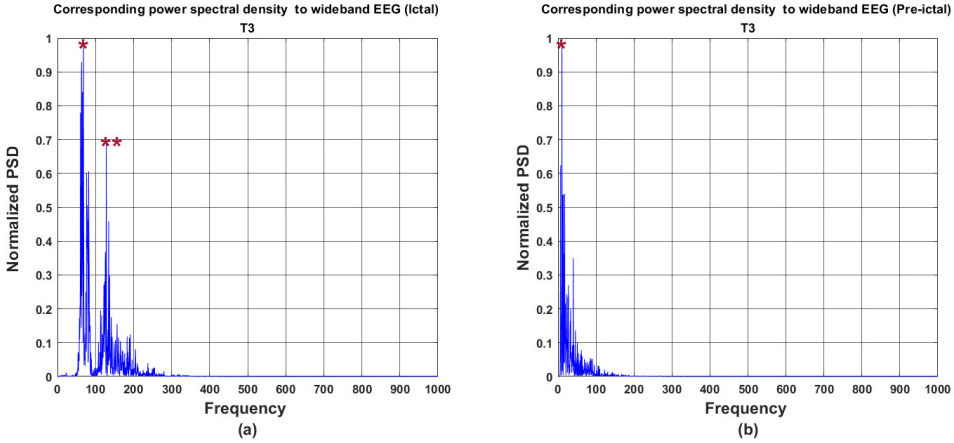

Figure 3.19 : Corresponding power spectral density to wideband ictal and pre-ictal EEG signal (T3 channel).

as a low-frequency swing (indicated as *) that turns into a much higher-frequency swing (indicated as **). The maximum power of F4 and T3 channels for all patients included only delta and theta subbands. In addition, HFOs are detected in the F4 (seen 3.18) channel of four patients and in the T3 (seen 3.19) channel of all patients. Patient 1 in Figure 3.20 and 3.21, patient 2 in Figure 3.22 and 3.23, patient 3 in Figure 3.24 and 3.25, patient 4 in Figure 3.26 and 3.27, and patient 5 in Figure 3.28 and 3.29 there are wideband normalized incremental power graphs of ictal and pre-ictal data for all channels of.

Frequency above 80 Hz was common in the Fp2, C4, P4, O2, and Pz channels in five patients. Table 3.3 shows the ripples and fast ripples found in these channels of five patients. In Fp2 and C4, ripples were present for all five patients, while in P4

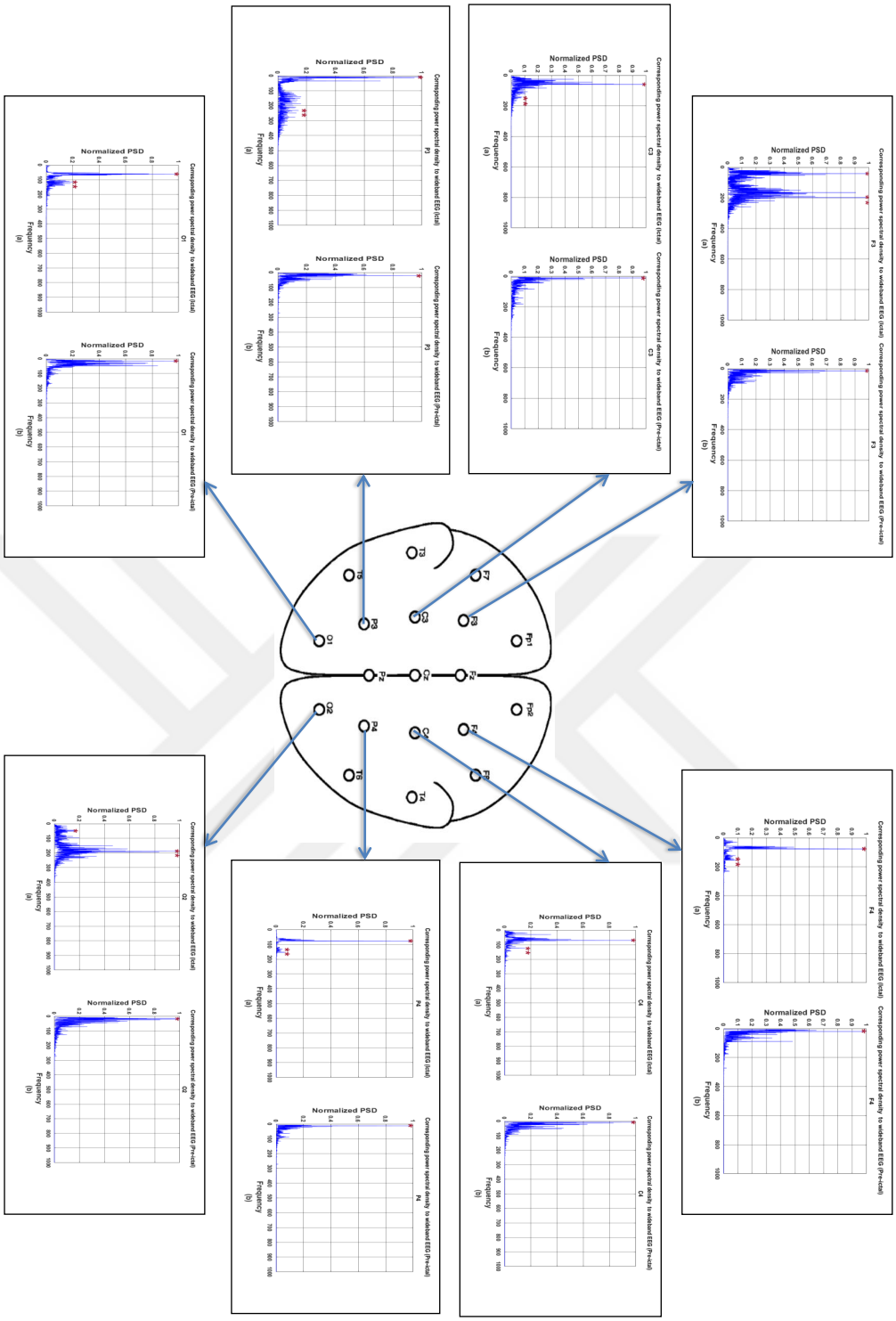

Figure 3.20 : Corresponding power spectral density to wideband ictal and pre-ictal EEG signal (some channel-Patient/1).

ripples were detected for four patients and fast ripples for one patient. Ripples in the O2 channel were detected for two patients, and fast ripples for three patients.

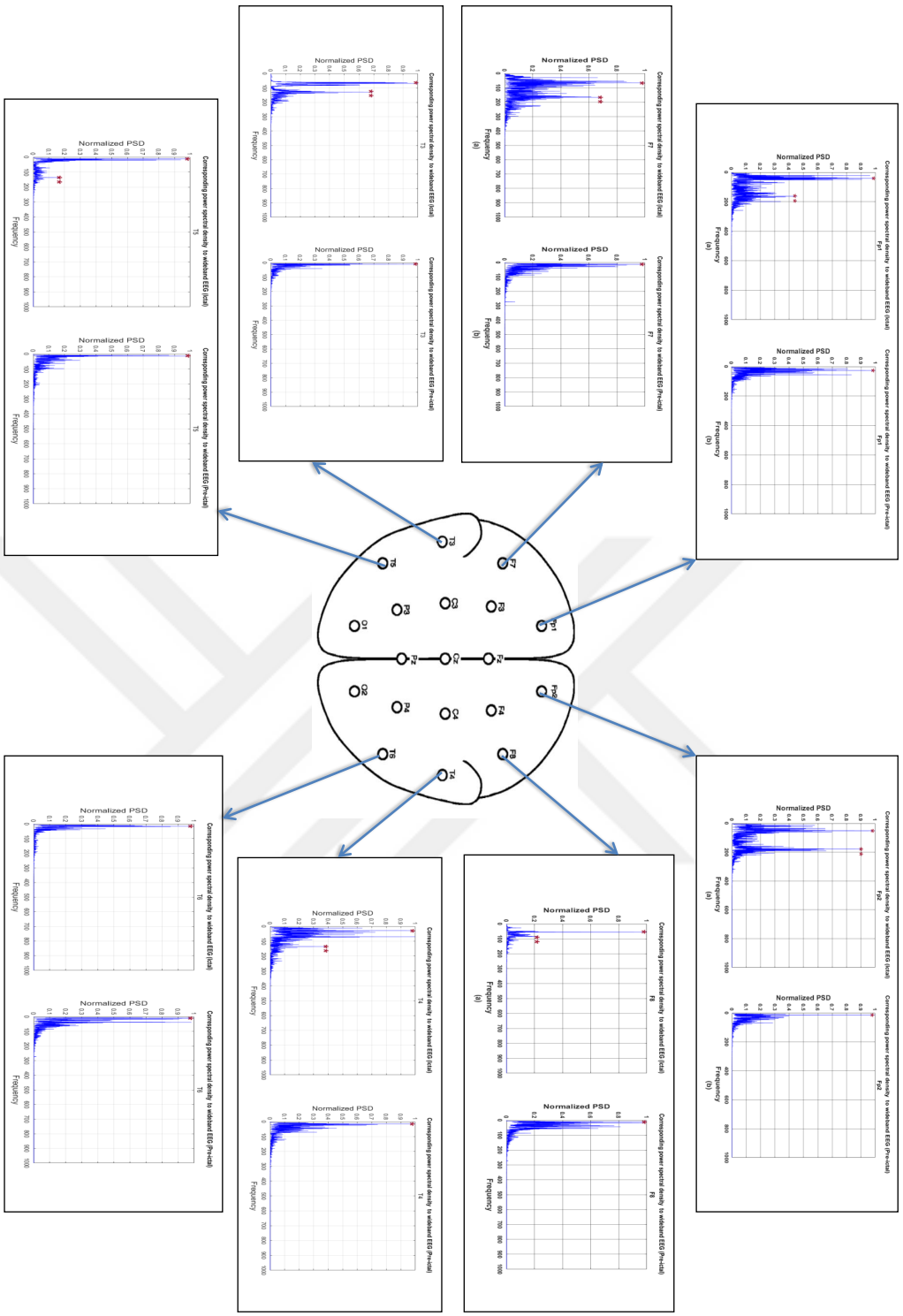

Figure 3.21 : Corresponding power spectral density to wideband ictal and pre-ictal EEG signal (some channel-Patient/1).

Ripples in the Pz channel were detected in five patients. In other channels, ripples and fast ripples were detected, but they are not common for all patients. The frequencies of the A and C data sets were generally found below 80 Hz. Thus, with

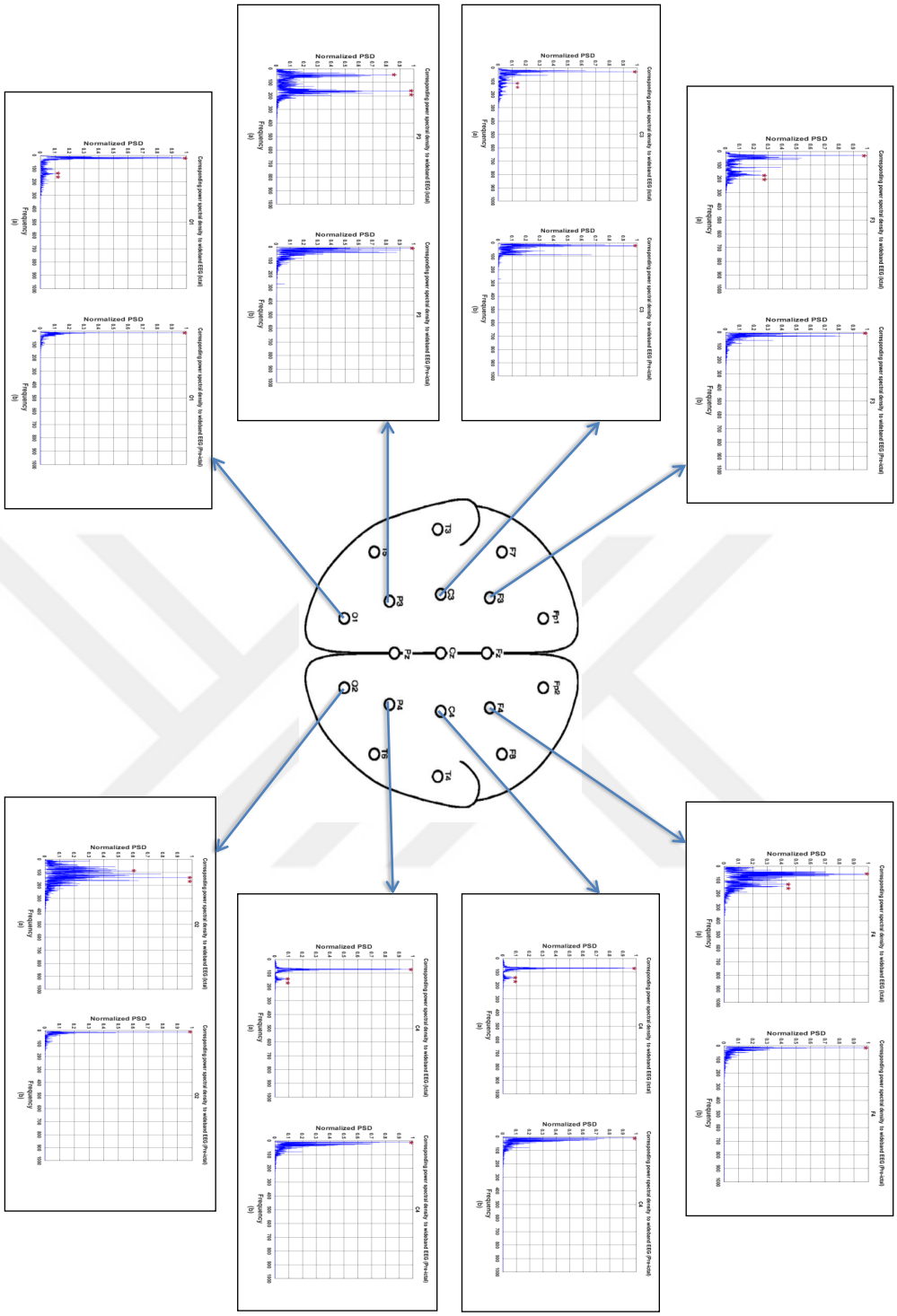

Figure 3.22 : Corresponding power spectral density to wideband ictal and pre-ictal EEG signal (some channel-Patient/2).

this method, these data sets were distinguished from each other.

In addition, we calculated the ratios of the frequency values between the reference electrode and all channels of these five patients' data in order to examine

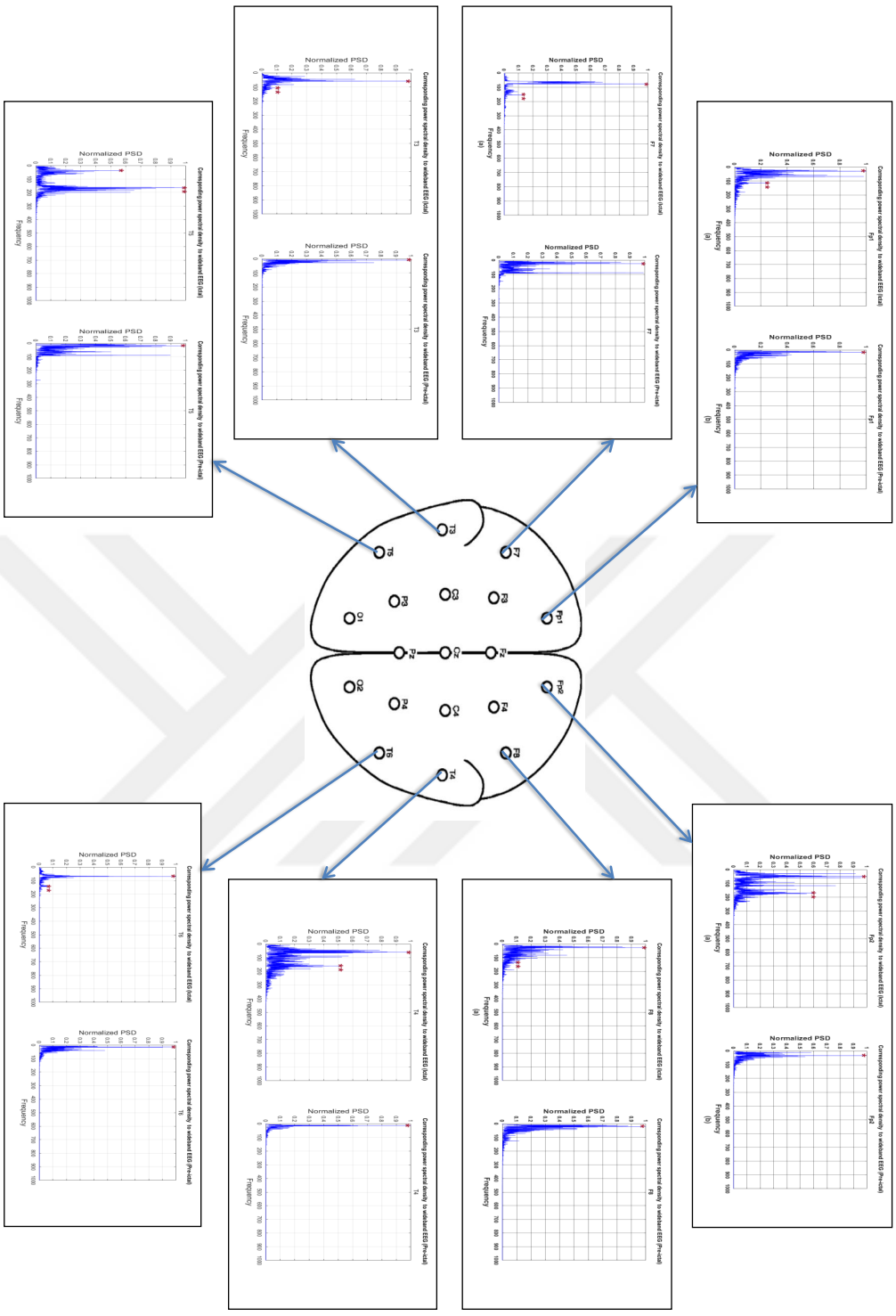

Figure 3.23 : Corresponding power spectral density to wideband ictal and pre-ictal EEG signal (some channel-Patient/2).

the frequency change between pre-ictal and ictal data. As it is aforementioned in Section 2.4.2, HFOs increase during the transition from a seizure-free period to a seizure. As can be seen from Table 3.4, large frequency variations are observed

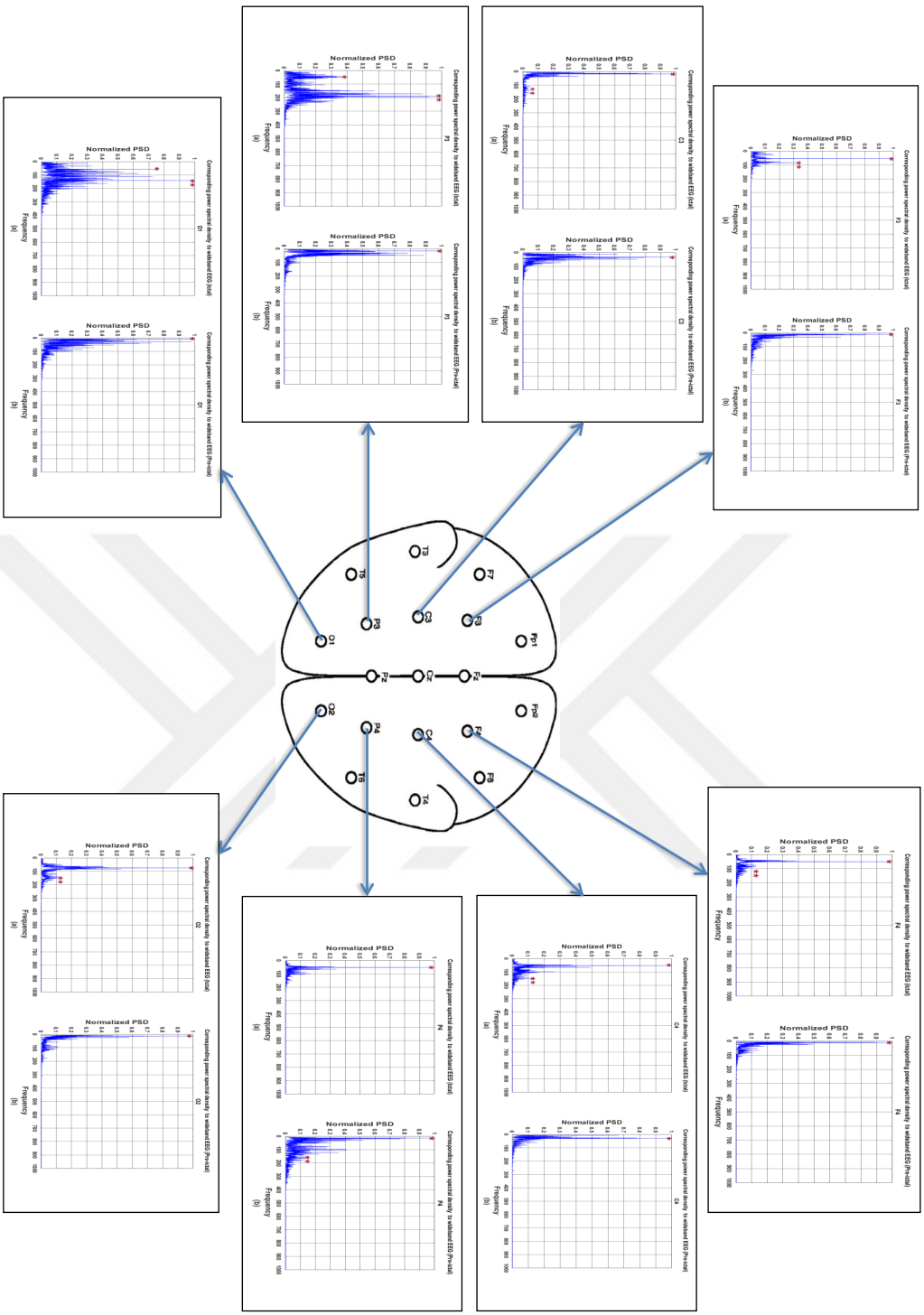

Figure 3.24 : Corresponding power spectral density to wideband ictal and pre-ictal EEG signal (some channel-Patient/3).

between the epileptic signal and the pre-seizure signals. Thus, these frequency changes, which are usually observed as increases, indicate that there is a pathological difference between the two signals. Thus, epileptic patterns can be detected

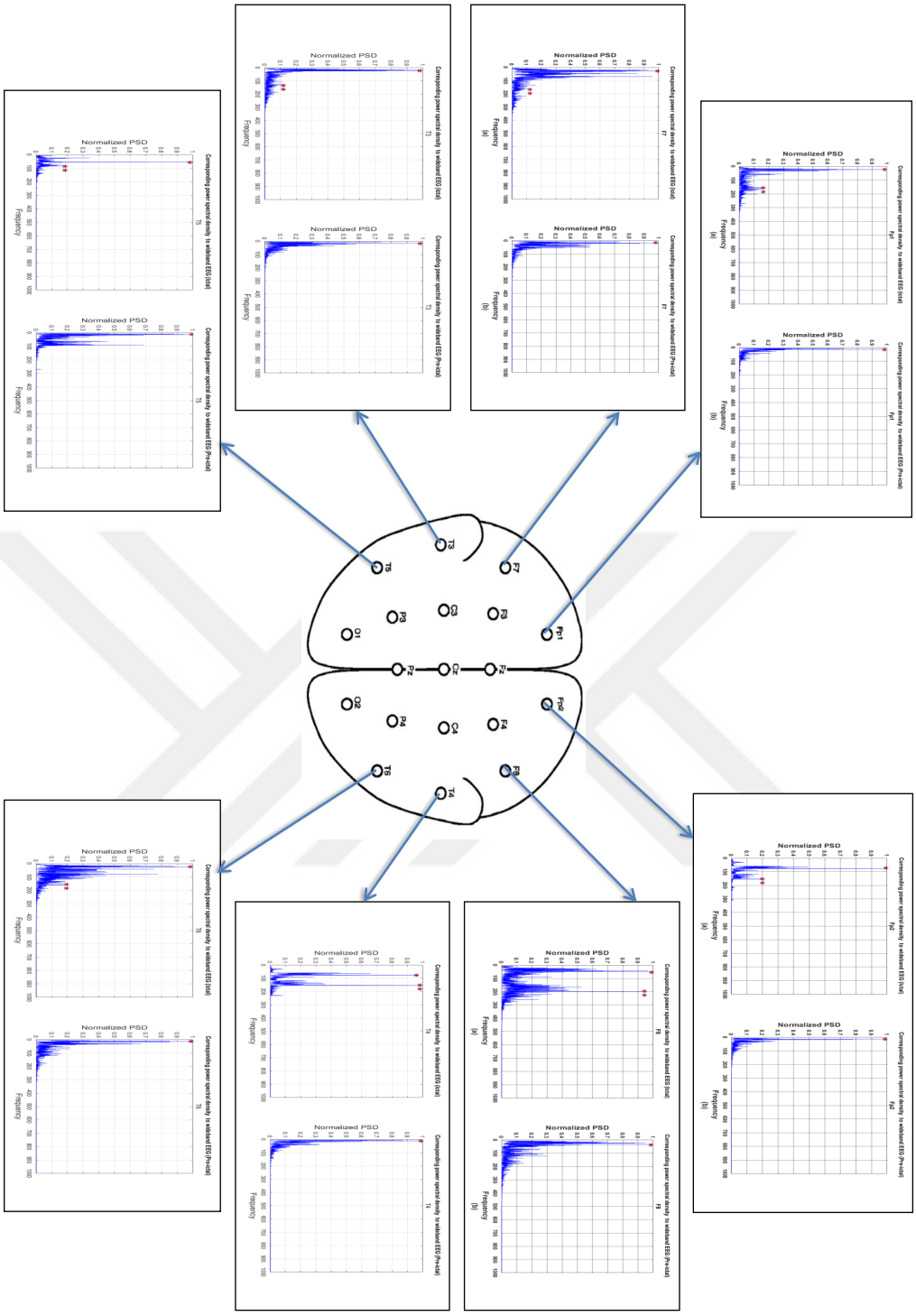

Figure 3.25 : Corresponding power spectral density to wideband ictal and pre-ictal EEG signal (some channel-Patient/3).

with these rates, although not as much as other methods (PSD and HFO). The P3 channel, highlighted in this table, is the common channel with an 80% amplitude increase when the amplitude ratios between the pre-ictal and ictal signals are exam-

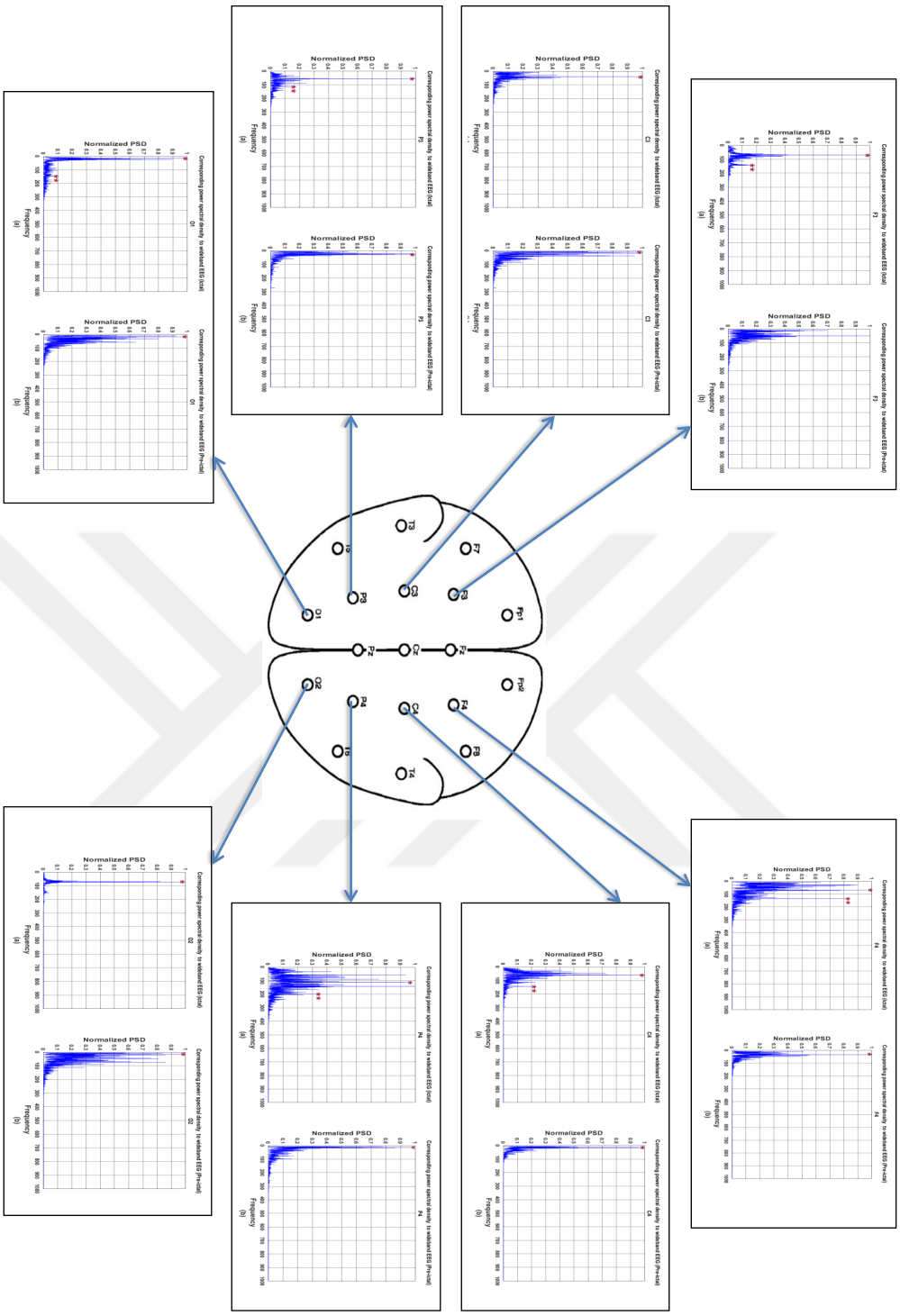

Figure 3.26 : Corresponding power spectral density to wideband ictal and pre-ictal EEG signal (some channel-Patient/4).

ined. As seen in Table 3.4, in this channel, the frequency rates for five patients are 80% and above. This result can be used in channel selection studies.

Our second dataset consists of the database collected at Boston Children's Hos-

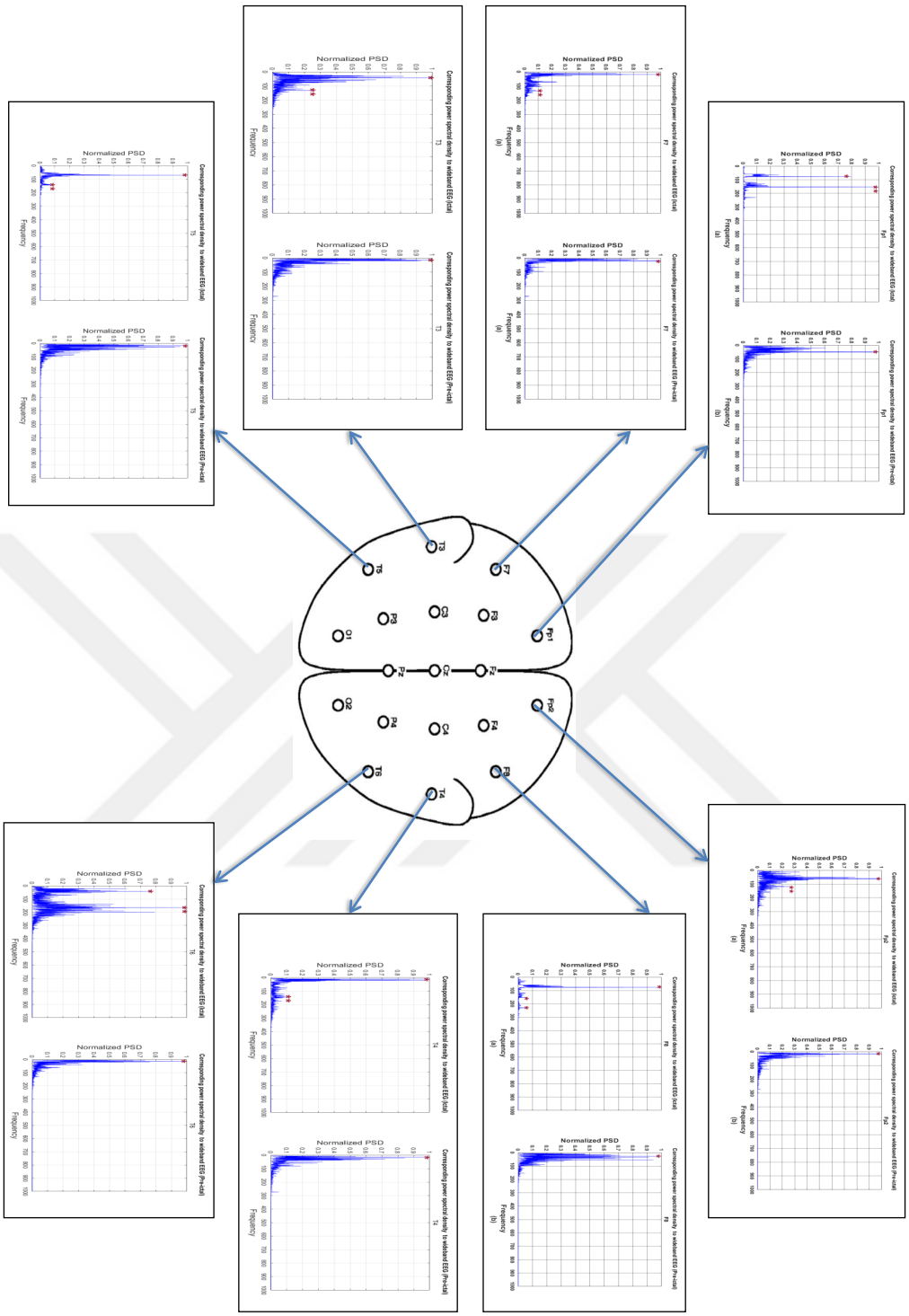

Figure 3.27 : Corresponding power spectral density to wideband ictal and pre-ictal EEG signal (some channel-Patient/4).

pital. The methods used for the first data set were applied to this data set. However, in this part, pre-seizure differences in EEG signals were also given. In this data set, which includes a total of 24 patients, it is known in which time interval the signals

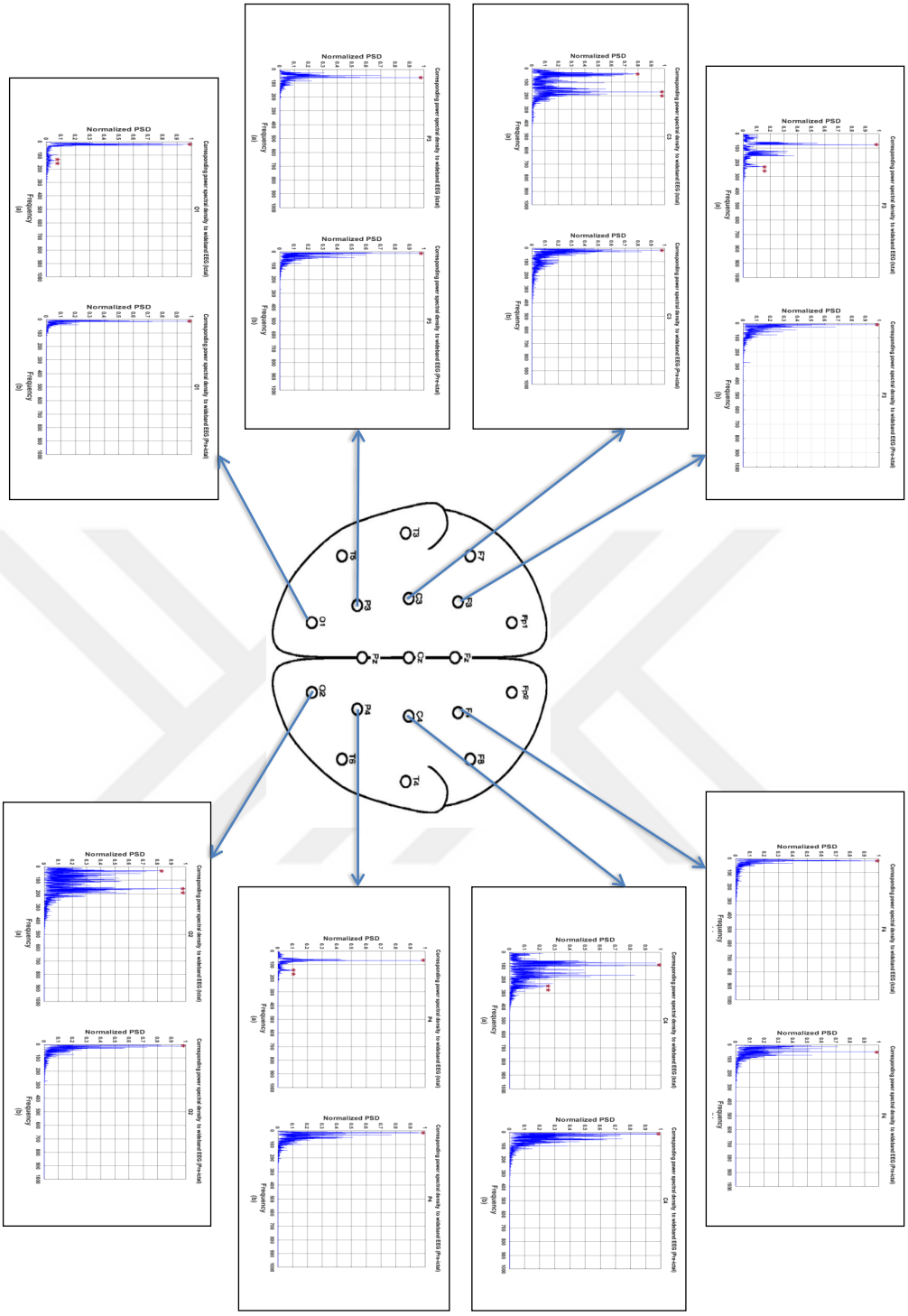

Figure 3.28 : Corresponding power spectral density to wideband ictal and pre-ictal EEG signal (some channel-Patient/5).

contain seizures. However, during the study, this situation was ignored and studies were carried out, and then the information on the seizures given was examined and the results were checked to see if they were correct. After passing the prepro-

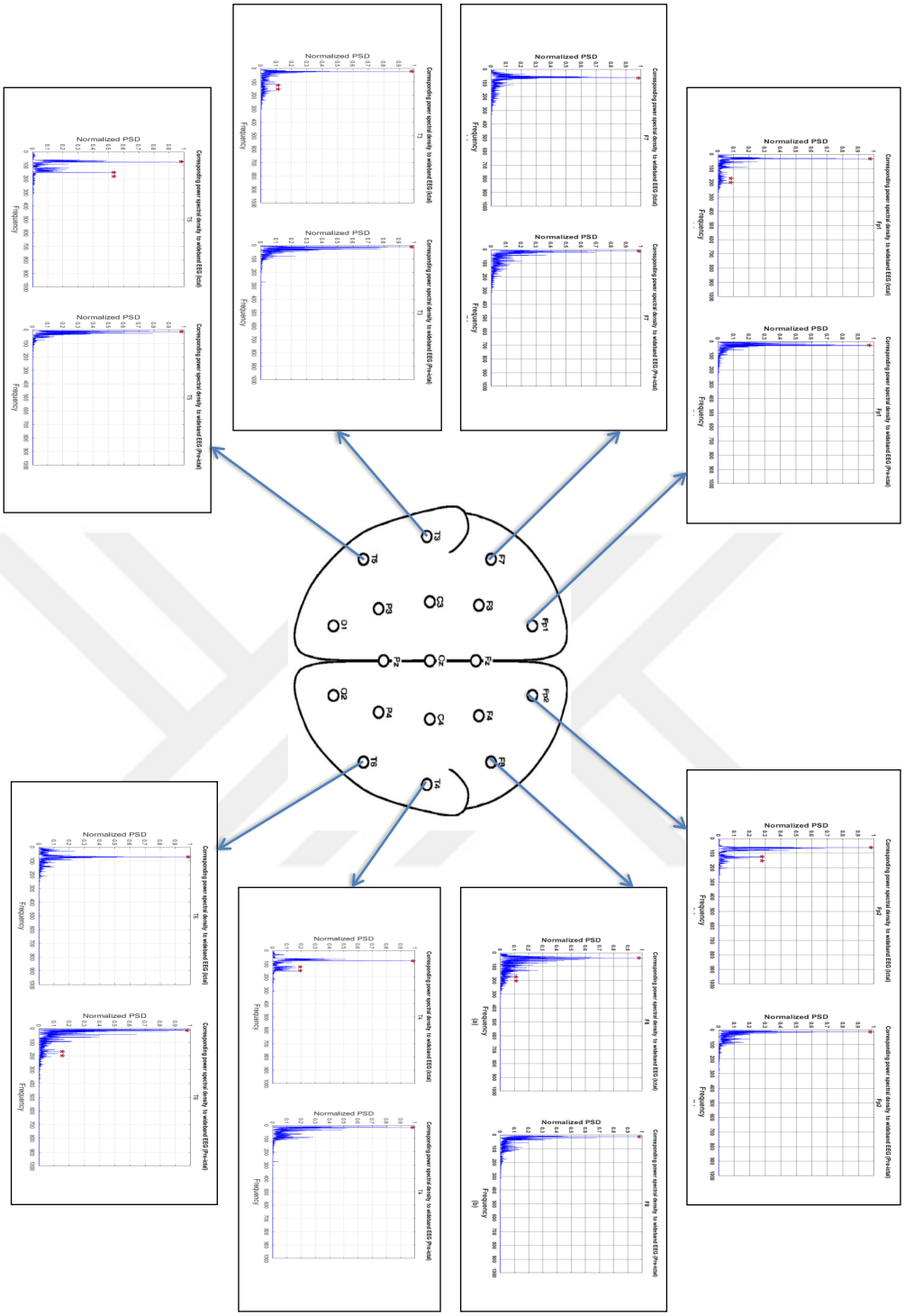

Figure 3.29 : Corresponding power spectral density to wideband ictal and pre-ictal EEG signal (some channel-Patient/5).

cessing step, the EEG signals from each channel of each patient were divided into pre-seizure and seizure moments. Then, their PSDs were examined, and results similar to those obtained from the first data set were obtained. In other words, it

Table 3.3 : Ripples(R) and fast ripples(FRs) in Fp2, C4,P4,O2 and Pz channels for all patients.

		Fp2	C4	P4	O2	Pz
Patients	Patient-1	R	R	R	FRs	R
	Patient-2	R	R	R	FRs	R
	Patient-3	R	R	R	R	R
	Patient-4	R	R	FRs	R	R
	Patinet-5	R	R	R	FRs	R

Table 3.4 : The ratios of the frequency values of the pre-ictal and ictal data between the reference electrode and all channels.

		Patient-1	Patient-2	Patient-3	Patient-4	Patient-5
Ref-Ch	Fp1	138.8	195.45	-1100	62.4	153.7
	Fp2	109.8	81.6	109.1	81.4	200
	F3	109.7	309.5	123.07	600	116.6
	F4	100	140.8	119.3	328.5	181.05
	C3	88.57	176.19	372.7	77.3	95.4
	C4	7.6	132.7	62.06	91.6	100
	P3	115.5	112.5	101.4	161.5	80
	P4	-100	104.5	124.1	106.7	0
	O1	125.9	-100	109.1	100	104.3
	O2	100.8	113.2	109.5	0	99.5
	F7	100	93.1	100	109.1	75
	F8	84.1	250	40.3	100	107.8
	T3	64.7	150	-600	90.2	96.4
	T4	114.2	135.3	105.9	95.4	64
	T5	100.7	106.4	112.3	76.9	76
	T6	96.03	127.8	350	103.8	75
	Fz	102	733.3	85.3	87.6	-4
	Cz	98.2	-100	145.4	100	-164
	Pz	116.6	129.05	77.5	190.6	95.7

was determined that the PSD of the seizure signal was much higher than the PSD of the pre-seizure signal. In addition, it has been determined that the PSD of the pre-seizure signal is in the wider frequency range, while the PSD of the seizure signal is in the narrower frequency range. Figure 3.30 for the FP1-F7 channel of the first patient (chb01), and Figure 3.31 for the T8-P8 channel of the second patient (chb02) show the PSDs of the signals. We chose these channels as an example among 23 channels.

Table 3.5 : Table including proportionality of maximum amplitude for preictal and ictal EEG frequency subbands (channels 1-5).

		Subbands(Hz)	P-1	P-2	P-3	P-4	P-5
Channels	Fp1	alpha:	0.81	-0.11	0.81	0.81	0.88
		beta:	0.80	0.5	0.94	0.39	0.93
		delta:	0.92	-2.1	0.99	0.83	0.96
		theta:	0.89	0.37	0.58	0.88	0.87
		gamma:	0.85	0.6	0.93	0.79	0.95
	Fp2	alpha:	0.76	0.32	0.59	0.84	0.32
		beta:	0.75	0.49	0.27	0.81	0.29
		delta:	0.96	0.75	0.89	:0.92	-0.13
		theta:	0.85	0.79	0.84	0.94	0.43
		gamma:	0.78	0.65	0.72	0.89	0.84
	F3	alpha:	0.43	0.81	-0.43	0.44	0.62
		beta:	0.74	0.85	0.12	0.64	0.57
		delta:	-1.52	0.97	-2.24	0.97	0.72
		theta:	0.18	0.83	0.36	0.49	0.17
		gamma:	0.87	0.86	0.48	0.33	0.74
	F4	alpha:	0.03	0.52	0.27	0.61	0.65
		beta:	0.52	0.15	0.67	0.49	0.67
		delta:	-0.06	0.27	0.96	0.88	0.97
		theta:	0.57	0.57	0.88	0.79	0.58
		gamma:	0.65	0.76	0.91	0.58	0.51
	C3	alpha:	-0.31	0.79	0.81	0.89	0.73
		beta:	0.23	0.88	0.77	0.89	0.67
		delta:	0.69	0.85	0.69	0.91	0.97
		theta:	0.47	0.72	0.73	0.75	0.92
		gamma:	0.71	0.85	0.68	0.87	0.87

Secondly, the sample and frequency subband, which includes the maximum power and maximum power of the signals, are examined. It has been determined that these samples obtained are within the sample range included in the seizure information. In addition, the maximum power calculation was made for each signal 1 (one) second before the start of the seizure and it was checked in which frequency subband it was. This process was done in one-second steps until 94 seconds ago. But after 94. seconds, 2-3-4-5, and 10 minutes ago (according to the length of the signals) are checked. We found that the maximum power during the seizure is mostly in the frequency ranges of the delta and theta subbands. However, although the duration varies in each patient before the seizure, we found that the frequencies

Table 3.6 : Table including proportionality of maximum amplitude for preictal and ictal EEG frequency subbands (channels 6-10).

		Subbands(Hz)	P-1	P-2	P-3	P-4	P-5
Channels	C4	alpha:	-0.58	0.07	0.81	-0.49	0.54
		beta:	0.35	0.28	0.74	0.57	0.49
		delta:	0.96	0.92	0.92	-0.02	0.94
		theta:	-0.04	0.9	0.83	-0.71	0.59
		gamma:	0.53	0.87	0.89	0.67	0.67
	P3	alpha:	0.82	0.89	0.73	0.85	0.77
		beta:	0.64	0.94	0.6	0.85	0.88
		delta:	0.21	0.96	0.99	0.99	0.87
		theta:	0.56	0.95	0.92	0.79	0.84
		gamma:	0.64	0.92	0.77	0.95	0.93
	P4	alpha:	0.25	0.83	0.39	0.73	0.53
		beta:	0.30	0.81	0.67	0.73	0.49
		delta:	0.94	0.98	-0.16	0.96	0.93
		theta:	0.74	0.81	0.78	0.95	0.92
		gamma:	0.88	0.97	0.81	0.75	0.8
	O1	alpha:	0.68	0.62	0.86	0.78	0.39
		beta:	0.12	0.69	0.77	0.8	0.71
		delta:	0.91	0.62	0.9	0.8	0.41
		theta:	0.87	0.87	0.89	0.89	0.35
		gamma:	0.72	0.63	0.81	0.65	0.44
	O2	alpha:	0.68	0.45	-0.7	0.038	0.75
		beta:	0.81	0.65	-1.09	-0.68	0.85
		delta:	0.99	0.95	0.98	0.99	-0.33
		theta:	0.94	0.87	0.66	0.59	0.72
		gamma:	0.83	0.89	0.63	g0.55	0.85

of the alpha and beta subbands were higher than the delta and theta subbands in 75% of the patients before a certain period of time. We aforementioned earlier that EEG signals of healthy individuals contain alpha and beta subbands, and delta and theta subbands are caused by pathological conditions and are a sign of disease. This situation shows us both the accuracy of the results we obtained and that we can use these results for pre-seizure prediction. In Figure 3.32 for patient 1 (chb01), Figure 3.33 for patient 15 (chb15), and in Figure 3.34 for patient 10 (chb10), the percentile sums of delta-theta subbands with the maximum power in the EEG signals, and alpha-beta subbands' percentile sums changes are shown for certain periods.

Table 3.7 : Table including proportionality of maximum amplitude for preictal and ictal EEG frequency subbands (channels 11-15).

		Subbands(Hz)	P-1	P-2	P-3	P-4	P-5
Channels	F7	alpha:	0.87	0.47	-0.002	0.34	-0.22
		beta:	0.81	0.53	0.49	0.58	0.5
		delta:	0.96	0.92	0.72	0.36	0.35
		theta:	0.89	0.87	0.56	-0.37	0.82
		gamma:	0.91	0.81	0.32	0.52	0.86
	F8	alpha:	0.63	0.16	-0.3	0.25	-0.09
		beta:	0.75	0.77	0.51	0.58	0.57
		delta:	0.96	0.95	0.96	-2.08	0.96
		theta:	0.84	0.53	0.71	0.45	0.46
		gamma:	0.86	0.53	0.7	0.54	0.72
	T7	alpha:	0.46	0.26	0.69	0.37	0.92
		beta:	0.2	0.61	0.78	0.84	0.93
		delta:	0.99	0.95	0.99	0.51	0.86
		theta:	0.68	0.51	0.74	0.86	0.81
		gamma:	0.87	0.85	0.51	0.89	0.94
	T8	alpha:	0.72	0.22	-0.95	0.82	0.56
		beta:	0.76	0.56	0.004	0.76	0.19
		delta:	0.98	0.98	0.93	-1.2	0.97
		theta:	0.88	0.74	0.25	0.75	0.89
		gamma:	0.66	0.84	0.76	0.72	0.77
	P7	alpha:	0.65	0.78	0.11	0.31	-0.26
		beta:	0.65	0.9	0.47	0.24	-0.56
		delta:	0.89	0.95	-0.17	0.75	0.67
		theta:	0.59	0.92	0.55	0.69	0.39
		gamma:	0.26	0.87	0.78	0.72	0.43

The percentage calculations here are obtained by dividing the number of channels in which the maximum power is in the delta and theta or alpha and beta subbands by the total number of channels.

Table 3.8 : Table including proportionality of maximum amplitude for preictal and ictal EEG frequency subbands (channels 16-20).

		Subbands(Hz)	P-1	P-2	P-3	P-4	P-5
Channels	P8	alpha:	0.7	-0.37	-0.54	0.59	-1.3
		beta:	0.62	0.07	0.58	0.84	-0.07
		delta:	0.95	-16.6	0.96	d0.71	0.83
		theta:	0.69	-3.44	0.59	0.31	-1.9
		gamma:	0.44	0.54	0.41	0.84	0.35
	Fz	alpha:	0.79	0.84	0.9	-0.19	0.9
		beta:	0.83	0.85	0.85	0.15	0.8
		delta:	0.97	0.98	0.94	-0.5	0.95
		theta:	0.94	0.77	0.96	-0.5	0.95
		gamma:	0.91	0.87	0.92	0.57	0.96
	Cz	alpha:	0.88	0.71	0.15	-1.92	0.7
		beta:	0.83	0.76	0.8	0.14	0.39
		delta:	0.17	0.96	0.76	-3.7	0.93
		theta:	0.77	0.62	-0.48	-0.43	0.93
		gamma:	0.53	0.7	0.84	0.56	0.72
	Pz	alpha:	0.41	-1.6	0.94	0.39	0.15
		beta:	0.77	-0.5	0.92	0.59	0.41
		delta:	0.7	0.41	0.97	0.79	0.98
		theta:	0.86	-0.3	0.9	0.79	0.78
		gamma:	0.85	0.3	0.96	0.83	0.76
	FCz	alpha:	-0.77	0.64	0.85	0.53	0.23
		beta:	-0.26	0.79	0.87	0.04	0.14
		delta:	-11.8	0.49	0.85	0.98	0.84
		theta:	-0.08	0.63	0.68	0.83	0.67
		gamma:	0.74	0.4	0.78	0.84	0.83

As can be seen in Figures 3.32, 3.33, delta and theta subbands were replaced by alpha and beta subbands at certain times before the seizure in patients 1 and 15. However, this was not the case with the 10th patient (Figure 3.34). All EEG signals of all patients were studied with this approach. While the claimed change was not observed in 25% of the patients, this change was observed in 75% of the patients.

Table 3.9 : Table including frequency values for ictal data .

		Patient-1	Patient-1	Patient-3	Patient-4	Patient-5
Channels	Fp1	85 Hz	62 Hz	47 Hz	314Hz	65 Hz
	Fp2	106 Hz	100 Hz	157 Hz	130 Hz	130 Hz
	F3	85 Hz	61 Hz	113 Hz	144 Hz	156 Hz
	F4	157 Hz	11 Hz	106 Hz	143 Hz	37 Hz
	C3	122 Hz	61 Hz	37 Hz	82 Hz	353 Hz
	C4	144 Hz	150 Hz	106 Hz	121 Hz	193 Hz
	P3	18 Hz	335 Hz	384 Hz	118 Hz	122 Hz
	P4	157 Hz	106 Hz	106 Hz	290 Hz	144 Hz
	O1	130 Hz	40 Hz	290 Hz	33 Hz	40 Hz
	O2	384 Hz	290 Hz	153 Hz	150 Hz	333 Hz
	F7	135 Hz	157 Hz	58 Hz	37 Hz	124 Hz
	F8	113 Hz	52 Hz	100 Hz	157 Hz	81 Hz
	T7	140 Hz	122 Hz	47 Hz	85 Hz	48 Hz
	T8	143 Hz	122 Hz	315 Hz	24 Hz	157 Hz
	P7	24 Hz	335 Hz	113 Hz	144 Hz	157 Hz
	P8	31 Hz	144 Hz	52 Hz	339 Hz	144 Hz
	Fz	107 Hz	46 Hz	157 Hz	278 Hz	157 Hz
	Cz	42 Hz	40 Hz	81 Hz	238 Hz	157 Hz
	Pz	85 Hz	157 Hz	106 Hz	125 Hz	226 Hz
	FCz	157 Hz	40 Hz	48 Hz	157 Hz	132 Hz

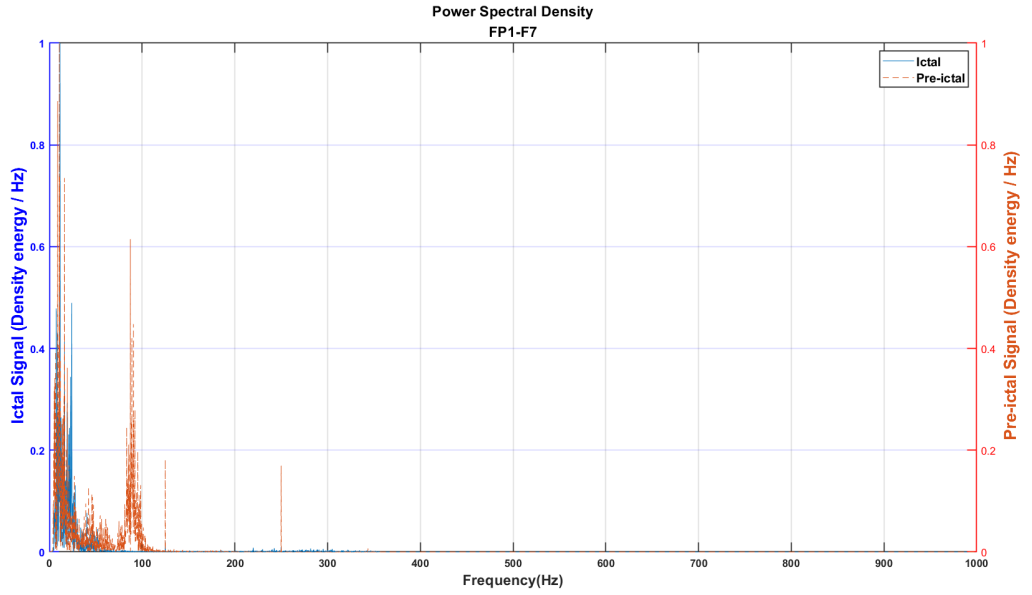

Figure 3.30 : Corresponding power spectral density to wideband ictal and pre-ictal EEG signal (FP1-F7 channel/ patient-chb01 (patient-1)).

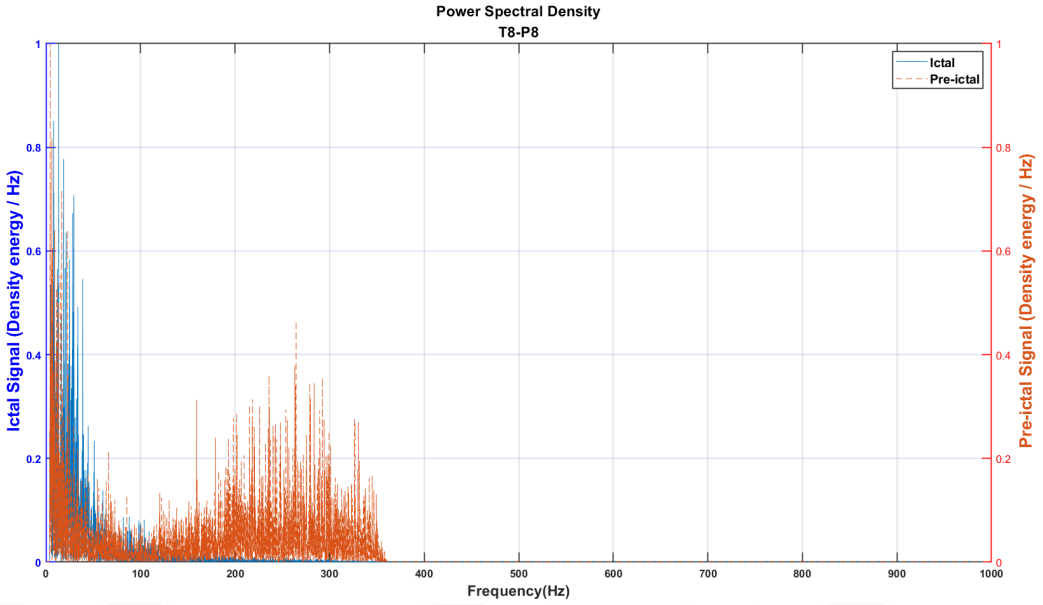

Figure 3.31 : Corresponding power spectral density to wideband ictal and pre-ictal EEG signal (T8-P8 channel/ patient-chb02 (patient-2)).

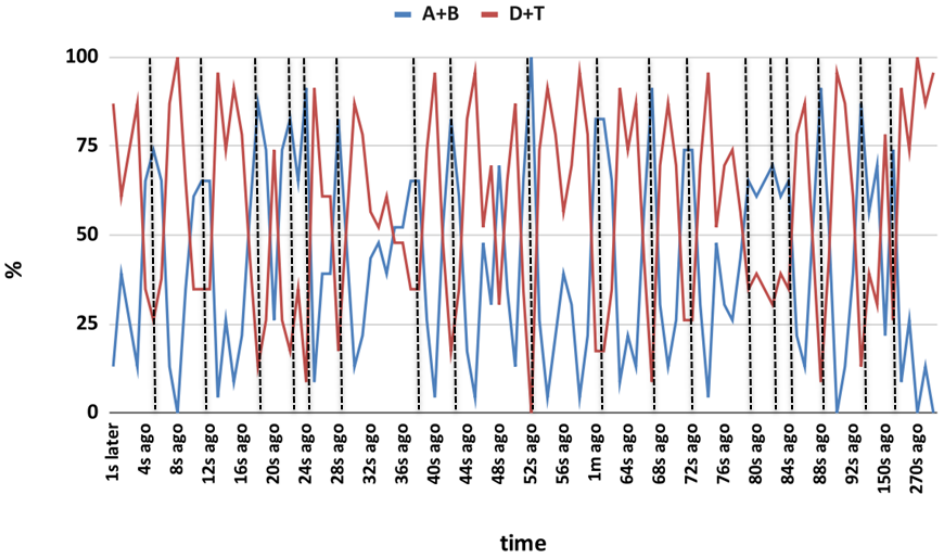

Figure 3.32 : The percentile sums of delta-theta subbands with the maximum power in the EEG signals, and alpha-beta subbands' change of percentile sums for certain periods. (patient-chb01).

We detected low-frequency ripples followed by much higher frequency ripples in % of the channels of the 24 patients (MIT database), respectively. Figures 3.35, 3.36, 3.37, 3.38, and 3.39 show the graphs obtained by using broadband EEG seg-

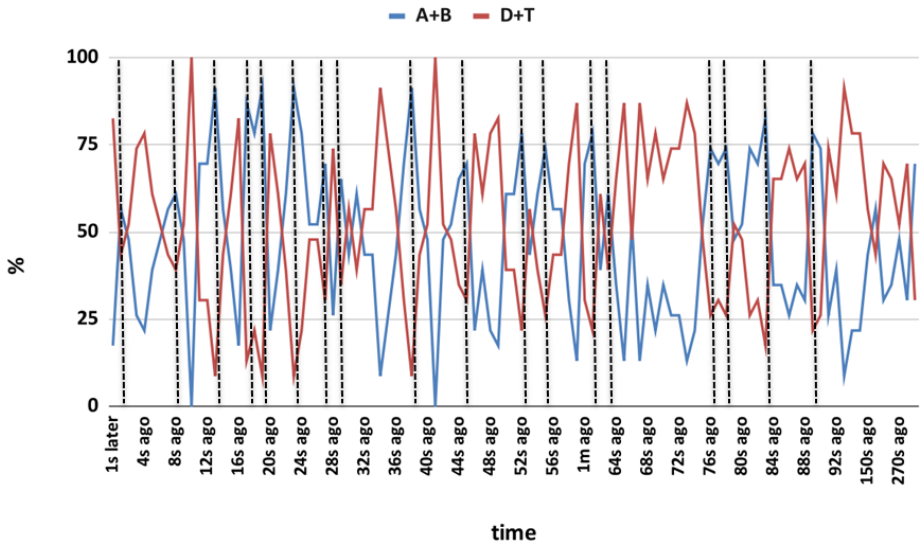

Figure 3.33 : The percentile sums of delta-theta subbands with the maximum power in the EEG signals, and alpha-beta subbands' change of percentile sums for certain periods. (patient-chb15).

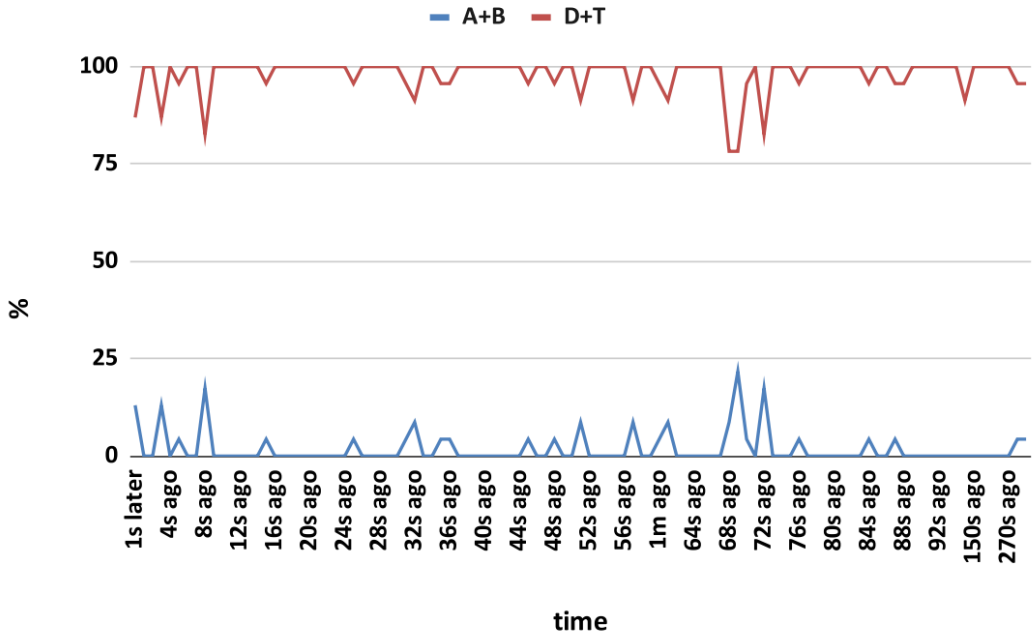

Figure 3.34 : The percentile sums of delta-theta subbands with the maximum power in the EEG signals, and alpha-beta subbands' change of percentile sums for certain periods. (patient-chb10).

ments representing HFOs power spectral analysis using the criteria described in the methods (see Section 2.4.2). Figure 3.35a, 3.36a, 3.37a, 3.38a, and 3.39a shows

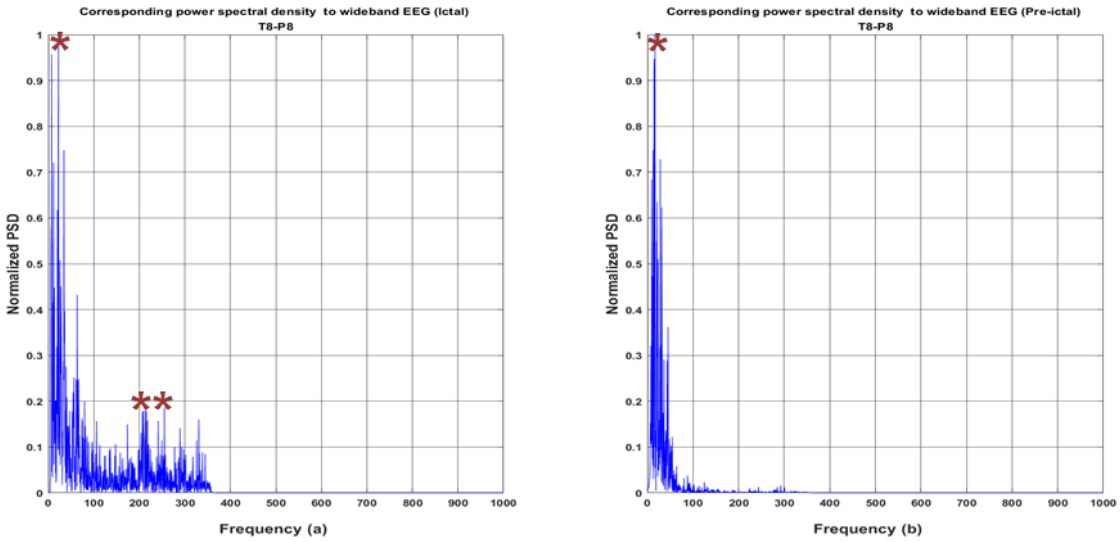

Figure 3.35 : Corresponding power spectral density to wideband pre-ictal EEG singal (chb14 (patient-14) / T8-P8 channel).

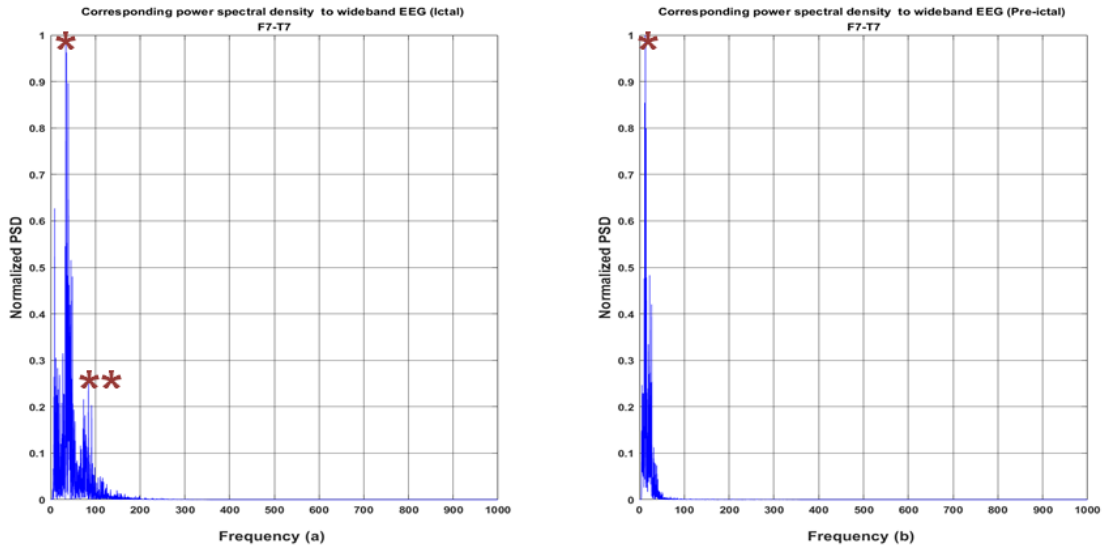

Figure 3.36 : Corresponding power spectral density to wideband ictal EEG singal (chb10 (patient 10) / F7-T7 channel).

how the HFO starts out as a low-frequency swing(indicated as *) that turns into a much higher frequency swing (indicated as **). In Figure 3.35b, 3.36b, 3.37b, 3.38b, and 3.39b however, a much higher frequency ripple is not seen following the low-frequency. This fact proves to us that Figure 3.35a and 3.36a, 3.37a, 3.38a, and 3.39a contains the epileptic patterns. HFOs were detected in 19 of 24 patients. For example, in Figure 3.40 much higher frequency ripple is not seen following the low-

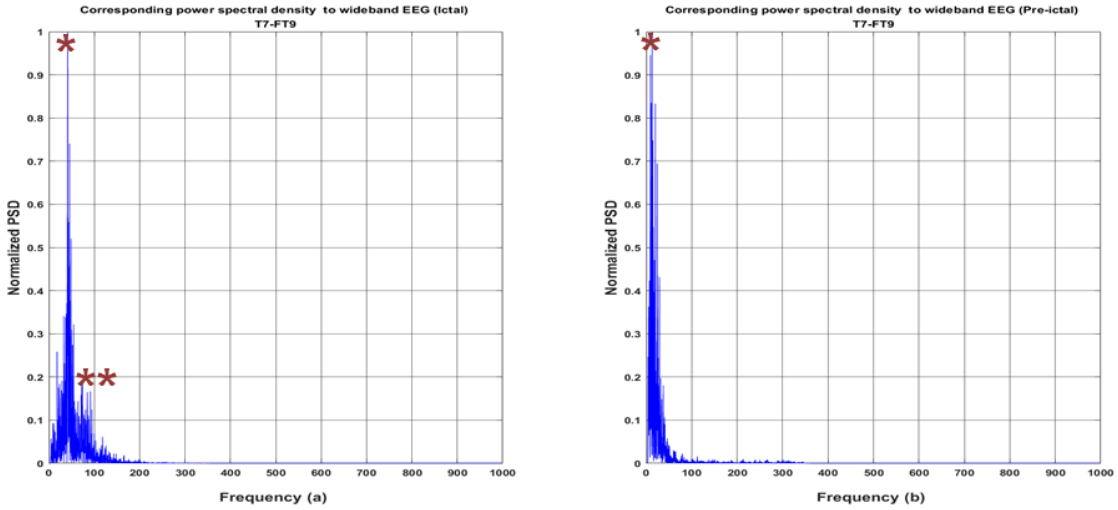

Figure 3.37 : Corresponding power spectral density to wideband ictal EEG singal (chb10 (patient 10) / T7-FT9 channel).

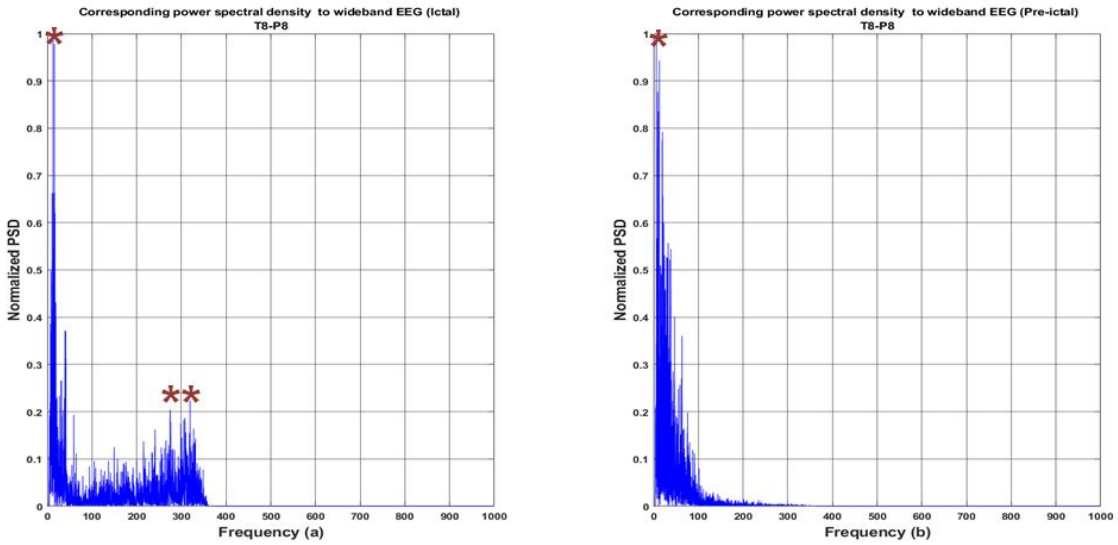

Figure 3.38 : Corresponding power spectral density to wideband ictal EEG singal (chb18 (patient 18) / T8-P8 channel).

frequency ripple for the ictal data.

Table 3.10 and Table 3.11 contain the percentile values for patient 1, in which subbands the maximum power took place in how many seconds before. Checked boxes indicate that the majority of the maximum power per second is located more in the alpha and beta subbands.

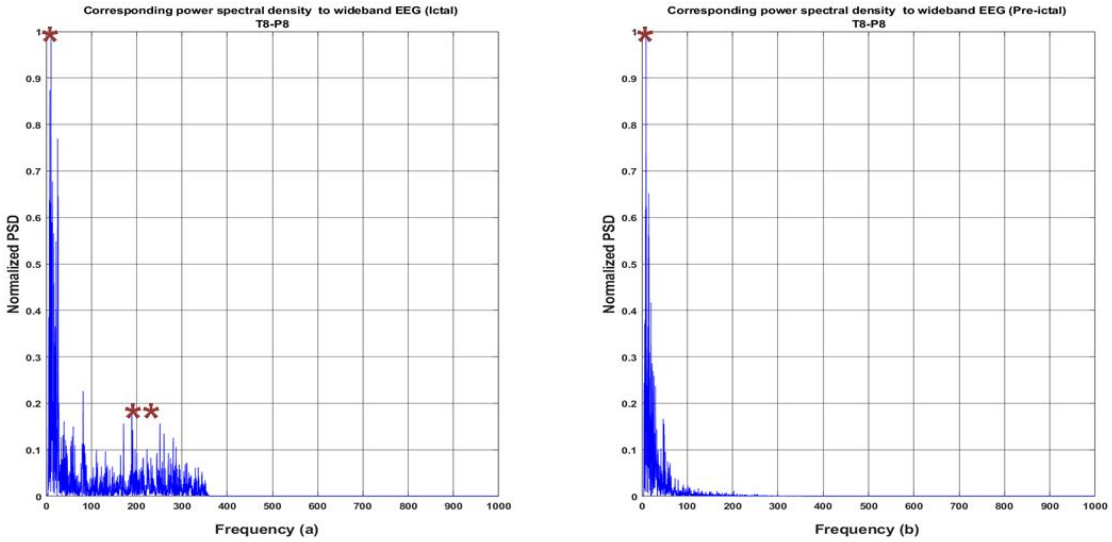

Figure 3.39 : Corresponding power spectral density to wideband ictal EEG singal (chb20 (patient 20) / T8-P8 channel).

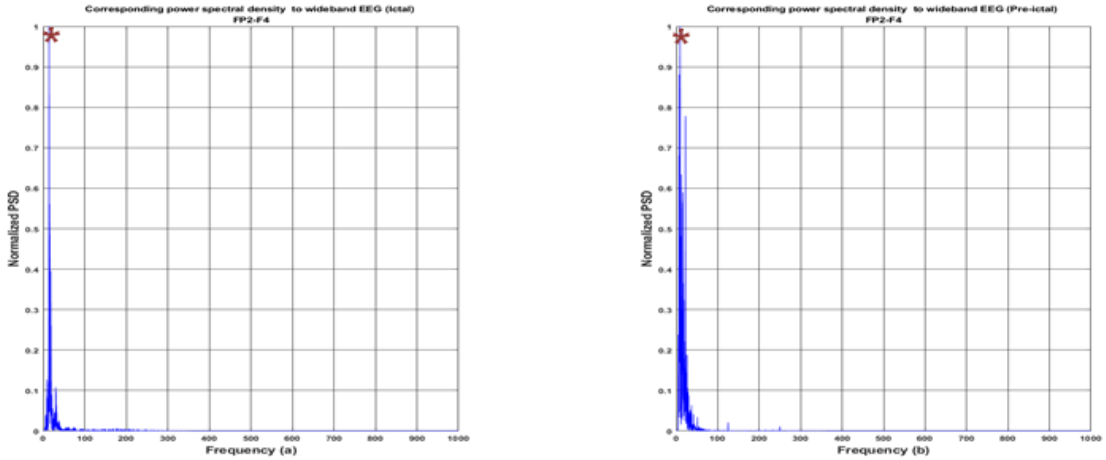

Figure 3.40 : Corresponding power spectral density to wideband ictal EEG singal (chb24 (patient 24) / FP2-F4 channel).

Table 3.12 and Table 3.13 contain the percentile values for patient 1, in which subbands the maximum power took place in how many seconds before. Checked boxes indicate that the majority of the maximum power per second is located more in the alpha and beta subbands. Especially, when the subbands with the maximum power before seizure were examined, it was determined that the T8-P8 and P7-T7 channels had alpha and beta subbands in most of the patients.

Table 3.10 : Table including the percentile sums of delta-theta subbands with the maximum power in the EEG signals, and alpha-beta subbands' values of percentile sums for certain periods (patient-chb01).

chb01 (%)	1sec later	1sec ago	2sec ago	3sec ago	4sec ago	5sec ago	6sec ago	7sec ago	8sec ago
A+B	13,04	39,13	26,08	13,04	65,21	73,91	65,21	13,04	0
D+T	86,95	60,86	73,91	86,95	34,78	26,08	34,78	86,95	99,99
chb01 (%)	9sec ago	10sec ago	11sec ago	12sec ago	13sec ago	14sec ago	15sec ago	16sec ago	17sec ago
A+B	34,78	60,86	65,21	65,21	4,34	26,08	8,69	21,73	56,52
D+T	65,21	34,78	34,78	34,78	95,65	73,91	91,3	78,26	43,47
chb01 (%)	18sec ago	19sec ago	20sec ago	21sec ago	22sec ago	23sec ago	24sec ago	25sec ago	26sec ago
A+B	86,95	73,91	26,08	73,91	82,6	65,21	91,3	8,69	39,13
D+T	13,04	26,08	73,91	26,08	17,39	34,78	8,69	91,3	60,86
chb01 (%)	27sec ago	28sec ago	29sec ago	30sec ago	31sec ago	32sec ago	33sec ago	34sec ago	35sec ago
A+B	39,13	82,6	47,82	13,04	21,73	43,47	47,82	39,13	52,17
D+T	60,86	17,39	52,17	86,94	78,26	56,52	52,17	60,86	47,82
chb01 (%)	36sec ago	37sec ago	38sec ago	39sec ago	40sec ago	41sec ago	42sec ago	43sec ago	44sec ago
A+B	52,17	65,21	65,21	26,08	4,34	52,17	82,6	60,86	17,39
D+T	47,82	34,78	34,78	73,91	95,64	47,82	17,39	34,78	82,6
chb01 (%)	45sec ago	46sec ago	47sec ago	48sec ago	49sec ago	50sec ago	51sec ago	52sec ago	53sec ago
A+B	4,34	47,82	30,43	69,56	34,78	13,04	65,21	100	26,08
D+T	95,64	52,17	69,56	30,43	65,21	86,94	34,78	0	73,91

Table 3.14 and Table 3.15 contain the percentile values for patient 1, in which subbands the maximum power took place in how many seconds before. These tables show that most of the maximum power per second is found mostly in the delta and theta subbands.

Table 3.11 : Table including The percentile sums of delta-theta subbands with the maximum power in the EEG signals, and alpha-beta subbands' values of percentile sums for certain periods (patient-chb01).

chb01 (%)	54sec ago	55sec ago	56sec ago	57sec ago	58sec ago	59sec ago	60sec ago	61sec ago	62sec ago
A+B	4,34	21,73	39,13	30,43	4,34	21,73	82,6	82,6	65,21
D+T	91,3	78,26	56,52	69,56	95,65	78,26	17,39	17,39	34,78
chb01 (%)	63sec ago	64sec ago	65sec ago	66sec ago	67sec ago	68sec ago	69sec ago	70sec ago	71sec ago
A+B	8,69	21,73	13,04	56,52	91,3	30,43	13,04	26,08	73,91
D+T	91,3	73,91	86,95	43,47	8,69	69,56	86,95	69,56	26,08
chb01 (%)	72sec ago	73sec ago	74sec ago	75sec ago	76sec ago	77sec ago	78sec ago	79sec ago	80sec ago
A+B	73,91	30,43	4,34	47,82	30,43	26,08	43,47	65,21	60,86
D+T	26,08	69,56	95,65	52,17	69,56	73,91	56,52	34,78	39,12
chb01 (%)	81sec ago	82sec ago	83sec ago	84sec ago	85sec ago	86sec ago	87sec ago	88sec ago	89sec ago
A+B	65,21	69,56	60,86	65,21	21,73	13,04	52,17	91,3	52,17
D+T	34,78	30,43	39,13	34,78	78,26	86,95	47,82	8,69	43,47
chb01 (%)	90sec ago	120sec ago	150sec ago	180sec ago	210sec ago	240sec ago	270sec ago	5min ago	10min ago
A+B	0	69,56	21,73	73,91	8,69	26,08	0	13,04	0
D+T	95,64	30,43	78,26	26,08	91,3	73,91	99,99	86,95	95,64

Table 3.12 : Table including The percentile sums of delta-theta subbands with the maximum power in the EEG signals, and alpha-beta subbands' values of percentile sums for certain periods (patient-chb15).

chb15 (%)	1sec later	1sec ago	2sec ago	3sec ago	4sec ago	5sec ago	6sec ago	7sec ago	8sec ago
A+B	17,39	56,52	47,82	26,08	21,73	39,12	47,82	56,52	60,86
D+T	82,56	43,46	52,17	73,9	78,26	60,86	52,17	43,47	39,13
chb15 (%)	9sec ago	10sec ago	11sec ago	12sec ago	13sec ago	14sec ago	15sec ago	16sec ago	17sec ago
A+B	47,82	0	69,56	69,56	91,3	56,52	39,13	17,39	86,95
D+T	52,17	99,99	30,43	30,43	8,69	43,47	60,86	82,6	13,04
chb15 (%)	18sec ago	19sec ago	20sec ago	21sec ago	22sec ago	23sec ago	24sec ago	25sec ago	26sec ago
A+B	78,26	91,3	21,73	39,13	60,86	91,3	78,26	52,17	52,17
D+T	21,73	8,69	78,26	60,86	39,13	8,69	21,73	47,82	47,82
chb15 (%)	27sec ago	28sec ago	29sec ago	30sec ago	31sec ago	32sec ago	33sec ago	34sec ago	35sec ago
A+B	69,56	26,08	65,21	43,47	60,86	43,47	43,47	8,69	26,08
D+T	30,43	73,91	34,78	56,51	39,13	56,52	56,52	91,3	73,9
chb15 (%)	36sec ago	37sec ago	38sec ago	39sec ago	40sec ago	41sec ago	42sec ago	43sec ago	44sec ago
A+B	43,47	69,56	91,3	56,52	47,82	0	47,82	52,17	65,21
D+T	56,52	30,43	8,69	43,47	52,17	99,99	52,17	47,82	34,78
chb15 (%)	45sec ago	46sec ago	47sec ago	48sec ago	49sec ago	50sec ago	51sec ago	52sec ago	53sec ago
A+B	69,56	21,73	39,13	21,73	17,39	60,86	60,86	78,26	43,47
D+T	30,43	78,26	60,86	78,26	82,6	39,13	39,13	21,73	56,52

Table 3.13 : Table including The percentile sums of delta-theta subbands with the maximum power in the EEG signals, and alpha-beta subbands' values of percentile sums for certain periods (patient-chb15).

chb15 (%)	54sec ago	55sec ago	56sec ago	57sec ago	58sec ago	59sec ago	60sec ago	61sec ago	62sec ago
A+B	60,86	73,9	56,52	56,52	30,43	13,04	69,56	78,26	39,13
D+T	39,13	26,08	43,47	43,47	69,56	86,95	30,43	21,73	60,86
chb15 (%)	63sec ago	64sec ago	65sec ago	66sec ago	67sec ago	68sec ago	69sec ago	70sec ago	71sec ago
A+B	60,86	34,78	13,04	52,17	13,04	34,78	21,73	34,78	26,08
D+T	,13	65,21	86,95	47,82	86,95	65,21	78,26	65,21	73,91
chb15 (%)	72sec ago	73sec ago	74sec ago	75sec ago	76sec ago	77sec ago	78sec ago	79sec ago	80sec ago
A+B	26,08	13,04	21,73	52,17	73,91	69,56	73,91	47,82	52,17
D+T	73,91	86,95	78,26	47,82	26,08	30,43	26,08	52,17	47,82
chbchb (%)	81sec ago	82sec ago	83sec ago	84sec ago	85sec ago	86sec ago	87sec ago	88sec ago	89sec ago
A+B	73,91	69,56	82,6	34,78	34,78	26,08	34,78	30,43	78,26
D+T	26,08	30,43	17,39	65,21	65,21	73,91	65,21	69,56	21,73
chb15 (%)	90sec ago	120sec ago	150sec ago	180sec ago	210sec ago	240sec ago	270sec ago	5min ago	10min ago
A+B	73,91	21,73	43,47	56,52	30,43	34,78	47,82	30,43	69,56
D+T	26,08	78,26	56,52	43,47	69,56	65,21	52,17	69,56	30,43

Table 3.14 : Table including the percentile sums of delta-theta subbands with the maximum power in the EEG signals, and alpha-beta subbands' values of percentile sums for certain periods (patient-chb10).

chb10 (%)	1sec later	1sec ago	2sec ago	3sec ago	4sec ago	5sec ago	6sec ago	7sec ago	8sec ago
A+B	13,04	0	0	13,04	0	4,34	0	0	17,39
D+T	86,95	99,99	99,99	86,95	99,99	95,65	99,99	99,99	82,6
chb10 (%)	9sec ago	10sec ago	11sec ago	12sec ago	13sec ago	14sec ago	15sec ago	16sec ago	17sec ago
A+B	0	0	0	0	0	0	4,34	0	0
D+T	99,99	99,99	99,99	99,99	99,99	99,99	95,65	99,99	99,99
chb10 (%)	18sec ago	19sec ago	20sec ago	21sec ago	22sec ago	23sec ago	24sec ago	25sec ago	26sec ago
A+B	0	0	0	0	0	0	0	4,34	0
D+T	99,99	99,99	99,99	99,99	99,99	99,99	99,99	95,65	99,99
chb10 (%)	27sec ago	28sec ago	29sec ago	30sec ago	31sec ago	32sec ago	33sec ago	34sec ago	35sec ago
A+B	0	0	0	0	4,34	8,69	0	0	4,34
D+T	99,99	99,99	99,99	99,99	95,65	91,3	99,99	99,99	95,65
chb10 (%)	36sec ago	37sec ago	38sec ago	39sec ago	40sec ago	41sec ago	42sec ago	43sec ago	44sec ago
A+B	4,34	0	0	0	0	0	0	0	0
D+T	95,65	99,99	99,99	99,99	99,99	99,99	99,99	99,99	99,99
chb10 (%)	45sec ago	46sec ago	47sec ago	48sec ago	49sec ago	50sec ago	51sec ago	52sec ago	53sec ago
A+B	4,34	0	0	4,34	0	0	8,69	0	0
D+T	95,65	99,99	99,99	95,65	99,99	99,99	91,3	99,99	99,99

Table 3.15 : Table including the percentile sums of delta-theta subbands with the maximum power in the EEG signals, and alpha-beta subbands' values of percentile sums for certain periods (patient-chb10).

chb10 (%)	54sec ago	55sec ago	56sec ago	57sec ago	58sec ago	59sec ago	60sec ago	61sec ago	62sec ago
A+B	0	0	0	8,69	0	0	4,34	8,69	0
D+T	99,99	99,99	99,99	91,3	99,99	99,99	95,65	91,3	99,99
chb10 (%)	63sec ago	64sec ago	65sec ago	66sec ago	67sec ago	68sec ago	69sec ago	70sec ago	71sec ago
A+B	0	0	0	0	0	8,69	21,73	4,34	0
D+T	99,99	99,99	99,99	99,99	99,99	78,26	78,26	95,65	99,99
chb10 (%)	72sec ago	73sec ago	74sec ago	75sec ago	76sec ago	77sec ago	78sec ago	79sec ago	80sec ago
A+B	0	17,39	0	0	0	4,34	0	0	0
D+T	99,99	82,6	99,99	99,99	99,99	95,65	99,99	99,99	99,99
chb10 (%)	81sec ago	82sec ago	83sec ago	84sec ago	85sec ago	86sec ago	87sec ago	88sec ago	89sec ago
A+B	0	0	0	4,34	0	0	4,34	0	0
D+T	99,99	99,99	99,99	95,65	99,99	99,99	95,65	99,99	99,99
chb10 (%)	90sec ago	120sec ago	150sec ago	180sec ago	210sec ago	240sec ago	270sec ago	5min ago	10min ago
A+B	0	0	0	0	0	0	0	4,34	4,34
D+T	99,99	91,3	99,99	99,99	99,99	99,99	99,99	95,65	95,65

4. CONCLUSION

In this study, we dealt with the methods for detecting epileptic seizure patterns. We determined the EEG signal subbands with maximum power for each signal in the A, C, and E data sets out of the EEG dataset from Bonn University. It was determined by the maximum PSD method whether the detected subbands were pathological or non-pathological. The total percentage figures in Table 3.2 show that we correctly detected the ictal status for all five patients. In addition, ripples and fast ripples were determined by frequency analysis of the signals. Frequencies in epileptic signals are generally found with 80 Hz and above. Furthermore, calculating the increased PSDs of ripples and fast ripples, it was observed that the HFO in epileptic data started as a low-frequency ripple and then turned into a much higher-frequency ripple. However, pre-seizure data did not show much higher frequency ripples following the low-frequency ripples. Thus, the separation of epileptic patterns from pre-seizure patterns was also determined by this method. We detected low-frequency ripple followed by much higher frequency ripple in 75%, 75%, 65%, 85%, and 75% of the channels of the five patients, respectively. For the pre-ictal data, we could not observe a much higher frequency ripple followed by a low-frequency ripple in 90%, 85%, 75%, 90%, and 90% of the channels, respectively. As seen in Table 3.4, large frequency changes were observed between the pre-seizure and seizure period in most of the channels for all five patients. This allows us to distinguish data containing epileptic patterns within five patients correctly. Table 3.5, 3.6, 3.7 ve 3.8 show the proportionality of maximum amplitude for preictal and ictal EEG frequency subbands. The P3 channel, highlighted in this table, is the common channel and for all subbands amplitude increase when the amplitude ratios between the pre-ictal and ictal signals are examined. As seen in these tables, the Gamma subband amplitude increased in all channels for all patients, and the delta subband amplitude increased in the left lob (Fp1, F3, F7, T3, T5, C3, P3, O1). Table 3.9 also includes frequency values for ictal data. According to this table, the frequency of signals is observed to be 80 Hz and above on all channels for all patients.

The same studies were applied to the EEG signals obtained from the Boston database. The signals were first passed through the preprocessing step. Then, the PSDs of

the EEG signals of each channel were examined. As obtained from the first data set, it was determined that the PSD of the pre-seizure signal was in a large frequency range, while the PSD of the seizure signal was in a narrow frequency range (seen Figure 3.30 and Figure 3.31). Secondly, the sample including the maximum power and maximum power of the signals was examined. It has been determined that these samples are within the sample range included in the seizure information. In addition, when the seizure moment of the signals is examined, it has been determined that the maximum power is mostly in the frequency ranges of the delta and theta subbands. However, although the duration varies for each patient before the seizure, we found that the frequencies of the alpha and beta subbands were higher than the delta and theta subbands in 75% of the patients for a certain period of time (seen Figure 3.32 and Figure 3.33). We could not observe this situation in 25% of the patients (seen Figure 3.34). Tables 3.10 and 3.11 contain the percentile values for patient 1, Tables 3.12 and 3.13 contain the percentile values for patient 15, and Tables 3.14 and 3.15 contain the percentile values for patient 10, in which subbands the maximum power took place in how many seconds before. Checked boxes indicate that the majority of the maximum power per second is located more in the alpha and beta subbands. As seen in Tables 3.14 and 3.15, the maximum power is always in the delta and theta subbands in patient 10. These tables of patient 10 do not give us information about seizure prediction. We were aforementioned that EEG signals of healthy individuals contain alpha and beta subbands, while delta and theta subbands are caused by pathological conditions and are a sign of disease. Also, when the subbands with the maximum power before seizure were examined, it was determined that the T8-P8 and P7-T7 channels had alpha and beta subbands in most of the patients. Moreover, calculating the increased PSDs of ripples and fast ripples for the Boston database, it was observed that the HFO in epileptic data started as a low-frequency ripple and then turned into a much higher-frequency ripple. However, pre-seizure data did not show much higher frequency ripples following the low-frequency ripples. Thus, the separation of epileptic patterns from pre-seizure patterns was also determined by this method. We detected low-frequency ripple followed by much higher frequency ripple in 19 patients out of 24 patients ($\% \ 79,16$). This situation shows us both the accuracy of the results we obtained and that we

can use these results for seizure prediction.

In the future, these studies will be carried out to determine pre-ictal status with a larger data set. The aim is to create a communication system that automatically detects epileptic seizure signals for a certain period of time before the seizure occurs so that epileptic patients can get through the seizure moment with the least damage by obtaining the pre-seizure differences of the brain signals.

REFERENCES

[1] **World Health Organization.** (2022). Epilepsy, 2022. pp. 1-2.

[2] **Sirven JI.** (2015). Epilepsy: A Spectrum Disorder. Cold Spring Harb Perspect Med. 2015 Sep; 5(9): a022848.

[3] **Akdağ et al.** (2016). Epilepsy" Osmangazi Medical Journal. 2016; 38 (Special Issue 1): 35-41.

[4] **Varsavsky A, Mareels I, Cook M.** (2011). Epileptic Seizures and the EEG/Measurement, Models, Detection, and Prediction. CRC Press, International Standard Book Number-13: 978-1-4398-1204-4 (eBook - PDF), 2011.

[5] **Thoracic Key.** (2022). Introduction to EEG. Website https://thoracickey.com/introduction-to-eeg/ [accessed 4 June 2022].

[6] **Aktekin B.** (2020). Epilepsi Nedir? Yeditepe EpilepsiSİZ. http://www.yeditepeepilepsisiz.com/epilepsi/ [accessed 4 December 2020].

[7] **UCB.** (2021). Inspired by patients driven by science, "Epilepsi ve Tedavisi" https://www.ucb.com.tr/hastalar/ko%C5%9Fullar/Santral-Sinir-Sistemi/Epilepsi/Epilepsi-N%C3%B6betleri-ve-Sendromlar%C4%B1 [accessed 20 June 2021].

[8] **Uysal P.** (2008). İlk Kez Afebril Konvülsiyon Geçiren Çocuklarda Etiyolojik Ve Prognostik Faktörler. Master thesis, 2008, pp. 13-14.

[9] **UPMC.** (2021). Children's Hospital of Pittsburgh. Epilepsy Syndromes. https://www.chp.edu/our-services/brain/neurology/epilepsy/types/syndromes [accessed 21 June 2021].

[10] **Memorial Tıbbi Yayın Kurulu.** (2021). Epilepsi nedir? Epilepsi belirtileri ve tedavi yöntemleri nelerdir? https://www.memorial.com.tr/hastaliklar/epilepsi-nedir-epilepsi-belirtileri-ve-tedavi-yontemleri-nelerdirepilepsi-tanisi-nasil-konulur [accessed 20 June 2021].

[11] **Sezer E.** (2008). Epilepsi Teşhisi için EEG Sinyal Analizi. 2008, pp. 127.

[12] **Baykan B, Altındağ E,Elmalı AD.** (2020) Elektroensefalografi. http://www.itfnoroloji.org/semi2/eeg.htm, [accessed 21 January 2020].

[13] **Öztura İ.** (2016). Elektrofizyolojinin Temelleri. Dokuz Eylül University, Faculty of Medicine, Department of Neurology, İzmir, 2016.

[14] **Morley A, Hill L, Kaditis AG.** (2016). 10-20 EEG Placement. European Respiratory Society Every Breath Counts, 2016.

[15] **Vikipedi.** (2021). 10–20 sistem (EEG) - 10–20 system (EEG). https://tr.xcv.wiki/wiki/10%E2%80%9320system(EEG) [accessed 20 June 2021].

[16] **Schafer NF, Damberger MG.** (2012). Identifying Interictal and Ictal Epileptic Activity in Polysomnograms. DOI: 10.1016/j.jsmc.2012.01.002, Article in Sleep Medicine Clinics, March 2012.

[17] **Yıldız O, Yılmaz Öz B, Yeni SN.** (2021). Writing and Reporting of Scalp Electroencephalography. DOI: 10.14744/epilepsi.2020.54366, Epilepsi 2021; 27(1): 1-7.

[18] **Çabalar M, Selçuk Ö, Yazar T, Karamanlı Y, Yetkin T, Yayla V.** (2011). Rutin Elektroensefalografide Diken, Keskin ve Yavaş Dalga Aktivitelerinin Anatomik Lokalizasyonları. Medical Journal of Bakırköy, Volume 7, Number 3, 2011.

[19] **Türk Epilepsi ile Savaş Derneği. Epilepsi ve Tedavisi.** (2019). www.turkepilepsi.org.tr/menu/31/epilepsiyi-siniflandirma [accessed 1 June 2019].

[20] **Kaculini CM, Tate-Looney AJ,Seifi A.** (2021). The History of Epilepsy: From Ancient Mystery to Modern MisconceptionThe History of Epilepsy: From Ancient Mystery to Modern Misconception. Cureus, Mar; 13(3): e13953, 2021.

[21] **WHO.** (2015). Epilepsy: the disorder. Epilepsy Atlas, 2015; pp. 15-18.

[22] **Magiorkinis E, Sidiropoulou K, Diamantis A.** (2010). Hallmarks in the history of epilepsy: Epilepsy in antiquity. Epilepsy & Behavior; Volume 17, Issue 1,January 2010; pp. 103-108

[23] **George M, Doolittle MD.** (1934). Acid base equilibrium in epilepsy. Psybbchiatric Quarterly, volume 8, 1934; pp. 754–759

[24] **Fisch BJ.** (1991). Spehlmann's EEG Primer. Elsevier, 1991; pp. 634

[25] **Meldrum BS, Chapman AG.** (1999). Excitatory amino acids receptors and antiepileptic drug development. Delgado-Escueta, A. V. Wilson, W. Olsen, R. W. Porter, R. J. eds. Jasper's Basic Mechanisms of the Epilepsies. Third Edition: Advances in NeurologyVol. 79, Chapter 65:965–978 Lippincott Williams & Wilkins Philadelphia. 1999.

[26] **Andrzejak RG, Lehnertz K, Mormann F, Rieke C, David P, Elger CE.** (2001). Indications of nonlinear deterministic and finite-dimensional structures in time series of brain electrical activity: Dependence on recording region and brain state. PHYSICAL REVIEW E, VOLUME 64, 061907, The American Physical Society, 2001.

[27] **Zhao M, Suh M, Ma H, Perry C, Geneslaw A ve Schwartz TH.** (2007). Focal Increases in Perfusion and Decreases in Hemoglobin Oxygenation Precede Seizure Onset in Spontaneous Human Epilepsy. Epilepsia, 2007; 48(11): 2059–2067.

[28] **Schwartz TH.** (2007). Neurovascular Coupling and Epilepsy: Hemodynamic Markers for Localizing and Predicting Seizure Onset. Epilepsy Curr. 2007 Jul; 7(4): 91–94.

[29] **Bek S, Erdoğan E, Gökçil Z.** (2012). Vagal Nerve Stimulation and Patient Selection. Epilepsy 2012; 18(Appendix 1): 63-67

[30] **Meenakshi et al.** (2014). Frequency Analysis of Healthy Epileptic Seizure in EEG using Fast Fourier Transform. International Journal of Engineering Research and General Science Volume 2, Issue 4, June-July, 2014.

[31] **Moghim N, Corne DW.** (2014). Predicting Epileptic Seizures in Advance. PLoS One, 2014; 9(6): e99334

[32] **Kılıç TY, Yesilaras M, Atilla ÖD, Sever M, Aksay E.** (2014). Can venous blood gas analysis be used for predicting seizure recurrence in emergency department? World J Emerg Med, Vol 5, No 3, 2014.

[33] **Aguiar K, França FMG, Barbosa VC, Teixeria CS.** (2016). Early detection of epilepsy seizures based on a weightless neural network. 2016.

[34] **Fujiwara K, Miyajima M, Yamakawa T, Abe E, Suzuki Y, Sawada Y, Kano M, Maehara T, Ohta K, Sakuma TS, Sasano T, Matsuura M, Matsushima E.** (2016). Epileptic Seizure Prediction Based on Multivariate Statistical Process Control of Heart Rate Variability Features. IEEE TRANSACTIONS ON BIOMEDICAL ENGINEERING, VOL. 63, NO. 6, JUNE 2016.

[35] **Aggarwal G, Gandhi TP.** (2017). Prediction of Epileptic Seizures based on Mean Phase Coherence. bioRxiv preprint doi: https://doi.org/10.1101/212563; November 1, 2017.

[36] **Lai YF, Chiang GS.** (2017). Automatic Detection of Epileptic Seizures in EEG Using Machine Learning Methods. E-ISSN: 2224-2902, Volume 14, 2017.

[37] **Billeci L, Marino D, Insana L, Vatti G, Varanini M.** (2018). Patient-specific seizure prediction based on heart rate variability and recurrence quantification analysis. Sep 25; 13(9): e0204339. doi: 10.1371/journal.pone.0204339. eCollection 2018.

[38] **Wang et al.** (2017). Automated Recognition of Epileptic EEG States Using a Combination of Symlet Wavelet Processing, Gradient Boosting Machine, and Grid Search Optimizer. Epilepsi 2017; 23(3): 109-117.

[39] **Hussein R, Palangi H, Ward RK, Wang ZJ.** (2019). Optimized deep neural network architecture for robust detection of epileptic seizures using EEG signals. Clinical Neurophysiology 130, 2019; 25–37.

[40] **Abedin MZ, Akther S, Hossain MS.** (2019). An Artificial Neural Network Model for Epilepsy Seizure Detection. 5th International Conference on Advances in Electrical Engineering (ICAEE), 2019.

[41] **Slimen IB, Boubchir L, Seddik H.** (2020). Epileptic seizure prediction based on EEG spikes detection. J Biomed Res. 2020 May; 34(3): 162–169.

[42] **Stirling RE, Cook MJ, Grayden DB, Karoly PJ.** (2020). Seizure forecasting and cyclic control of seizures. 2020.

[43] **Zhang Z, Parhi KK.** (2015). Seizure detection using regression tree based feature selection and polynomial SVM classification. 37th Annual International Conference of the IEEE Engineering in Medicine and Biology Society (EMBC), 2015.

[44] **McGrogan N.** (1999). Neural network detection of epileptic seizures in the electroencephalogram. Oxford University, 1999.

[45] **Srinivasan V, Eswaran C, Sriraam N.** (2005). Artificial Neural Network Based Epileptic Detection Using Time-Domain and Frequency-Domain Features. Journal of Medical Systems, Vol. 29, No. 6, December 2005.

[46] **Tzallas AT, Tsipouras MG, Fotiadis DI.** (2009). Epileptic Seizure Detection in EEGs Using Time-Frequency Analysis. IEEE Transactions on Information Technology in Biomedicine, Volume: 13, Issue: 5, Sept. 2009.

[47] **Ubeyli ED.** (2009). Statistics over features: EEG signals analysis. Computers in Biology and Medicine 39 (2009) pp. 733 - 741

[48] **Bandarabadi M, Teixeira CA, Rasekhi J, Dourado A.** (2015). Epileptic seizure prediction using relative spectral power features. Volume 126, Issue 2, February 2015; pp. 237-248.

[49] **Balasaraswathy N, Rajavel R.** (2015). Automatic seizure detection system with low complex PSD using TMS320C6713 DSP. Int. J. Biomedical Engineering and Technology, Vol. 18, No. 2, 2015.

[50] **Ashokkumar SR, Anupallavi S, Premkumar M, Jeevanantham V.** (2021). Implementation of deep neural networks for classifying electroencephalogram signals using fractional S-transform for epileptic seizure detection. Int J Imaging Syst Technol.2021; 31: 895–908.

[51] **Nanthini K, Tamilarasi A, Pyingkodi M, Kaviya SM, Mohideen PA.** (2022). Epileptic Seizure Detection and Prediction Using Deep Learning Technique. 2022 International Conference on Computer Communication and Informatics (ICCCI), Jan. 25 – 27, 2022, Coimbatore, INDIA

[52] **Singh K, Malhotra J.** (2022). Smart neurocare approach for detection of epileptic seizures using deep learning based temporal analysis of EEG patterns. Multimedia Tools and Applications. 2022.

[53] **Ma D, Zheng J, Peng L.** (2021). Performance Evaluation of Epileptic Seizure Prediction Using Time, Frequency, and Time–Frequency Domain Measures. Processes 2021, 9(4), 682.

[54] **Park Y, Luo L, Parhi KK, Netoff T.** (2011). Seizure prediction with spectral power of EEG using cost-sensitive support vector machines. Volume52, Issue10, October 2011; pp. 1761-1770

[55] **Parhi KK, Zhang Z.** (2019). Discriminative Ratio of Spectral Power and Relative Power Features Derived via Frequency-Domain Model Ratio With Application to Seizure Prediction. IEEE Transactions on Biomedical Circuits and Systems (Volume: 13, Issue: 4, Aug. 2019); pp. 645 - 657.

[56] **Tsipouras MG.** (2019). Spectral information of EEG signals with respect to epilepsy classification. EURASIP Journal on Advances in Signal Processing volume 2019, Article number: 10. 2019.

[57] **Ge L, Parhi KK.** (2022). Applicability of Hyperdimensional Computing to Seizure Detection. IEEE Open Journal of Circuits and Systems (Volume: 3), 2022; pp. 59-71.

[58] **Zweiphenning WJEM, Ellenrieder NV, Dubeau F, Martineau L, Minotti L, Hall JA, Chabardes S, Dudley R, Kahane P, Gotman J, Frauscher B.** (2022). Correcting for physiological ripples improves epileptic focus identification and outcome prediction. Epilepsia. 2022; 63: 483–496.

[59] **Kramer MA, Ostrowski LM, Song DY, Thorn EL, Stoyell SM, Parnes M, Chinappen D, Xiao G, Eden UT , Staley KJ , Stufflebeam SM, Chu CJ.** (2019).

Scalp recorded spike ripples predict seizure risk in childhood epilepsy better than spikes. Brain . 2019 May 1; 142(5): 1296-1309.

[60] **Lachner-Piza D, Jacobs J, Bruder JC, Schulze-Bonhage A, Stieglitz T, Dümpelmann M.** (2020). Automatic detection of high-frequency-oscillations and their sub-groups co-occurring with inter-ictal-epileptic-spikes. J Neural Eng . 2020 Jan 14; 17(1): 016030.

[61] **Nadalin JK, Eden UT, Han X, Richardson RM, Chu CJ, Kramer MA.** (2021). Application of a convolutional neural network for fully-automated detection of spike ripples in the scalp electroencephalogram. J Neurosci Methods . 2021 Aug 1; 360: 109239.

[62] **Schönberger J, Knopf A, Dümpelmann M, Schulze-Bonhage A, Jacobs J.** (2021). Distinction of Physiologic and Epileptic Ripples: An Electrical Stimulation Study. Brain Sci. 2021, 11, 538.

[63] **Andrzejak RG, Lehnertz K, Mormann F, Rieke C, David P, Elger CE.** (2001). Indications of nonlinear deterministic and finite-dimensional structures in time series of brain electrical activity: Dependence on recording region and brain state. PHYSICAL REVIEW E, VOLUME 64, 061907, DOI: 10.1103/PhysRevE.64.061907, ©2001 The American Physical Society.

[64] **Bairagi RN, Maniruzzaman Md, Pervin S, Sarker A.** (2021). Epileptic seizure identification in EEG signals using DWT, ANN and sequential window algorithm. Soft Computing Letters 3 (2021) 100026.

[65] **Libenson M.** (2009). Practical approach to electroencephalography. First ed., Saunders, United States, 2009.

[66] **LeVan P,Urrestarazu E, Gotman J.** (2006). A system for automatic artifact removal in ictal scalp EEG based on independent component analysis and Bayesian classification. Clinical Neurophysiology 117. 2006. 912–927.

[67] **Al-Fahoum AS, Al-Fraihat AA.** (2014). Methods of EEG Signal Features Extraction Using Linear Analysis in Frequency and Time-Frequency Domains. Volume 2014 |Article ID 730218.

[68] **Nayak CS, Anilkumar AC.** (2021). EEG Normal Waveforms. Last Update: July 31, 2021.

[69] **Park CJ, Hong SB.** (2019). High Frequency Oscillations in Epilepsy: Detection Methods and Considerations in Clinical Application. J Epilepsy Res. 2019 Jun; 9(1): pp. 1–13.

[70] **Moctezuma LA, Molinas M.** (2020). EEG Channel-Selection Method for Epileptic-Seizure Classification Based on Multi-Objective Optimization. Frontiers in Neuroscience, Volume 14, Article 593, June 2020.

[71] **MathWorks Inc.** (2021). MATLAB [online]. Website https://www.mathworks.com/products/matlab.html [accessed 13 March 2022].

[72] **Shoeb AH.** (2009). Application of Machine Learning to Epileptic Seizure Onset Detection and Treatment. Massachusetts Institute of Technology 2009.

RESUME

Name Surname : Rabia TUTUK

EDUCATION STATUS :

- **Bachelor :** 2020, Inonu University, Faculty of Engineering, Department of Biomedical Engineering

- **Master :** 2022, Inonu University, Department of Biomedical Engineering, Department of Biomedical Engineering

PROFESSIONAL EXPERIENCE:

- 2019 OTTOMAN GROUP IMPLANT (Summer internship).

- 2020 SASTEK Conformity Assessment Inc. (Intern).